Analysis of Manufacturing Methods and Die Design for Agricultural Parts in Bangladesh

A Thesis
Presented to
The Academic Faculty

By

William Schalch

In Partial Fulfillment
Of the Requirements of the Degree
Master of Science in Mechanical Engineering in the
School of Mechanical Engineering

Georgia Institute of Technology

August 2022

Analysis of Manufacturing Methods and Die Design for Agricultural Parts in Bangladesh

Approved by:

Dr. Jonathan S. Colton
School of Mechanical Engineering
Georgia Institute of Technology

Dr. Shreyes N. Melkote
School of Mechanical Engineering
Georgia Institute of Technology

Dr. Christopher J. Saldana
School of Mechanical Engineering
Georgia Institute of Technology

Date Approved: July 21, 2022

ACKNOWLEDGMENTS

Table of Contents

LIST OF TABLES

LIST OF FIGURES

LIST OF SYMBOLS AND ABBREVIATIONS

Abbreviation	Definition
ABLE	Agricultural Based Light Engineering
AISI	American and Iron Steel Institute
ASTM	American Society for Testing and Materials
BDT	Bangladesh Taka
BITAC	Bangladesh Industrial Technical Assistance Centre
BRRI	Bangladesh Rice Research Institute
CAD	Computer Aided Design
CNC	Computer numerical control
CSISA-MEA	Cereal Systems Initiative for South Asia - Mechanization Extension Activity
FEA	Finite Element Analysis
FEM	Finite Element Method
HRB	Rockwell hardness B scale
HRC	Rockwell hardness C scale
IRRI	International Rice Research Institute
NVA	Non value added
OEM	Original Equipment Manufacturer
OES	Optical emission spectrometer
RPM	Revolutions per minute
RTC	Rice transplanter Claw
SIPM	Surface inch per minute
SFPM	Surface feet per minute
SS	Stainless steel
USAID	United States Agency for International Development
USD	United States Dollar
VA	Value added
WDXRF	Wavelength dispersive x-ray fluorescence
XRF	X-ray fluorescence

SUMMARY

High labor wages brought on by a decreasing agricultural labor force as well as promises of decreased drudgery and increased yield have spurred the adoption of agricultural mechanization among farmers in Bangladesh. However, a combination of skill-based, logistical, and economic constraints has limited the complexity and production rates of spare parts for agricultural machinery currently produced locally within Bangladesh. This thesis provides a framework for the manufacturing of two key spare parts for the mechanization of planting and harvesting in Bangladesh: rice transplanter claws and combine harvester blades. The work presented in this thesis incorporates the development of rice transplanter claw and combine harvester blade manufacturing processes that have been tailored to the conditions and machinery that is available within small machine shops in Bangladesh.

The thesis is divided into four main sections: the introduction, development of rice transplanter claw manufacturing process, development of combine harvester blade manufacturing process, and the conclusion. The introduction provides a brief overview of mechanization within Bangladesh as well as the current state of local production of agricultural spare parts. The two chapters regarding the manufacturing of rice transplanter claws and combine harvester blades proceed through multiple stages including a manufacturing process analysis, cost analysis, design of required tools and dies, experimental testing, finite element analysis (FEA) in DEFORM-3D, and results analysis. The conclusion summaries the work presented in the thesis as well as the drawbacks of the study.

The manufacturing process analysis contains multiple stages including the characterization of the original rice transplanter claws and combine harvester blades, development of manufacturing process charts and cost analyses, and selection of the most appropriate manufacturing process for the agricultural spare parts manufacturers in Bangladesh.

The thesis then proceeds through the design of the blanking, bending, and forging die sets required for the manufacturing of claws and blades. Next, prototype bending and forging die sets were machined and tested for validation of the design and DEFORM-3D simulations. After the testing of the prototype die sets, the results were analyzed and design changes were made to the bending and forging die sets.

The results of the rice transplanter prototype bending die testing and DEFORM-3D simulation of the prototype testing validate the model because the width differences of the two were found to be 0.05 mm or 0.29%. The validation of the combine harvester forging die testing and corresponding DEFORM-3D model demonstrate the accuracy of the model because the difference in die stroke between the prototype forging die set and DEFORM-3D simulation was found to be 0.08 mm or 2.3%. The results of the DEFORM-3D simulations of the final rice transplanter claw bending and forging die sets demonstrate low deviations in the dimensions of the original rice transplanter claw and the combine harvester blade following the bending and forging operations, respectively. The difference in width of the original rice transplanter blade and the DEFORM simulation width of the final bending punch and die set with springback was found to be 0.05 mm. The DEFORM simulation of the final forging die set of the four combine harvester blade revealed that a pressing force of 100-300 metric tons was needed to reach

an adequete die stroke. The specific press force required depends on the model of

combine harvester blade in question. Finally, a sensitivy analysis of the bending and

forging die sets revealed that deviation in stock material yield strength can be accoutned

for though proper characterization of the stock material prior to manufacturing.

CHAPTER 1

Introduction

1.1 Mechanization of Rice and Wheat Production in Bangladesh

Bangladesh is among the world's most populated countries with a population of 167.9 million and a population density of 1,265 people per square kilometer (United Nations, 2022; The World Bank, 2020). Rice is the staple food for the majority of the population of Bangladesh as it provides two thirds of the total daily caloric intake of an average Bangladeshi (Bangladesh Rice Research Institute, 2011). Over a three-year period of 2020-2022, Bangladesh has been the third largest rice producer in the world, allocating three fourths of its agricultural land to the crop (Daily Sun, 2022). However, as of 2021 less than one percent of rice planting and eight percent of harvesting has been mechanized (Alam, 2022). The dependence on manual labor for planting and harvesting has left farmers open to the effects of labor shortages and wage hikes brought on by a decreasing agricultural labor force (Fuad and Flora, 2019). Projects such as USAID's Cereal Systems Initiative for South Asia - Mechanization and Extension Activity (CSISA-MEA) have brought the public and private sector together to promote the mechanization of agriculture and manufacturing of agricultural machinery and spare parts in Bangladesh to improve both the agricultural and industrial sectors. Support of agricultural-based light engineering workshops (ABLEs) is provided to the business owners and workers through a variety of machine shop and business training activities. Specific support is also provided to businesses in developing manufacturing processes for more complex agricultural machines and spare parts.

1.2 Bangladesh Agricultural Mechanization Spare Parts Market

In 2017, reports from Alam et al. indicated that the Bangladesh agricultural spare parts market consisted of approximately 70 foundries, 800 agricultural machinery manufacturers, and 1500 spare parts manufacturers. Figure 1 shows the estimated market size of agricultural spare parts in Bangladesh over a period from 2004-2020. In 2004, the estimated agricultural spare parts market size was $89.3 million with two percent or $1.78 million from local production. After a period of seven years, the market size had grown considerably to $309.5 million with 77% or $237.9 million from production within Bangladesh. By 2020, the agricultural spare parts market size had risen to $381.0 million with 77% or $293.4 million from production in Bangladesh (Alam, 2017; Alam, 2022). The rapid growth of the local agricultural machinery and spare parts market can be attributed to the fast adoption of the mechanization of land preparation (power tilling), pesticide application, irrigation, threshing, and post-harvest processing (Hossen, 2019). The local production of spare parts for the respective machinery soon followed with local production of centrifugal pumps, wells pumps, and various pulley covers dominating the local market. However, local agricultural machinery and spare part manufacturers face issues of the lack of worker skills, proper raw materials, and modern capital machinery, which affect the ability of the ABLEs to produce more complex spare parts or agricultural machinery such as rice transplanters and combine harvesters (Alam, 2017). As the adoption of mechanization increases for other agricultural operations such as planting and harvesting, the need for spare parts for these machines is predicted to increase rapidly creating a potential market for local spare parts manufacturers.

Figure 1: Estimated market size of agricultural spare parts market in Bangladesh. Adapted [reprinted] from *Trend of Agricultural Machinery and Spare Parts Manufacturing and Sales in Bangladesh* (p. 13), by M. M. Alam, 2022, Agricultural Mechanization in Bangladesh - The Future.

The two major agricultural machinery involved in the planting and harvesting of rice are the rice transplanter and the combine harvester. Specific spare parts for these machines were identified by their propensity to wear and their need for replacement due to contact with either the ground, crop stalks, or field debris. The two parts identified for local manufacturing are the rice transplanter claw and combine harvester blade. Figure 2, Figure 3, and Figure 4 show the rice transplanter claw and combine harvester blades with basic dimensions. This work provides a framework for local agricultural machinery and spare parts manufacturers to produce rice transplanter claws and combine harvester blade given the skill-based, logistical, and economic constraints faced in Bangladesh. This is accomplished through a combination of manufacturing process analysis, cost analysis, and designing of the required tooling for the chosen manufacturing processes.

3
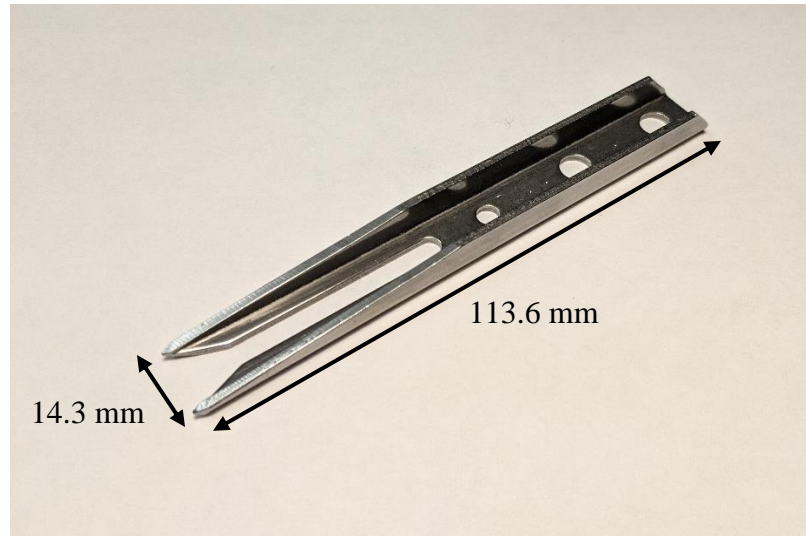
Figure 2: Original rice transplanter claw
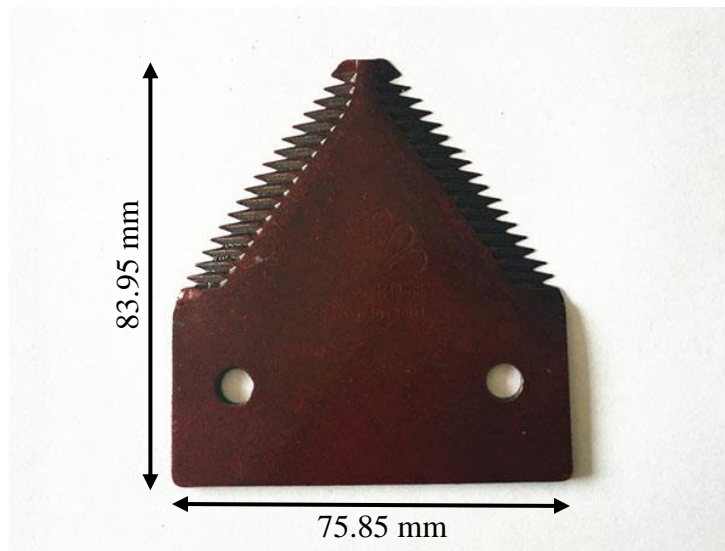
Figure 3: Full feed combine harvester blade
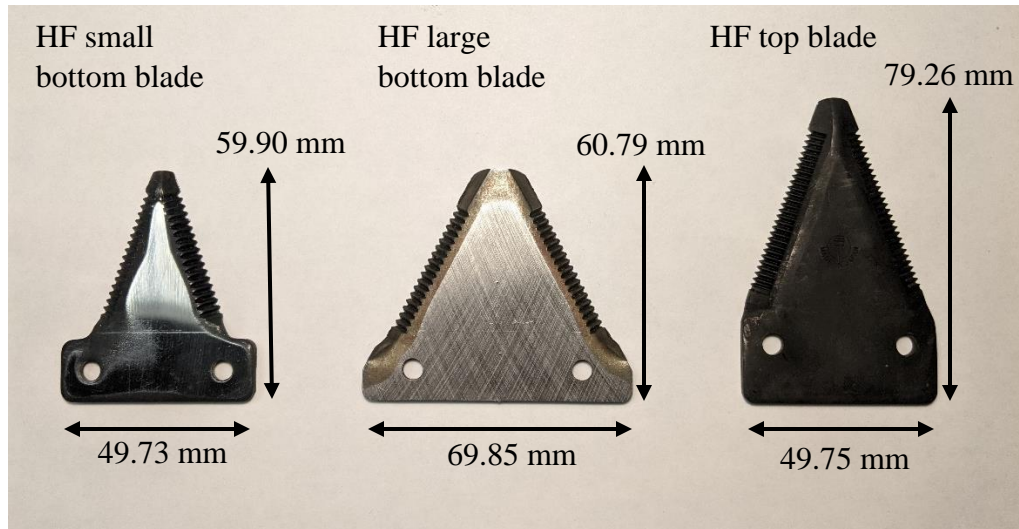
Figure 4: Half-feed combine harvester blades

1.3 Thesis Overview

This thesis is organized into four chapters: the introduction, development of rice transplanter claw manufacturing process, development of combine harvester blade manufacturing process, and conclusions and suggestions for future work. Chapter 1 provides background information on rice and wheat production in Bangladesh, agricultural mechanization, and the growth of Bangladesh agricultural spare parts market. Chapter 2 provides a comprehensive breakdown on the development of the rice transplanter claw manufacturing process through a combination of manufacturing process and cost analysis as well as designing and testing of the required tooling for the chosen manufacturing processes. Chapter 3 provides a breakdown of the development of the combine harvester blade manufacturing process using the same process as found in Chapter 2. Chapter 4 provides a conclusion summary for the thesis along with drawbacks of the thesis and plan for future work.

1.4 Chapter Summary

This chapter begins by discussing the dependence on manual labor for planting and harvesting, which has left farmers open to the effects of labor shortages and wage hikes brought on by a decreasing agricultural labor force. The support of agricultural mechanization and agricultural base light engineering workshops through a variety of machine shop and business training activities are then discussed.

The current state of the Bangladesh agricultural spare parts manufacturers, which consist of 70 foundries, 800 agricultural machinery manufacturers, and 1500 spare parts manufacturers, was presented alongside the rapid growth of the Bangladesh agricultural spare parts market over a period of 2004-2020. The potential for mechanization of planting and harvesting operations was discussed and the key spare parts for each operation, rice transplanter claws and combine harvester blades, were introduced. Finally, a thesis overview was provided.

The next chapter discusses the development of the rice transplanter claw manufacturing process.

CHAPTER 2

Development of Rice Seedling Transplanter Claw Manufacturing Process

2.1 Introduction

2.1.1 Rice Transplanter Operation

Rice seedlings are grown in a dense seedling mat as shown in Figure 5 (IRRI, 2014). The seedling mat resembles sod with a root structure and thin layer of soil. After growing to the desired height, the seedling mat is cut into smaller sections and placed onto the rear of the rice transplanter as shown in Figure 6. The rice transplanter planting arm, located at the bottom rear of the machine, rotates and plants the individual rice seedlings into the rice paddy as seen in the lower right of Figure 6. The preparation and transplanting of rice seedlings by a walk-behind rice transplanter is shown in the YouTube video by Discover Agriculture (2020).

Figure 5: Rice seedling mat

Figure 6: Rice transplanter in rice paddy field

Figure 7 shows the design schematic of the rice transplanter plating arm with planting claw/fork. The planting arm consists of two rotating planting claws/forks which cut the individual rice seedlings from the seedling mat and then plants the rice seedling

into the ground. The rotation of the planting arms is accomplished using a drive shaft,

cam, and push rods as shown in Figure 7 (Hoshino, 1974). Modern rice transplanters

have an additional part which sits inside the rice transplanter claw and pushes out the rice

seedling when the claw makes contact with the rice paddy. Figure 8 shows a Kubota rice

transplanter planting arm assembly (Kubota SPV6C, n.d.).
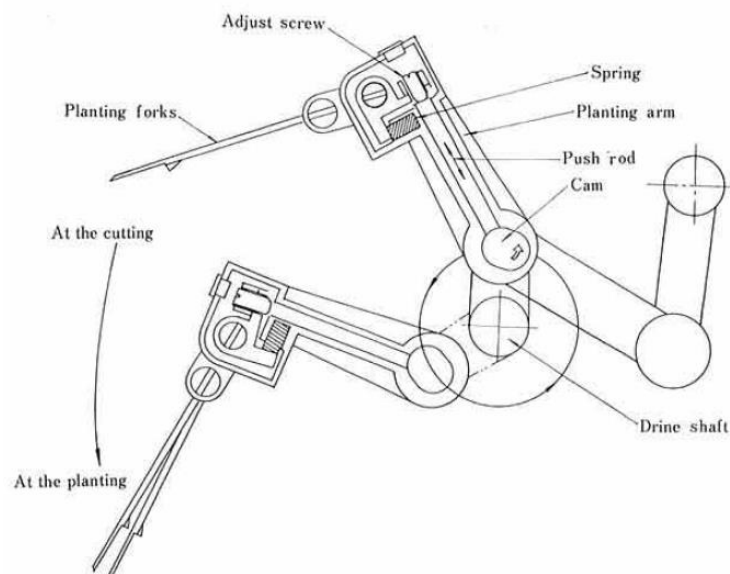
Figure 7: Rice transplanter planting arm schematic. Adapted [reprinted] from *Recent Advances on Rice Transplanter* (p. 210), by Seiji Hoshino, 1974, Japanese Agricultural Research Quarterly.
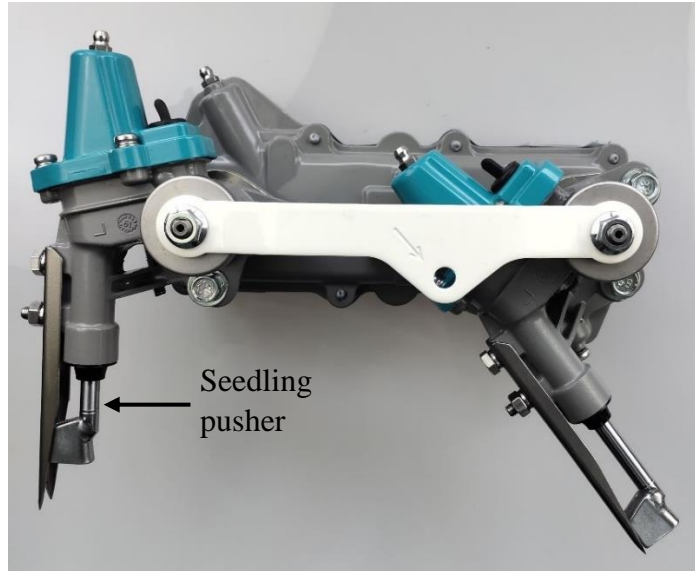
Figure 8: Kubota rice transplanter planting arm assembly

Figure 9 shows a rice transplanter claw mounted onto a rice transplanter planting arm assembly. The rice transplanter claw is mounted with two bolts through the back two mounting holes.
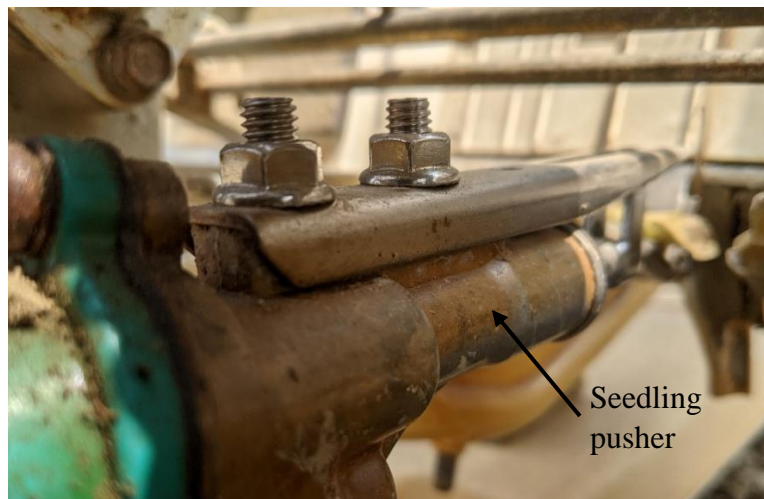
Figure 9: Rice transplanter claw mounted on planting arm assembly

2.1.2 Rice Transplanter Claw Manufacturing

The OEM rice seedling transplanter claws provided from the factory wear down

or break due to rapid and repeated contact with the rice seedling mat, rice field, and

debris within the rice paddy (rocks, etc.). Therefore, the need to manufacture spare rice

seedling transplanter claws has been identified as a requirement to continue the

mechanization of rice seedling transplanting. Multiple small machine shops within

Bangladesh have expressed interest in the manufacturing of the rice seedling transplanter

claws alongside the other agricultural spare parts that they currently manufacture.

However, due to the economic situation of many of these small machine shops, the

current domestic production of spare rice transplanter claws utilizes sand casting. The

iron used in the castings often comes from the dismantled decommissioned ships, which

are cut into pieces in various shipyard in the Chittagong region of Bangladesh. Therefore,

the specific elemental composition of the metal used in the castings is not known to any

degree of certainty. After the claws have been removed from the molds, the risers and

other imperfections are removed using bench and hand grinders. This method of

manufacturing results in the production of rice transplanter claws with unpredictable

mechanical properties such as hardness and tensile strength. Sand casting and the manual

grinding of the individual rice transplanter claws also result in large variations in product

dimensions that do not allow for adherence to any tolerance standards. Figure 10 shows

an example of a cast rice transplanter claw with an original claw for reference. The length

and width dimensions of the original rice transplanter claw are shown in Figure 2.
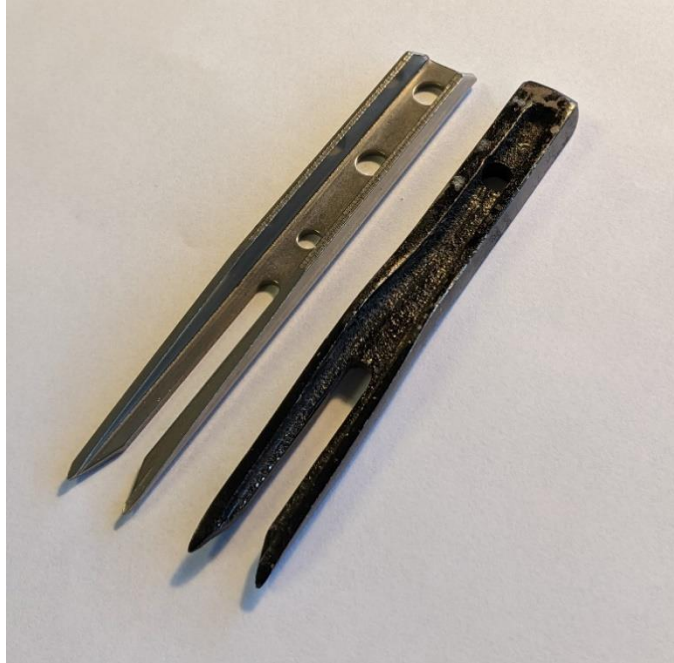
Figure 10: Original rice transplanter claw (left); sand cast rice transplanter claw (right)

The goal of the work reported in this chapter is to improve the quality of the rice transplanter claws manufactured by the small machine shops given both the economic and skill constraints within Bangladesh. The ability to manufacture these products will allow for the domestic production of high-quality rice transplanter claws reducing the need to import spare parts from the Chinese and Japanese markets. Domestic production of the spare parts will reduce lead times and headaches on both repair shops and farmers by eliminating the hassle of ordering and receiving long distance shipments of foreign manufactured rice transplanter claws. The addition of domestic products to the Bangladeshi markets will also result in the growth of the agricultural machinery manufacturing industry, which is one of the main goals of Bangladesh's agricultural mechanization policy (Ministry of Agriculture, 2020).

The work presented in this chapter incorporates the development of a rice transplanter claw manufacturing process that has been tailored to the conditions and machinery that are available in small machine shops in Bangladesh. The first section contains a survey of published literature, video media, and online marketplaces regarding the current rice transplanter spare parts market and the manufacturing of rice transplanter claws. The second section presents the manufacturing method selection, which explains the process taken to characterize the original rice transplanter claws, develop manufacturing process charts and cost analysis, and select the most appropriate manufacturing process for the agricultural spare parts manufacturers in Bangladesh. The third section contains the modeling, simulation, and experimentation used in the development of the blanking and bending die sets required to manufacture the rice transplanter claws. The fourth section presents the results found during characterization of the rice transplanter claws, experimental testing and FEM simulations. The validation of the FEM model is also presented in the fourth section.

2.2 Literature Review

A survey of literature, video media, online marketplaces, and the Bangladesh spare parts market was completed regarding the current rice transplanter claw spare parts market and the current manufacturing practices for producing rice transplanter claws. The survey of published literature revealed no published papers regarding the manufacturing of rice transplanter claws. The survey of video media did not identify any videos showing the current state of the rice transplanter claw manufacturing process. The survey of online marketplace such as Alibaba (alibaba.com) identified the rice transplanter spare parts

currently available. The survey of the Bangladesh spare parts market, by CSISA-MEA staff in Bangladesh, revealed the price of imported rice transplanter claw to be $2.15 per part. The goal of the work presented in this section is to review the published literature and online marketplace listings found during the literature review to develop an understanding of the operation of the rice transplanter planting arm and materials used in the rice transplanter claw spare parts market.

The survey of online marketplaces helped identify replacement rice transplanter claws manufactured in China. Common steel grades used in the manufacturing of rice transplanter claws is 45# steel with a hard chromium plating surface treatment (Qingdao, n.d.). The equivalent AISI grade for 45# steel is AISI 1045 (China 45 Steel, 2022). The hard chromium plating is applied to reduce friction, increase wear resistance, and increase surface hardness. Therefore, the rice transplanter claw has the advantages of heat-treated stainless steel without the increased cost of purchasing high quality hardened stainless steel.

The next section describes the characterization of the original rice transplanter claws using hardness and material composition testing as well as an analysis of the manufacturing markers on the OEM rice transplanter claws. Then, the development of the manufacturing process is presented through a combination of manufacturing morphological charts, production cost analysis, and market analysis.

2.3 Manufacturing Method Selection

2.3.1 Material Characterization

The process of developing a rice transplanter claw manufacturing process suitable for use

in Bangladesh started with the characterization of the OEM rice transplanter claw to best

determine the material qualities as well as to estimate the original manufacturing

processes as closely as possible. The first step in the characterization process was to

conduct hardness and x-ray fluorescence spectroscopy tests to determine the material

properties and composition of the metal used to produce the original rice transplanter

claws. The determination of the original material used by the OEM allowed material

recommendations to be provided to the CSISA-MEA partners in Bangladesh so that the

availability of such materials for the manufacturing of the spare parts in Bangladesh

could be determined. The results from the hardness testing of the original material

established an additional testing metric to determine if the stock materials available in

Bangladesh are suitable for manufacturing of the rice transplanter claws or if additional

materials must be imported. Characterization of the original rice transplanter claw

through hardness testing also established production quality checks for locally

manufactured parts.

 The first step taken to characterize the original and casted rice transplanter blades

was to determine the elemental composition using an x-ray fluorescence (XRF)

spectroscopy. The specific XRF used was the Niton FXL Field XRF manufactured by

Thermo Fisher Scientific, Waltham, Massachusetts (Niton™ FXL field X-ray lab, n.d.).

An XRF determines the elemental composition of a part by exciting electrons using x-ray

radiation. The radiation causes electrons in the outer rings of the atoms to jump down

energy levels and produce secondary x ray radiation. The specific wavelength of the

secondary x-ray radiation is determined and matched to the correct element. The

disadvantages of using this method for characterizing the elemental makeup of the rice

transplanter blades is the lack of the ability to determine the composition of elements

with an atomic number less than 11, which is sodium (Wirth & Barth, 2020). Therefore,

as the atomic number of Carbon is 6, the specific carbon content of the materials was not

able to be identified using XRF spectroscopy.

Wavelength dispersive XRF systems can be used to determine the percentage of

carbon in a properly prepared sample, however the system is not portable and is often

more expensive than standard an XRF (ARL™ OPTIM'X WDXRF Spectrometer, n.d.).

Optical emission spectroscopy (Spark OES) testing is a method of elemental analysis that

can determine the carbon percentage of metals by analyzing the vaporized atoms created

by an arc between the machine and the sample (Acuren, 2019). Spark OES systems are

portable and therefore are better suited for determining the elemental composition of

scrap material in Bangladesh.

Next, hardness testing was performed on both the cast and original rice

transplanter claws. This was performed using a Wilson Rockwell 874 hardness tester

manufactured by Buehler, Lake Bluff, Illinois (Buehler, n.d.). The hardness of the cast

and original rice transplanters was tested three times to obtain more data to identify the

specific materials for each part respectively. The average of the three Rockwell hardness

tests was calculated for each part and used as the final hardness value. The average

Rockwell hardness from the hardness tests were then used to estimate the tensile strength

of the original and sand casted rice transplanter claws. Three different methods of converting Rockwell hardness to tensile strength were used so that potential error in one estimation would not drastically affect the estimated tensile strength.

The first tensile strength estimate for the rice transplanter claws were determined by first converting the Rockwell hardness to Brinell hardness using ASTM E140-12B standard's Table 1 and Table 2 (pp. 3-5). Next, the ultimate tensile strength is determined by multiplying the Brinell hardness by a constant value as shown in Equation 1 (Callister, 2003, p.139).

$$\sigma_{UTS} \ (MPa) = \ 3.45 * H_{Brinell}$$

(1)

The second tensile strength estimate was determined by using a second order polynomial regression. The inputs of the second order polynomial are the Rockwell C and B hardness values, and the output of the polynomial is the estimated tensile strength. To determine the regression coefficients, Excel was used (Statology, 2020). The Rockwell hardness and tensile strength data found in Table A1, which can be found in Appendix A, were used as the input to the Excel function. Table A1 contains estimated tensile strengths for various Rockwell B and C harnesses, however gaps exist in the data (OnlineMetals, 2019). Therefore, a polynomial regression was performed on the data to allow for a continuous range of estimated tensile strengths. The third tensile strength estimation came directly from the ASTM A370-20 standard's Table 2 and Table 3, which list approximate tensile strengths based upon the Rockwell C and B scales respectively (pp.13-15). The results of all three estimate techniques were averaged to determine the final estimated tensile strength of the original and sand casted rice transplanter claws.

The estimated tensile strengths, along with the Rockwell hardness values, of the original and sand cast rice transplanter blades were determined so that an objective comparison could be made between them. The tensile strength and hardness of the original rice transplanter claw provide reference values to CSISA-MEA partners in Bangladesh so that the appropriate stock materials can be produced for local manufacturing. As proper channels of sourcing high quality stock materials currently do not exist in Bangladesh, these reference values will also provide manufacturers the ability to test their stock material, often sourced from ship breaking, as well as their final product for the correct hardness and tensile strength.

2.3.2 Manufacturing Method Selection

The manufacturing methods used by the original manufacturer were evaluated through characterization of various manufacturing marks on the claws. This was performed to 'reverse engineer' the manufacturing process so it could then be adjusted based on the various constraints of the small manufacturers in Bangladesh. After this was completed, a morphological chart of possible manufacturing methods for each product feature was created ranging from the least to most needed capital investment. Various manufacturing methods were eliminated from the morphological chart based upon their feasibility within Bangladesh as well as by evaluation using basic economic analysis. Collaboration with colleagues in Bangladesh also provided advice on the tooling and machinery available in the local machine shops as well as the amount of capital owners were willing to invest in the creation of a new product line. A cost analysis including machinery, labor, and material costs was then completed to evaluate the remaining

manufacturing processes and determine the most appropriate manufacturing model. The tooling required was developed using design references, FEA analysis, and experimental testing. After the completion of the experimental testing, process flow diagrams were created for the chosen manufacturing method and adjusted based on feedback from partners in Bangladesh. Finally. a factory layout analysis was performed to find the safest and most efficient layout of the stock material and required machinery.

The first step in creating the optimal manufacturing process for production in Bangladesh was to determine the possible manufacturing methods used by the OEM through the identification of various marks created during the manufacturing process. The initial step in determining the original manufacturing process was to identify the features of the rice transplanter claw. Figure 11 shows a top view of the rice transplanter claw with reference dimensions and labels for the left and right side of the claws. Figure 12 shows the original claw with the following features identified: general shape, bend, slot, mounting holes, and the slope toward the front of the claw. The general shape of the claw is defined as the shape of the rice transplanter claw before the operations which create the bend, slot, mounting holes, and slope (i.e., rice transplanter claw blank).
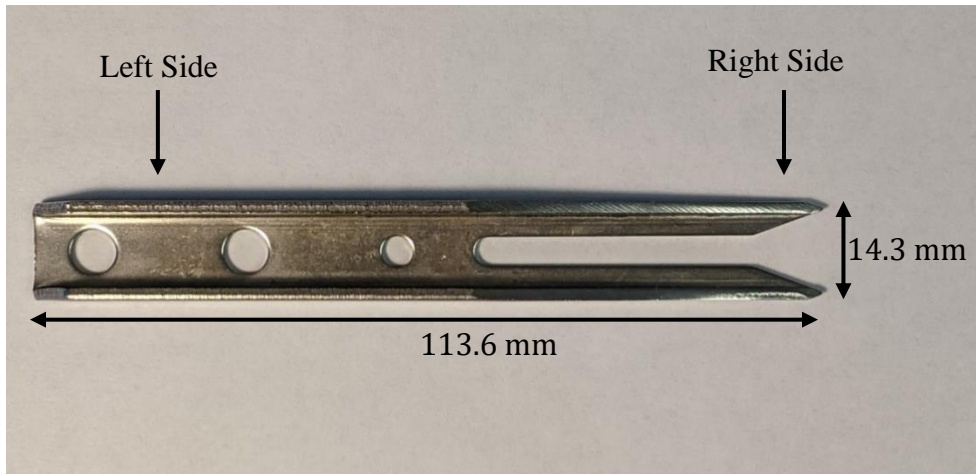
Figure 11: Original rice transplanter claw with basic size dimensions
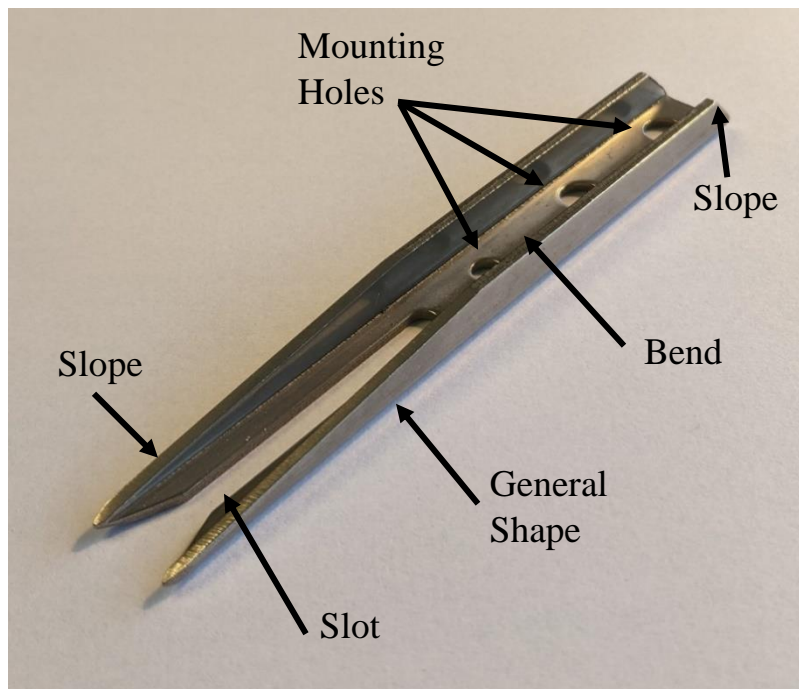
Figure 12: Original rice transplanter claw with labeled features

Visual analysis of the original rice transplanter blades led to the discovery of multiple witness marks, which led to the determination that the general shape, mounting holes, and slot were created using a blanking/piercing operation. Figure 13, Figure 14, and Figure 15 show the witness marks on the outside edge, mounting holes, and slot. The

slope on the front of the claw shows a distinct pattern of grinding on the top, side, and

underside of the front of the claw, which is shown in Figure 15.
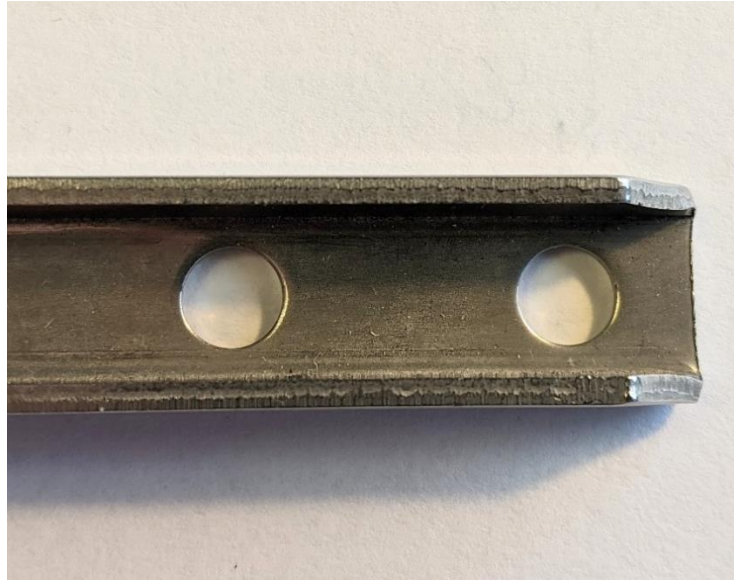
Figure 13: Blanking witness marks on outside edge of original rice transplanter claw

Figure 14: Piercing witness marks on inside of mounting holes
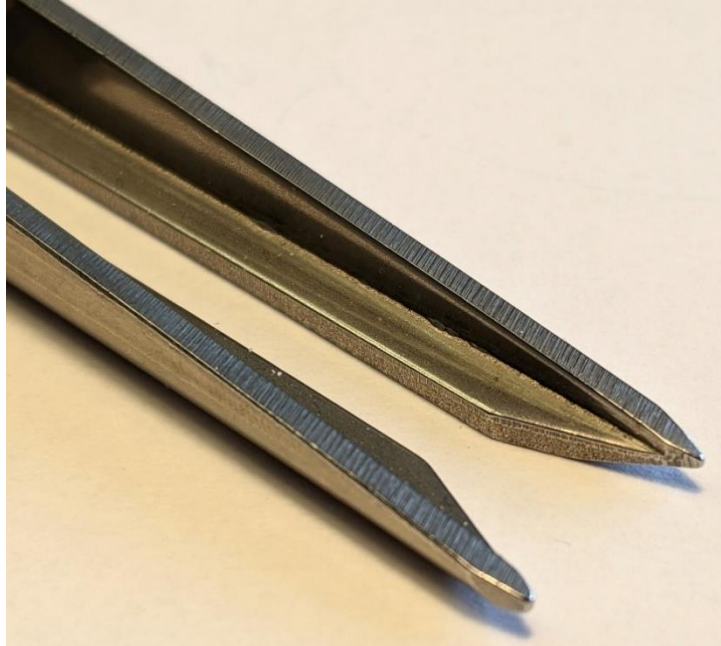
Figure 15: Witness marks from piercing of slot and grinding marking on slope
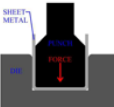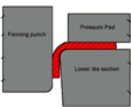
On the sides of the claw a strip along the length of the part through the middle of the claw is distinctively more polished than the rest of the side of the material. Figure 16 shows this area, which is believed to be created during a rolling operation used to produce the main bend of the part.

Figure 16: Rice transplanter claw side view showing the metal finish difference along the center

After the initial characterization of the rice transplanter claws, a morphological chart of possible manufacturing techniques was developed (Boeijen et al., 2020). The morphological chart shown in Table 2 is a proposed list of manufacturing methods based upon the inspection of the rice transplanter claw manufacturing markers as well as additional possible manufacturing methods. Morphological charts traditionally are used for idea generation by listing the product functions on the left most column and possible solutions across the rows. However, the morphological chart shown in Table 2 lists the product features in the left column and possible manufacturing processes in columns to the right.

Table 2: Morphological chart of rice transplanter claw manufacturing processes

Feature	Solution #1	Solution #2	Solution #3
General Shape	Blanking	Shears	
Bend	Bending Die	Gooseneck	Wiping Die
Mounting Holes	Drilling	Blanking	Piercing
Slot	Grinding	Blanking	Piercing
Slope	Grinding	Blanking	

Once the morphological chart was finalized, three manufacturing processes were established and categorized as low, medium, and high relative to their volume of production. The low-, medium-, and high-volume manufacturing processes are shown in Table 2.

Table 3: Rice transplanter claw manufacturing processes by production volume

Features / Manufacturing Processes	Low Volume	Medium Volume	High Volume
General Shape	Shears	Blanking	Blanking
Bend	Bending Die/Press Brake	Bending Die/Press Brake	Bending Die/Press Brake
Mounting Holes	Drilling	Drilling	Piercing
Slot	Grinding	Grinding	Piercing
Slope	Grinding	Grinding	Grinding

Low volume production, shown in the second column, utilizes manual labor the most and requires the least initial capital investment of the three manufacturing processes. The lower initial cost of the low-volume manufacturing process is attributable to differences between the low-volume and medium- and high-volume approaches. The main difference is the production of the general shape of the blanks using shears/grinder instead of a blanking die set, which removes the need for a blanking die set and reduces the initial cost when compared to the medium and high-volume production. The bend of the rice transplanter claw is created using either a bending die set in a forge or hydraulic press or a press brake depending on the manufacturer's preference and current machinery. The use of a drilling machine and angle grinder to create the mounting holes

and slot further reduces the initial cost over the high-volume approach, which utilizes piercing to create these features. This category of production is most like the current model of production in the majority of the machine shops in Bangladesh. Though the low-volume production method has the lowest initial cost of investment, the reliance on manual labor contributes to the fact that this option has the lowest product quality as the effects of human error is amplified in the creation of the blanks and slots.

The medium-volume approach improves the efficiency of operations by using a punch and die set to accomplish the blanking operation while maintaining the same manufacturing process for the bend, mounting holes, slot, and slope. The adoption of the blanking operation significantly increases the initial capital investment due to the manufacturing of an additional punch and die set. However, the addition of a punch and die set for the blanking operation increases the product quality and the production volume of the blanks. The increase in blank quality saves time which, if the low-volume approach were adopted, would be otherwise spent inspecting a larger number of blanks to determine if the specified tolerances were met. The dimensions of the blank must be within the specified tolerances to properly fit within the bending die. These improvements in blank quality and production rate potentially offset much of the higher initial cost incurred from the fabrication of the blanking punch and die set.

The high-volume approach utilizes piercing operations to create the mounting holes and slot instead of the drilling and grinding operations used in the low/medium volume approach. Utilizing a punch mounted on a press instead of using a drill press and grinder increases the production rate while also increases the product quality by removing human error in the grinding of the slot. However, the use of piercing operations requires

the machining of an additional punch and die set for the slot and the purchasing of appropriate punches for the piercing of the mounting holes. These additional costs further increase the initial cost of the high-volume manufacturing process when compared to the low- and medium-volume approaches. Along with the extra punches that require machining and their purchase, the addition of two piercing operations increases the number of operations that require a mechanical press thereby requiring the machine shops to either invest in additional presses or to swap punch and die sets more frequently. Due to these factors, the high-volume approach further increases the required capital investment to purchase machinery and develop punch and die sets over that of the low- and medium-volume approaches.

Process charts, factory layouts, and cost analysis were created for the low-, medium-, and high-volume manufacturing processes so that the economic differences of the processes could be studied quantitatively. Figure 17 shows a potential factory layout for the low-volume manufacturing process. The numbers associated with each machine tool indicate the number of workers in each area. The number of workers at each area was kept at one for all low-, medium-, and high-volume manufacturing processes as the production rate $[\frac{parts}{minute}]$ of each manufacturing process is determined by dividing the time taken for the slowest operation of the manufacturing process by the number of workers performing the operation. For example, if a drilling operation takes 2 minutes to complete, a single operator is expected to complete $0.5 \frac{parts}{minute}$ while two operators (on separate drill presses) would be expected to complete $1 \frac{parts}{minute}$. Therefore, the number of

workers at each area is set to one so that an objective comparison of the low-, medium-,

and high-volume manufacturing processes can be made.
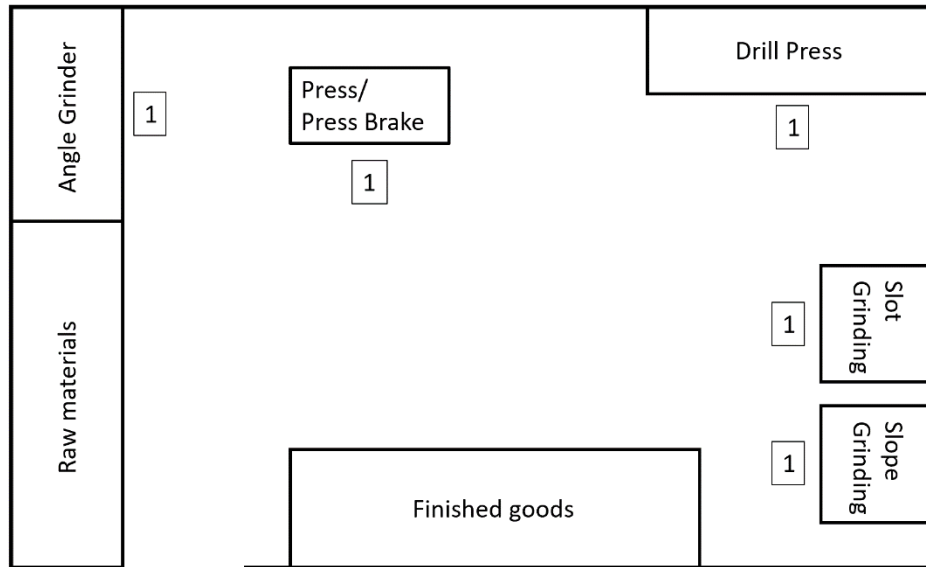
Figure 17: Proposed factory layout for low-volume production of rice transplanter claws

The process flow chart, shown in Figure 18 displays the steps of the low-volume

rice transplanter claw manufacturing process. A description of each activity is provided

on the left side of the process chart. The two columns to the right of the activity

description show the time required to complete the activity and the distance traveled for

each activity. The distances are intentionally left blank in Figure 18 as the layouts of the

individual factories are not known. Next, each activity is identified as either an operation,

transport, inspection, delay, or storage by placing an "X" under the specified column. The

total time for each activity type is summed under each column. Finally, each activity is

classified as either value added (VA) or non-value added (NVA). Operation and

inspection activities are value added while transport, delay, and storage activities are non-

value added. The number and time of all VA and NVA operations are shown at the bottom of the chart.

Step #	Activity description	Time (minutes)	Distance (meters)	Operation O	Transport ⇒	Inspection □	Delay D	Storage V	Value Category
1	Metal stored in storage							X	NVA
2	Move metal to cutting tools	2			X				NVA
3	Cut metal to form blanks	2		X					VA
4	Move metal strips to mechanical press	0.25			X				NVA
5	Bend blanks using mechanical press	0.1		X					VA
6	Inspect bends	0.1				X			VA
7	Move pickup forks to drill	0.25			X				NVA
8	Setup drill machine	2					X		NVA
9	Create holes using drill	1		X					VA
10	Move pickup forks to grinder	0.25			X				NVA
11	Create slot using grinder	0.75		X					VA
12	Grind down pickup forks	0.5		X					VA
13	Inspect pickup fork	0.15					X		NVA
14	Store finished part	0.25						X	NVA
	Count:			5	4	1	2	2	
	Time per process step:			4.35	2.75	0.1	2.15	0.25	

Total VA	6		Total NVA	8		Total ENVA	0
VA Time	4.45	Minutes	NVA Time	5.15	Minutes	ENVA Time	0
Distance traveled	0	Meters	Lead Time	10	Minutes	VS Ratio	46.354%

Figure 18: Process chart for low-volume manufacturing process utilizing mechanical press

Finally, a cost analysis was performed on the low-volume production method to determine the selling price of the rice transplanter claws so that the initial equipment costs are recouped in 18 months of operation. It is assumed that a loan for the entire cost of the machinery is borrowed by the spare parts manufacturers with a length of 18 months and an interest rate of 9%. Payments for the loan are made monthly. The loan length, interest rates, and payment plan are the standard for loans provide to ABLEs in Bangladesh. The loan information was provided by CSISA-MEA staff in Bangladesh. Table 3 shows the cost analysis breakdown for the proposed low-volume production factory. The first step in determining the selling price was to determine the cost of the initial capital investment for machinery. Equipment prices were determined through

online sellers within Bangladesh as well as from listings on indiamart.com because prices

of larger machinery are difficult to determine within Bangladesh due to import duties and

other regulations. Table B1 in Appendix B lists the individual machinery costs and links

for purchasing. The base machinery costs then are determined for both the press break

and mechanical press processes. Next, the total machinery costs were determined by

calculating the monthly loan payments and multiplying by the length of the loan.

Equation 2 displays the equation for determining the total machinery cost.

$$Total\ Machinery\ Cost = 18 \cdot Base\ Machinery\ Cost \cdot \left[\frac{0.09(1 + 0.09)^{18}}{(1 + 0.09)^{18} - 1}\right]$$

(2)

Next, the wage rates for the factory are calculated using an hourly wage for one

employee. The hourly wages for a factory worker in the agricultural spare parts industry

were established by converting and averaging the daily and monthly wages of medium

skilled workers throughout three cities in Bangladesh. Worker's salary data were

obtained through contact between members of the CSISA-MEA project in Bangladesh

and individual factory managers. Material cost per part was then determined by

multiplying the price of stainless steel per kg by the weight of a single blank. The parts

produced per minute were estimated by determining the parts per minute for the slowest

operation within the manufacturing process. As shown in the low-volume process control

chart in Figure 18 the operation which requires the longest time is the cutting of the

blanks by the angle grinder at 2 minutes per operation. Therefore, the parts per minute for

the low-volume manufacturing process is $\frac{1}{2}$ or 0.5 parts per minute. Finally, the cost per

part is determined using Equation 3.

$$\frac{Total\ Machinery\ Cost\ +\ 1.5\ [yr] \cdot \left[\frac{Parts}{yr} \cdot \frac{Material\ cost}{part} \cdot (1 - Downtime[\%]) + \frac{Wages}{yr}\right]}{\left[\frac{Parts}{yr}\right] \cdot 1.5\ [yr] \cdot (1 - Downtime[\%])}$$

(3)

The yearly material and wage costs as well as the yearly production are established by converting from a per minute or hourly basis to a yearly basis using the 2400 working hours per year. The working hours per year is based on a 6-day work week with 8 working hours per day, which is the standard work week in Bangladesh. A production line downtime of 20% is set for machine tool failures, maintenance, power outages and other events which result in production line being nonoperational. The results from the low volume cost analysis are shown in Table 4. The cost per with no loan part refers to the cost per part if no money is borrowed by the spare parts manufacturer. The loan cost per parts refers to the cost per part if all the money for the machinery is borrowed through an 18-month loan with a 9% interest rate. The cost per part required to recoup the loaned amount in 18 months is $0.39 for a mechanical press and $0.57 for a press brake used for the bending operation. If the spare parts manufacturer purchases the machinery without a loan the cost per part required to recoup the initial investment in 18 months is $0.36 for a mechanical press and $0.45 for a press brake.

Table 4: Low-volume manufacturing process cost analysis

Manufacturing Method:	Low Volume	
Equipment Costs		
Feature	Equipment	Price [USD]
General Shape	Angle grinder	43
Bend	Mechanical press	1300
	Bending punch/die set	450
	Press brake	9,178
	Press brake punch/die set	375
Mounting Holes	Drill press	140
Slot	Angle grinder	43
Slope	Bench grinder	72
	Base Cost (mechanical press)	2048
	Base Cost (press brake)	9,851
	Total Cost (mechanical press)	4210
	Total Cost (press brake)	20252
Labor Costs		
	# of workers	5
	Hourly rate	0.84
	Total wages per hour	4.20
Material Costs		
	Stainless steel per kg	3.77
	Material cost per part	0.17
Manufacturing Time Analysis		
	Parts per minute	0.50
	Parts produced per day	192
Cost per part		
	Hours per year	2400
	Payback period [yr]	1.5
	Downtime	20%
	Process cost per part (no loan - mechanical press)	0.36
	Process cost per part (no loan - press brake)	0.45
	Process cost per part (loan - mechanical press)	0.39
	Process cost per part (loan - press brake)	0.57

Factory layouts, process charts, and cost analysis were also created for the

medium- and high-volume manufacturing processes. Figure 19 and Figure 20 show the

factory layout and process chart for the medium-volume production process. The factory

layout and process charts have been modified to reflect the additional mechanical press

used in the blanking operation.
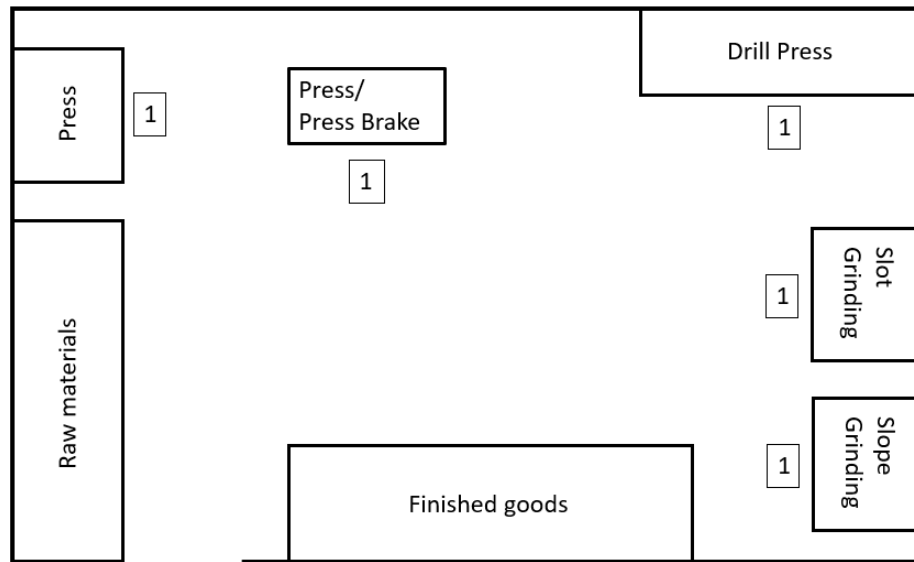
Figure 19: Proposed factory layout for medium-volume production of rice transplanter claws

Step #	Activity description	Time (minutes)	Distance (meters)	Operation O	Transport ⇨	Inspection ☐	Delay D	Storage V	Value Category
1	Metal stored in storage							X	NVA
2	Move metal to cutting tools	2			X				NVA
3	Cut metal to size to fit in blanking die	0.5		X					VA
4	Move metal strips to press	0.25			X				NVA
5	Create blanks using press	0.1		X					VA
6	Inspect blanks	0.1				X			VA
7	Store blanks	0.1						X	NVA
8	Move blanks to bending press/press brake	0.25			X				NVA
9	Bend Blanks	0.1		X					VA
10	Inspect bends	0.1				X			VA
11	Move pickup forks to drill	0.25			X				NVA
12	Setup drill machine	2					X		NVA
13	Create holes using drill	1		X					VA
14	Move pickup forks to grinder	0.25			X				NVA
15	Create slot using grinder	0.75		X					VA
16	Grind down pickup forks	0.5		X					VA
17	Inspect pickup fork	0.15					X		NVA
18	Store finished part	0.25						X	NVA
	Count:			6	5	2	2	3	
	Time per process step:			2.95	3	0.2	2.15	0.35	

Total VA	8		Total NVA	10		Total ENVA	0
VA Time	3.15	Minutes	NVA Time	5.5	Minutes	ENVA Time	0
Distance traveled	0	Meters	Lead Time	9	Minutes	VS Ratio	36.416%

Figure 20: Process chart for medium-volume manufacturing process utilizing mechanical press

Table 5 shows the cost analysis for medium-volume production process. As shown in the bottom of the far-right column, the cost per part with a loan to recoup the initial investment in 18 months is $0.28 for the mechanical press and $0.39 for the press brake. Relative to the low-volume process, the medium-volume production process reduces the cost per part by an average of $0.15 while doubling the number of parts produced. The reduction in production cost per part is due to the increased rate of production from 0.5 parts per minute to 1 part per minute. The addition of the blanking process eliminates the fabrication of the blanks as the slowest operation. Therefore, the slowest operation of the medium-volume production process is the drilling of the three mounting holes, which has a time of one minute per part.

Table 5: Medium-volume manufacturing process cost analysis

Manufacturing Method:	Medium Volume	
Equipment Costs		
Feature	Equipment	Price [USD]
General Shape	Mechanical press	1300
	Blanking punch/die set	540
Bend	Bending punch/die set	450
	Press brake	9,178
	Press brake punch/die set	375
Mounting Holes	Drill press	140
Slot	Grinder	43
Slope	Bench grinder	72
	Base price (mechanical press)	3845
	Base price (press brake)	11,648
	Total Cost (mechanical press)	5232
	Total Cost (press brake)	22836
Labor Costs		
	# of workers	5
	Hourly rate per worker [USD]	0.84
	Total wages per hour	4.20
Material Costs		
	Stainless steel per kg	3.77
	Material cost per part	0.17
Manufacturing Time Analysis		
	Parts per minute	1
	Parts produced per day	384
Cost per part		
	Hours per year	2400
	Payback period [yrs.]	1.5
	Downtime	20%
	Process Cost per part (Mechanical Press)	0.28
	Process Cost per part (Press Brake)	0.32
	Process cost per part (mechanical press)	0.28
	Process cost per part (press brake)	0.39

Figure 21 and Figure 22 display the example factory layout and process charts for

the high-volume manufacturing process. The factory layout in Figure 21 shows the three

additional presses used to fabricate the mounting holes and slot in replacement of the drill press and angle grinder. Due to these additions, the high-volume production process requires a minimum of six workers instead of the five required in the low- and medium-volume production processes.
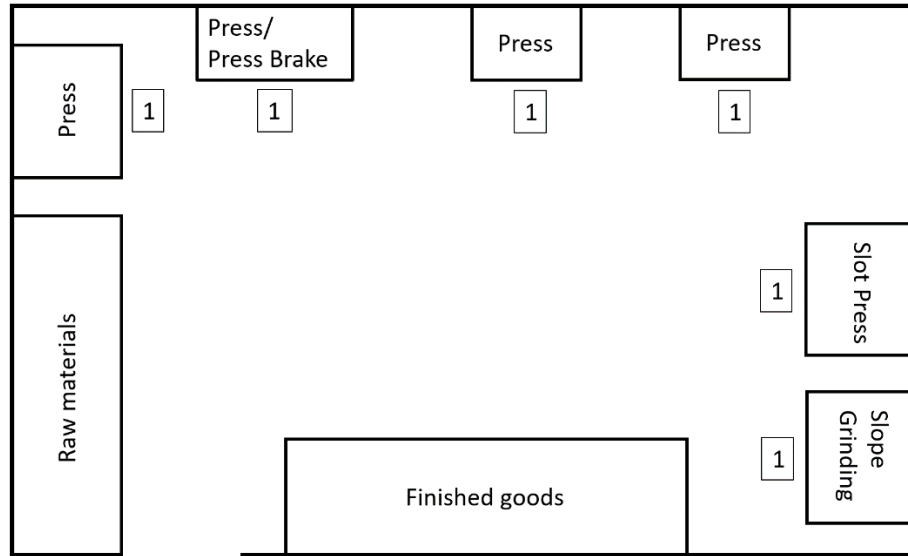
Figure 21: Proposed factory layout for high-volume production of rice transplanter claws

Step #	Activity description	Time (minutes)	Distance (meters)	Operation O	Transport ⇨	Inspection ☐	Delay D	Storage V	Value Category
1	Metal stored in storage							X	NVA
2	Move metal to cutting tools	2			X				NVA
3	Cut metal to size to fit in blanking die	0.5		X					VA
4	Move metal strips to press	0.25			X				NVA
5	Create blanks using press	0.1		X					VA
6	Inspect blanks	0.1				X			VA
7	Store blanks	0.1						X	NVA
8	Move blanks to bending press/press brake	0.25			X				NVA
9	Bend Blanks	0.1		X					VA
10	Inspect bends	0.1				X			VA
11	Move pickup forks to piercing press	0.25			X				NVA
12	Pierce holes using press	0.25		X					VA
13	Move pickup forks to slot press	0.25			X				NVA
14	Create slot using press	0.1		X					VA
15	Move pickup forks to grinder	0.25			X				NVA
16	Grind down pickup forks	0.5		X					VA
17	Inspect pickup fork	0.15					X		NVA
18	Store finished part	0.25						X	NVA
	Count:			6	6	2	1	3	
	Time per process step:			1.55	3.25	0.2	0.15	0.35	
	Total VA	8			Total NVA	10		Total ENVA	0
	VA Time	1.75	Minutes		NVA Time	3.75	Minutes	ENVA Time	0

Figure 22: Process chart for high-volume manufacturing process utilizing mechanical press

Table 4 displays the cost analysis for the high-volume manufacturing process. The production cost of producing the rice transplanter claws with a loan is $0.22 for the mechanical press and $0.24 for the press brake for the bending operation. This represents an average reduction in cost per part of $0.25 from the low-volume production method and $0.11 for the medium-volume production method. The production rate is increased to four parts per minute due to the fabrication of the mounting holes and slot with mechanical presses as opposed to the drilling and grinding operations used in the low- and medium-volume manufacturing processes.

Table 6: High-volume manufacturing process cost analysis

Manufacturing Method:	High Volume	
Equipment Costs		
Feature	Equipment	Price [USD]
General Shape	Mechanical press	1300
	Blanking punch/die set	540
Bend	Mechanical press	1300
	Bending punch/die set	450
	Press brake	9,178
	Press brake punch/die set	375
Mounting Holes	Mechanical press (2X)	1300
	Piercing punches (2X)	64
Slot	Mechanical press	1300
	Slot punch/die set	45
Slope	Bench grinder	72
	Base price (mechanical press)	7735
	Base price (press brake)	15,538
	Total Cost (mechanical press)	15901
	Total Cost (press brake)	31943
Labor Costs		
	# of workers	7
	Hourly rate per worker [USD]	0.84
	Total wages per hour	5.88
Material Costs		
	Stainless steel per kg	3.77
	Material cost per part	0.17
Manufacturing Time Analysis		
	Parts per minute	4
	Parts produced per day	1536
Cost per part		
	Hours per year	2400
	Payback period [yrs.]	1.5
	Downtime	20%
	Process cost per part (mechanical press)	0.21
	Process cost per part (press brake)	0.22
	Process cost per part (mechanical press)	0.22
	Process cost per part (press brake)	0.24

Table 7 lists the cost per part for the low-, medium-, and high-volume manufacturing processes along with the current dealer sales price for the imported rice transplanter claws. If it assumed that the dealer applies a 200% mark up on the sales price, the cost per part of the low, medium, and high-volume manufacturing processes are low enough so that the spare parts manufacturers make a profit from selling to the local spare parts dealers. Therefore, based upon the cost per part presented for the low-, medium-, and high-volume manufacturing processes, the manufacturing of spare rice transplanter claws by spare parts manufacturers in Bangladesh is economically viable.

Table 7: Comparison of cost of manufacturing versus dealer sales price

| Part | Manufacturing Methods | Cost per part (USD) | | | |
		Low volume	Medium volume	High volume	Dealer
Rice transplanter claw	Mechanical press	0.39	0.28	0.22	2.15
	Press brake	0.57	0.39	0.24	

The low-, medium-, and high-volume production process cost analyses show that as the rate of production increases the cost per part required to recoup the initial investment decreases despite the increase in the initial cost of the machinery. However, increasing a machine shop's rate of production is not as easy as reviewing a simple cost analysis and choosing the most efficient option. Factors such as the market demand, shop floor size, and the level of initial capital investment required must be considered when determining the appropriate manufacturing process for spare parts manufacturers in Bangladesh. Table 8 displays the machinery cost, cost per part, and production rate for the low-, medium-, and high-volume manufacturing methods.

Table 8: Total machinery cost and cost per part for low-, medium-, and high-volume rice transplanter claw manufacturing (interest included)

	Manufacturing Method	Low Volume	Medium Volume	High Volume
Machinery cost (USD)	Mechanical press	4210	5232	15901
	Press brake	20252	22836	31943
Cost per part (USD)	Mechanical press	0.39	0.28	0.22
	Press brake	0.57	0.39	0.24
Production rate $\frac{parts}{day}$		192	384	1536

As of 2021, an estimated 754 rice transplanters are in operation throughout Bangladesh (Alam, 2022). Interviews with farmers by CSISA-MEA project partners in Bangladesh have indicated that the most common rice transplanter in Bangladesh is a 4-row walk-behind transplanter. As rice transplanters have two claws per row the average number of claws per rice transplanter is estimated to be eight. Therefore, if it is assumed that all rice transplanter claws are replaced once per rice season, or three times per year, the current market size for rice transplanter claws per year can be estimated to be 18,096 as shown in Equation 4.

$$\frac{\text{Market Size}}{\text{yr.}} = 754 \text{ RT} \cdot 8 \frac{\text{claws}}{\text{RT}} \cdot 3 \frac{\text{replacement}}{\text{yr.}} = 18,096 \frac{\text{claws}}{\text{yr.}}$$

(4)

Table 9 shows the daily and yearly production rates for the low-, medium-, and high-production volume rice transplanter claw manufacturing processes. The yearly production rate is based on an 8-hour 6-day work week which equations to 2400 hours/300 days per year. This is the standard work week for the spare parts manufacturers in Bangladesh. The yearly production of the low volume manufacturing process is estimated to be approximately three times the current estimated market size. Therefore, it is recommended that the low-volume manufacturing process be implemented to produce

40

rice transplanter claws in Bangladesh for the Bangladesh market. The yearly production

of the medium- and high-volume manufacturing process is approximately six and twenty-

six times the current estimated market size within Bangladesh. Therefore, the

implementation of the medium- or high-volume manufacturing process is only

recommended if the rice transplanter claws are to be exported in large quantities.

Table 9: Daily and yearly production rates for low-, medium-, and high-volume rice transplanter claw manufacturing processes

Process	Low Volume	Medium Volume	High Volume
Daily Production Rate $\frac{parts}{day}$	192	384	1536
Yearly Production Rate $\frac{parts}{yr}$	57,600	115,200	460,800

A sensitivity analysis of the effect of batch size on part cost was completed using

the part cost estimator in Ansys Granta EduPack 2021 published by Ansys, Inc.

(Canonsburg, Pennsylvania). Figure 23 shows the part cost estimate as a function of

batch size from one hundred parts to one million parts for a primary process of closed die

forging and secondary process of press forming operation on annealed 304 stainless steel,

the proposed material for local manufacturing of rice transplanter claws. 304 stainless

steel was used due to its availability in Bangladesh (Inspira, 2022). The part length and

mass were set to 0.377 ft. and 0.0777 lb. respectively. The part complexities of the first

and second operation were set to simple and standard. The load factor was set to 50% and

the overhead rate was set to 4.20 $\frac{USD}{hr}$ for the medium-volume manufacturing process. The

remaining parameters of the rice transplanter part cost estimator can be found in Table B1

in Appendix B.

The part cost follows an exponential decay as the batch size increases. The current yearly demand of 18,096 rice transplanter claws corresponds to a part cost of approximately $0.23. As shown in Figure 23, a batch size of 10,000 to 1,000,000 is needed to maintain a low part cost over a large range of batch sizes. However, as the batch size decreases below 10,000 parts, a sharp increase in cost per part can be seen. A decrease in batch size results in a smaller number of parts to spread the fixed costs over, therefore the cost per part will increase relatively to a larger batch size. In Equation 3, the fixed costs are the cost of machinery and labor costs and do not change relative to the production rate. At the current market size of 18,096 rice transplanter claws per year, the cost per part is expected to not be very sensitive to small fluctuations in batch size as an increase of decrease of 10,000 parts per year corresponds to a cost per part of $0.21 and $0.25 respectively.
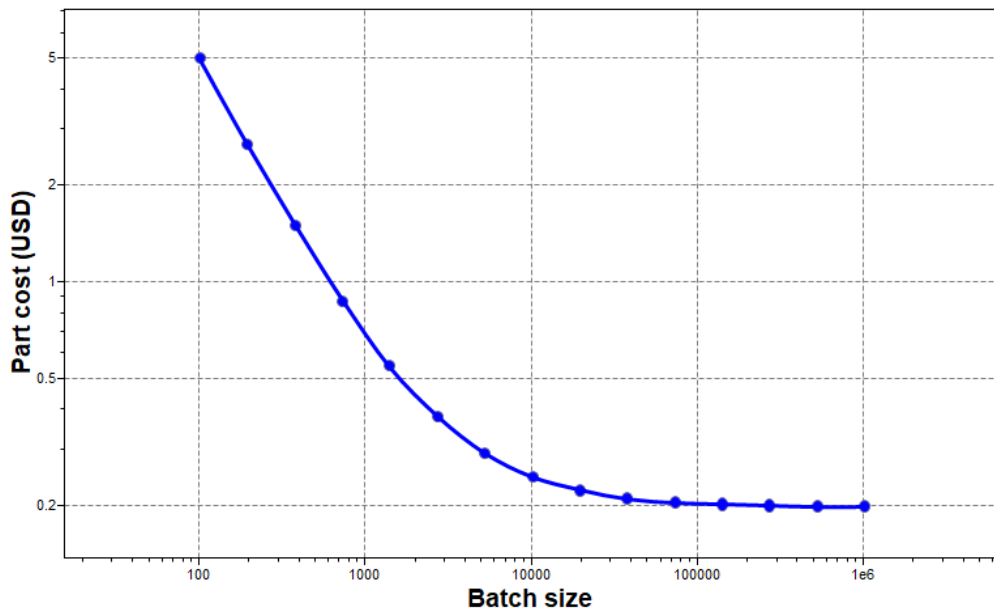
Figure 23: Part cost versus batch size for closed die forging and press forming operations

2.3.3 Section Review

The Manufacturing Method Selection section of Chapter 2 consists of two

separate subsections: material characterization and manufacturing method selection. The

material characterization section provides an overview of the XRF material composition

testing and Rockwell hardness tests performed on the original and locally produced rice

transplanter claws. Next, the original rice transplanter claws were inspected for

manufacturing markers such as the grinding pattern shown along the slope of the blade in

Figure 15. Next, in the manufacturing method selection section, a list of possible

manufacturing methods for each feature of the rice transplanter claw is presented. Three

manufacturing processes were then chosen based on low, medium, and high volumes of

production. Factory layouts, process charts, and cost analysis are then presented for the

three manufacturing processes. The results of the cost analysis determined that the cost

per part of the low-, medium-, and high-volume manufacturing processes are between

$0.22 and $0.57 as shown in Table 7. The dealer sale price of the spare rice transplanter

claws was found to be $2.15, therefore the manufacturing of spare rice transplanter claws

in Bangladesh is economically viable assuming a 200% markup by the dealers. Next, a

market size analysis of the rice transplanter claw spare parts market is performed based

upon the number of operational rice transplanters in Bangladesh. The three

manufacturing processes then are compared to the estimated market size and the low

volume manufacturing process was determined as the recommended method for locally

producing rice transplanter claws based upon the current estimated market size. Finally, a

sensitivity analysis was performed using the Granta EduPack part cost estimator. The

results of the part cost estimator revealed that the cost per part is not sensitive to changes

in market size under $10{,}000\ \frac{parts}{yr.}$.

The next section presents the design of the blanking and bending punch and die

sets for the rice transplanter claw manufacturing process. The calculation for the

maximum force and die angle of the press brake die are also shown in the next section.

2.4 Design of Required Tooling

2.4.1 Development of Rice Transplanter CAD Model

The design of the tooling began with the modeling of original the rice transplanter

claw in SolidWorks 2020 published by Dassault Systemes (Velizy-Villacoublay, France).

Before any CAD modeling of the claw was started, length, width, height, and thickness

measurements were taken at locations along three original rice transplanter claws using

an electronic caliper and micrometer with 0.01 mm resolution. The measurements across

the three rice transplanter claws were then averaged. The dimensions of the original rice

transplanter claw are shown in Table 10.

Table 10: Original rice transplanter claw dimensions

Dimension	Measurement (mm)
Overall Length	113.60
Overall Width	14.30
Overall Height	8.52
Thickness	1.80
Large Hole Diameter	6.50
Small Hole Diameter	4.50
Slot Width	4.22

The measurements listed in Table 10 as well as additional measurements were used to create a SolidWorks model of the rice transplanter claw. The SolidWorks model of the claw is shown in Figure 24.

Figure 24: SolidWorks rendering of rice transplanter claw

2.4.2 Design Theory for Blanking and Bending Punch and Die Sets

Once the initial CAD model was designed, the correctly sized blank was created such that it encompassed the size of the rice transplanter claw. To simplify the machining of the blanking die and punch, an oval shaped blank was used. This provided a symmetrical blank for bending so that the blank does not move during bending due to uneven pressures across the blank's horizontal axis.

The blanking die initial opening was made the exact size as the blank with a depth of 1.80 mm, the thickness of the stock material. After the 1.80 mm depth straight portion, a 0.5° taper is applied to the bottom of the die to allow for easy release of the blank from the die (Boljanovic & Pacquin, 2006, p. 92).

Next, the minimum thickness of the die block was determined using Equation 5 (Suchy, 2006, p. 196), where P_{max} is the maximum force in metric tons.

$$t_{\text{die block}} \geq \sqrt[3]{P_{max}}$$

(5)

P_{max} was approximated using F_{shear}, where σ_{UTS} is the ultimate tensile strength of stainless steel 304 (Equation 6) (Annealed 304 Stainless Steel, 2020).

$$F_{\text{shear}} = 0.7\sigma_{\text{UTS}} * \text{perimeter} * \text{thickness} = 0.7 * 515 \text{ MPa} * 275 \text{ mm} * 1.80 \text{ mm}$$
$$= 198275 \text{ N}$$

(6)

Equation (7 is formed by converting the shearing force from 198,275 Newtons to 20 metric tons,

$$F_{\text{shear}} = 198275 \text{ N} = 20.2 \text{ metric tons}$$

(7)

Therefore, the minimum thickness of the die block is found to be 27.2 mm (Equation 8),

$$t_{\text{die block}} \geq \sqrt[3]{20.2} \text{ metric tons} = 27.2 \text{ mm}$$

(8)

The final thickness of the die block was rounded up to 30 mm to account for tolerances in the die block opening and stock material thickness. Finally, the distance from the die block openings to the edge of the die block were determined using the guide which is shown in Figure 25 (Boljanovic & Paquin, 2006, p. 94).

Figure 25: Recommended minimum distances from die block opening to outside edge. Adapted [reprinted] from *Die Design Fundamentals* (p. 94), by V. Boljanovic and J.R. Paquin, 2006, Industrial Press Inc. Copyright 2006 by Industrial Press.

Starting with column A, the strip thickness falls within $\frac{1}{16}$" $-\frac{1}{8}$" or $1.59 -$

3.175 mm. A strip thickness in this range results in an estimated die block

height/thickness of approximately $1\frac{1}{8}$" or 28.575 mm under column B. The die block

thickness from Boljanovic and Paquin is 5% larger than the minimum die block thickness

found using Equation 8 derived from Suchy's formula for minimum die block thickness

in Equation 5. Next, the proper die contour was chosen from options 1, 2, and 3 under

column C. Due to the oval shape of the blank, the smooth die hole contour, option 1, was

chosen. The values, which are listed under column C in section 1, are die block thickness

multiplication factors that determine the minimum distance from the die openings to the

edge of the die block. In the row corresponding to a strip thickness of $\frac{1}{16}$" $- \frac{1}{8}$", the multiplication factor was found to be 1.2656. The die block thickness was found to be a minimum of 27.2 mm in Equation 8. Therefore, the minimum distance from the die opening to the edge of the die block was calculated to be 34.4 mm as shown in Equation 9.

$$1.2656 * t_{min} = 1.2656 * 27.2 \text{ mm} = 34.4 \text{ mm} \approx 35 \text{ mm}$$

(9)

To increase output in the manufacturing process, the blanking die was constructed to allow for two blanking operations to take place simultaneously. This is accomplished by creating two openings in the die plate separated by an appropriate distance as to not cause any deformation of the die plate due to the reduction in strength experienced due to the die openings. The blanking die also contains lineup blocks that are 5 mm in height, along the outside edge of the die block. These raised portions allow the operator to quickly line the stock material in the correct location so that the proper scrap thickness is left between consecutive blanking operations. The use of the raised portions decreases the amount of wasted material compared to the positioning of the stock material by hand without any aides. The material cost for a single rice transplanter claw was found to be $0.17 as shown in Table 5. The cost of the stainless-steel stock material contributes an average of 55% of the cost of the final product for the medium-volume manufacturing process. Therefore, a reduction in waste of material can significantly decrease the overall cost of production. Figure 26 shows the blanking die block.
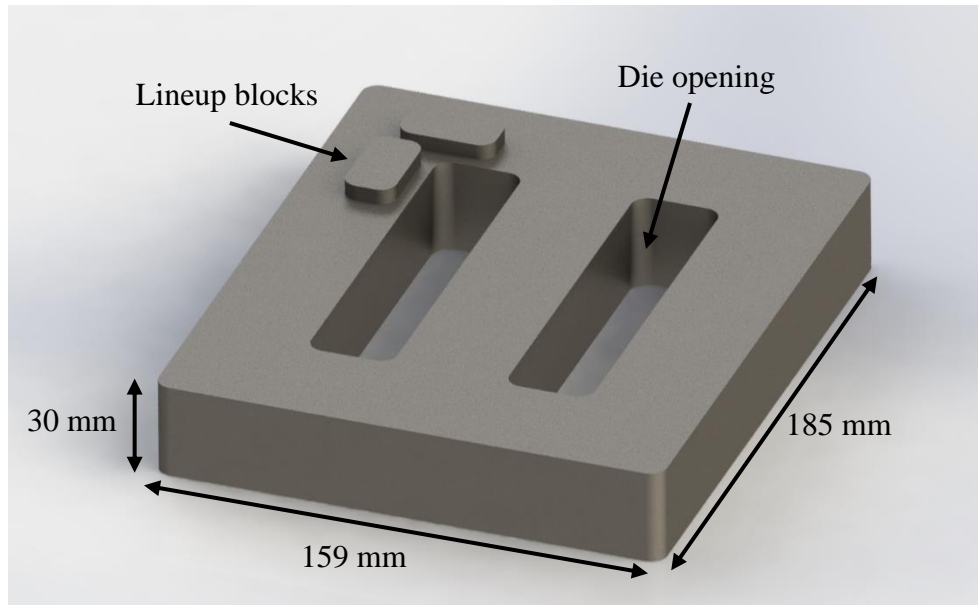
Figure 26: Rendering of rice transplanter claw blanking die

The two punches have a clearance of 22% of stock thickness or 0.40 mm between the individual punches and the corresponding opening of the die block which is the suggested clearance for blanking stainless steel (Clearance Calculation, 2019). The clearance ensures proper function of the punch as well as reduced wear and tear during repeated blanking of the stock material. The height of the punches is 10 mm, which allows for adequate clearance to blank the material with the presence of the raised portions of the die block. The two punches are separated by the width of a blank plus the blank thickness as recommended by the Handbook of Die Design (Suchy, 2006, p. 277). This ensures the proper amount of material is left between the punches to allow for the next blanking operation without unwanted deformation of the stock material. The separation between the two punches also allows for the ability to mount the punch to the press through the center of the punch block. Figure 27 shows the blanking punch.
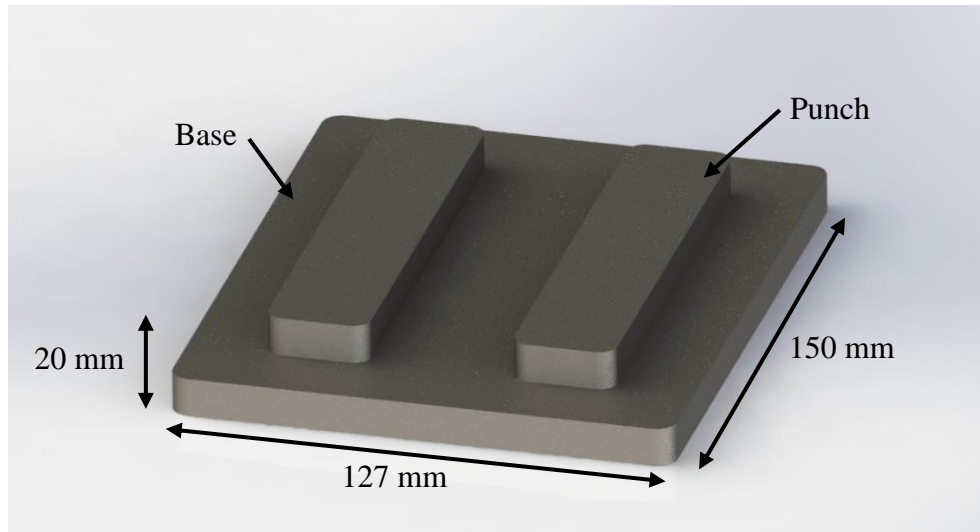
Figure 27: Rendering of rice transplanter claw blanking punch

Like the blanking punch and die set, the bending punch and die set completes two
bending operations simultaneously. This results in greater output of the manufacturing
process while maximizing the utility of the mechanical press. The bending die block was
designed to hold the blank within a recessed area with a depth of 1 mm or approximately
half of the blank's thickness. Recessing the blank by only half its thickness allows the
operator to remove the black from the bending punch and die set easier than if the blank
was fully recessed into the die block. The recessed area acts to position the blank in the
correct location to minimize the error in the lateral positioning of the blank. Error in the
lateral position of the blank results in uneven bending of the part as the centerline of the
bend is offset from the centerline of the blank. The valley of the bending die block was
designed such that the machining is completed using a single bull nose end mill with a
radius of 3.0 mm therefore reducing the needed machine tools and complexity of
machining. The valley was designed with a width of 13.5 mm, depth of 9 mm, and
radius of 3.0 mm. The valley also has a 1° draft angle applied to aid in post operation

removal of the part. The specific dimensions of the die valley were determined by a combination of analysis of the DEFORM bending punch and die model and calculations to determine the spring back due to unloading. Figure 28 shows the bending die block.
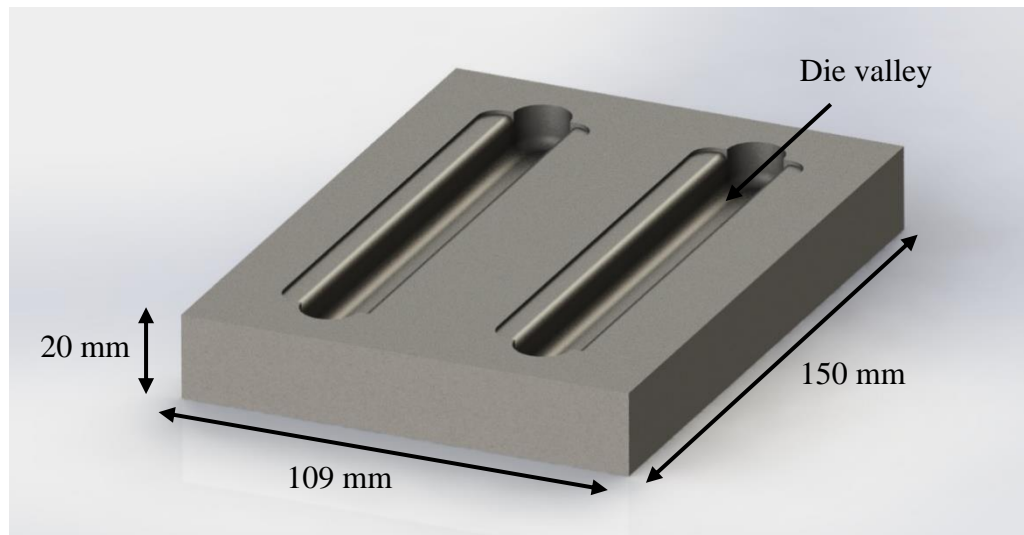
Figure 28: Rendering of rice transplanter bending die block

The bending punches were designed with a radius of 1.5 mm and no taper. As the radius of the bending die valley (3.0 mm) is double the radius of the punch (1.5 mm), extra pressure is applied on the formed radius during the bending operation (Auto Steel Partnership, 2000, p. 48). Figure 29 shows an example of this method of bending for a wiping die with the addition of back relief, which is not used in this design. Figure 30 shows the bending punch.
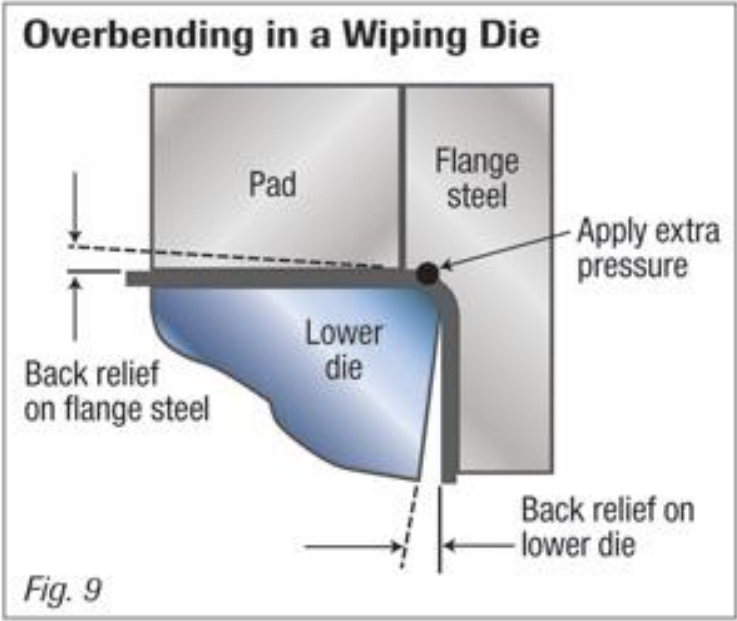
Figure 29: Overbending in a Wiping Die. Adapted [reprinted] from *High Strength Steel (HSS) Stamping Design Manual* (p. 48), by High Strength Steel Design/Formability Task Force of the Auto Steel Partnership, 2001.
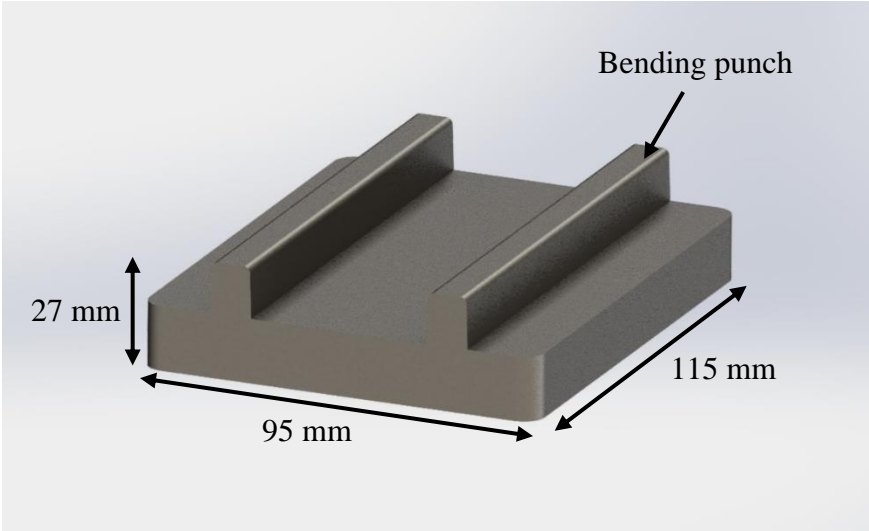
Figure 30: Rendering of rice transplanter bending punch

2.4.3 Press brake force and angle calculation

Force and angle calculations were completed to allow for a better understanding of the machinery and tooling needed to bend the rice transplanter claws using a press brake. The main equation driving the design of the press brake bending and bending punch and die set is for the strain in the sheet due to the bending of the material. This equation is used to determine the minimum radius to which a piece of sheet metal can be bent until it fails due to the formation of cracks, often along the radius of the bend (Kalpakjian & Schmid, 2008). Equation 10 shows the engineering strain in the sheet,

$$\frac{\Delta l}{l} = \frac{1}{1 + \frac{2r_p}{t}}$$

(10)

Solving for the radius of the bend, r_p, gives (Equation 11)

$$r_p = \frac{t}{2}(\frac{l}{\Delta l} - 1)$$

(11)

Substituting for the material thickness, 1.80 mm and the elongation at break of annealed stainless steel 304 of 43%, the minimum radius of the part is found to be 1.19 mm (Equation 12) (Annealed 304 Stainless Steel, 2020). Therefore, the internal radius created by the bending operation must be greater than 1.19 mm to not cause the failure of the material due to excessive strain.

$$r_p = \frac{1.80 \text{ mm}}{2}\left(\frac{1}{0.43} - 1\right) = 1.19 \text{ mm}$$

(12)

The punch radius for the press brake bending it set to 1.50 mm, so it must be

checked that the chosen punch radius will bend the part in the plastic region. The

engineering strain at the punch radius is calculated using Equation 10 and compared to

the engineering strain at the yield point. The yield stress and Young's modulus in

Equation 13 are 230 MPa and 200 GPa, respectively. These values are the respective

values for stainless steel 304 (Annealed 304 Stainless Steel, 2020). As the engineering

strain at the punch was found to be 0.375 and the engineering strain at the yield point was

found to be $1.15 \cdot 10^{-3}$, the bend will be in the plastic region.

$$e_p = \frac{1}{1 + \frac{2(r_p)}{t}} = 0.375 > \frac{\sigma_{yield}}{E} = 1.15 \cdot 10^{-3}$$

(13)

To determine the maximum force required during the bending process, the

bending moment for a strain hardening material must be calculated using Equation 14

(Kalpakjian & Schmid, 2008).

$$M_b = \frac{\sigma_{yield} \cdot bt^2}{12}\left(1 + \frac{2\sigma_1}{\sigma_{yield}}\right)$$

(14)

Since the yield stress, thickness, and width (b) of the material are known, only σ_1 must

be calculated using Equation 15. In Equation 15, k is the rate of strain hardening and e is

the engineering strain (Kalpakjian & Schmid, 2008).

$$\sigma_1 = \sigma_{yield} + ke$$

(15)

The rate of linear strain hardening is determined to be 816 MPa using the stress and engineering strain at yield and failure as shown in Equation 16 (Annealed 304 Stainless Steel, 2020).

$$k = \frac{\sigma_{UTS} - \sigma_{yield}}{e_{UTS} - e_{yield}} = \frac{\sigma_{UTS} - \sigma_{yield}}{e_{UTS} - \frac{\sigma_{yield}}{E}} = \frac{580 \text{ MPa} - 230 \text{ MPa}}{0.43 - 0.00115} = 816 \text{ MPa}$$

(16)

Substituting in the engineering strain at the punch radius from Equation 13, σ_1 is found to be 536 MPa (Equation 17)

$$\sigma_1 = 230 \text{ MPa} + 816 \text{ MPa} \cdot 0.375 = 536 \text{ MPa}$$

(17)

Therefore, using Equation 14, the bending moment can be calculated to be $3.06 \cdot 10^4 \text{ MPa} \cdot \text{m}^3$ (Equation 18)

$$M_b = \frac{215 \text{ MPa} \cdot 113.6 \text{ mm} \cdot 1.80 \text{ mm}^2}{12}\left(1 + \frac{2(536 \text{ MPa})}{230 \text{ MPa}}\right) = 3.73 \cdot 10^4 \text{ MPa} \cdot \text{m}^3$$

(18)

Next, the angle where the maximum force occurs must be determined using Equation 19 where μ is the coefficient of friction. The coefficient of sliding friction for mild steel on mild steel is 0.57 (*Handbook of Physical Quantities*, 1997). Therefore, the angle at which the maximum force occurs is found to be 15° (Kalpakjian & Schmid, 2008).

$$\alpha_{F_{max}} = \frac{1}{2}\tan^{-1}(\mu) = 14.8° \sim 15°$$

(19)

As the bending moment and angle of maximum force has been calculated, the maximum

force is found to be 10286 N or 1.05 metric ton-force (Equation 20). The length of the

bend, l, is set to 7.8 mm for this analysis.

$$F_{max} = \frac{2M_b}{l}\left[\cos^2(\alpha_{F_{max}}) + \mu \cdot \sin(\alpha_{F_{max}}) \cdot \cos(\alpha_{F_{max}})\right] = 10286 \text{ N}$$

$$= 1.05 \text{ metric tons}$$

(20)

Finally, the spring back due to unloading must be accounted for so the appropriate

punch and die angles are calculated. The spring back was calculated using a sheet metal

forming analysis which accounts for linear material strain hardening. Equation 21 shows

the equation for calculating the final bend angle (Kalpakjian & Schmid, 2008).

$$\alpha_{punch} = \frac{\alpha_{final}}{\left(1 + \frac{\Delta\alpha}{\alpha_{punch}}\right)}$$

(21)

α_{final} is set to 90 degrees to replicate the angle of the original rice transplanter claw.

Equation 22, shown below, is used to calculate $\frac{\Delta\alpha}{\alpha_{punch}}$, which was found to be 0.009.

$$\frac{\Delta\alpha}{\alpha_{punch}} = \left(r_{punch} + \frac{t}{2}\right)\frac{\sigma_{yield}}{Et}\left(1 + \frac{2\sigma_1}{\sigma_{yield}}\right) = 0.009$$

(22)

By substituting in this value into Equation 23, the final angle of the part is calculated to

be 89.1° (Equation 23)

$$\alpha_{\text{punch}} = \frac{90°}{(1 + 0.009)} = 89.1°$$

(23)

2.4.4. Section Summary

The Design of Required Tooling section of Chapter 2 is composed of two separate

subsections: the development of the rice transplanter CAD model and the design theory

for blanking and bending punch and die sets. The first subsection displays the basic rice

transplanter claw dimensions used to create the initial CAD model along with a rendering

of the rice transplanter claw CAD model. The second subsection provides the design

theory background for the development of the blanking and bending dies. First, the

blanking and press bending punch and die set is discussed with relevant equations for

punch and die clearances and die block thickness. Next, the final design of the blanking

and bending punch and die sets are discussed. Finally, the press brake bending is

discussed along with equations used to determine the maximum force and proper press

brake bending die angles.

The next section presents the experimental methods and procedures for the

prototype bending die testing. First the testing conditions are mentioned followed by the

design of the prototype bending punch and die set. Finally, the testing procedure is listed.

2.5 Experimental Methods and Procedures

Testing of the bending punch and die set were performed on the Wabash 50-ton/45.35 metric tons hot press shown in Figure 31. All tests were conducted at room temperature. During operation of the hydraulic press the entire bottom platen moves up, therefore the use of a die set with static guide rods was not possible because the rods would contact the platen before the punch reached the die block. An example of a standard die set as mentioned is shown in Figure 32.

Figure 31: Hydraulic pressed used for prototype testing

Figure 32: Die set

Due to this height restriction, the design of the punch and die block were altered to allow for operation in the hydraulic press. The design of the bending punch and die set was altered such that the die block contains a pocket which centers the punch without the need for any guide rods, which are traditionally used to position the punch in the proper position over the die block. Other changes made to the design of the prototype include the addition of holes in the bending die block to ensure that both the bending punch and blank could be removed from the die block if it jammed. To reduce the material used during testing, the design of the bending punch and die was altered by reducing the number of blanks bent in a single operation to one. Figure 33, Figure 34, and Figure 35 shows the bending punch, die, and punch and die set respectively.

Figure 33: Machined rice transplanter claw bending punch
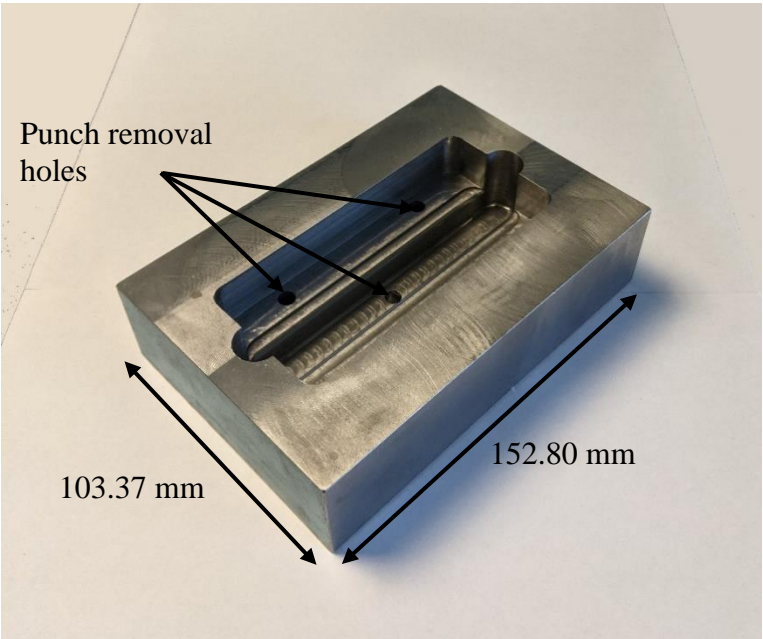
Figure 34: Machined rice transplanter claw bending die

Figure 35: Assembled machined rice transplanter claw bending punch and die set

The blanks used during the tests were machined using a water jet from 1.90 mm thick stainless-steel 304 sheeting. Figure 36 shows an example blank. Two sizes of blanks were tested to better determine the effects of a smaller blank resulting from looser tolerances. The first and largest blanks created were offset 0.25 mm from the size of the pocket in the bending die. The second blanks were offset 0.5 mm from the size of the pocket. Table 11 shows the average size for the water jet blanks compared to the designed values. The blanks were lubricated using molybdenum disulfide to prevent sticking during the bending operation.

Table 11: Testing blank width error

Part offset (mm)	0.25	0.50
Designed blank width (mm)	26.50	26.00
Actual blank width (mm)	26.56	26.11
Blank thickness (mm)	1.90	1.90
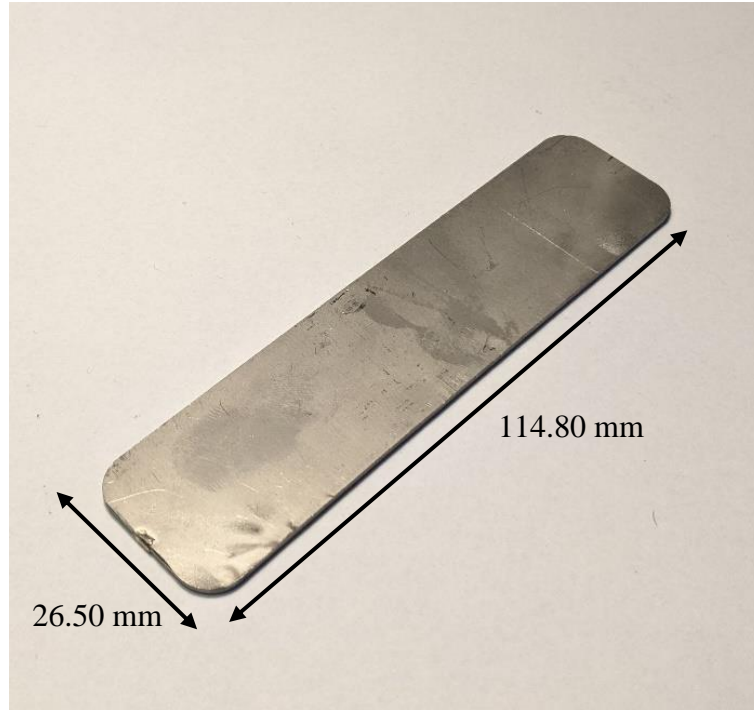
Figure 36: Water jet rice transplanter claw blank for bending

The testing procedure used in the testing of the rice transplanter bending punch and die set is listed as follows:

1. Lubricate the blank with a thin layer of molybdenum disulfide on both sides

2. Set blank into recessed area of bending die block

3. Lower bending punch into cavity until contact with blank

4. Place bending punch and die set onto bottom platen of press

5. Close hydraulic press until contact is made between the punch and top platen

6. Slowly increase hydraulic press force to 25 or 50 tons

7. Unload hydraulic press

8. Remove punch and die set from press and remove punch from punch and die set

9. Remove blank from die block.

2.5.1 Section Summary

The Experimental Methods and Procedures section looks to provide the necessary background information regarding the setup for the experimental testing of the bending punch and die set. The 50-ton hydraulic press used for testing is discussed along with the necessary changes to the design of the bending punch and die set to allow for proper alignment of the punch and die. Next, the blanks used during the experimental testing are discussed along with the variation in width between the designed and fabricated blanks. Finally, the testing procedure is listed.

The next section discusses the DEFORM-3D setup used for the finite element simulations of the bending punch and die set.

2.6 DEFORM Setup

DEFORM 3D (Version 11.1 published by Scientific Forming Technologies Corporation in Columbus, Ohio) is a process simulation system, which uses the finite element method to simulate manufacturing processes such as open and closed die forgings (Scientific Forming Technologies Corporation). In this study, DEFORM 3D was used to simulate both bending operations to study the effects of changes to various design parameters made prior to and after the machining and testing of the physical prototypes. This setup of the DEFORM 3D settings are discussed in this section with the results of the simulation are presented in the results section.

The settings used during the simulation of operations with DEFORM 3D were constant for all simulations in this study. The preprocessor used was 3D Forming

Express. 3D Forming Express sets many of the constraints to allow for ease of use when

conducting studies on cold or hot forming operations. An example of a constraint set by

the preprocessor is the constraint of the punch and die as rigid bodies. This sets the punch

and die as unable to be deformed which reduces the computing power needed as the

internal compressive forces experienced by the punch and die are not calculated. Figure

37 shows the settings of the 3D Forming Express preprocessor.
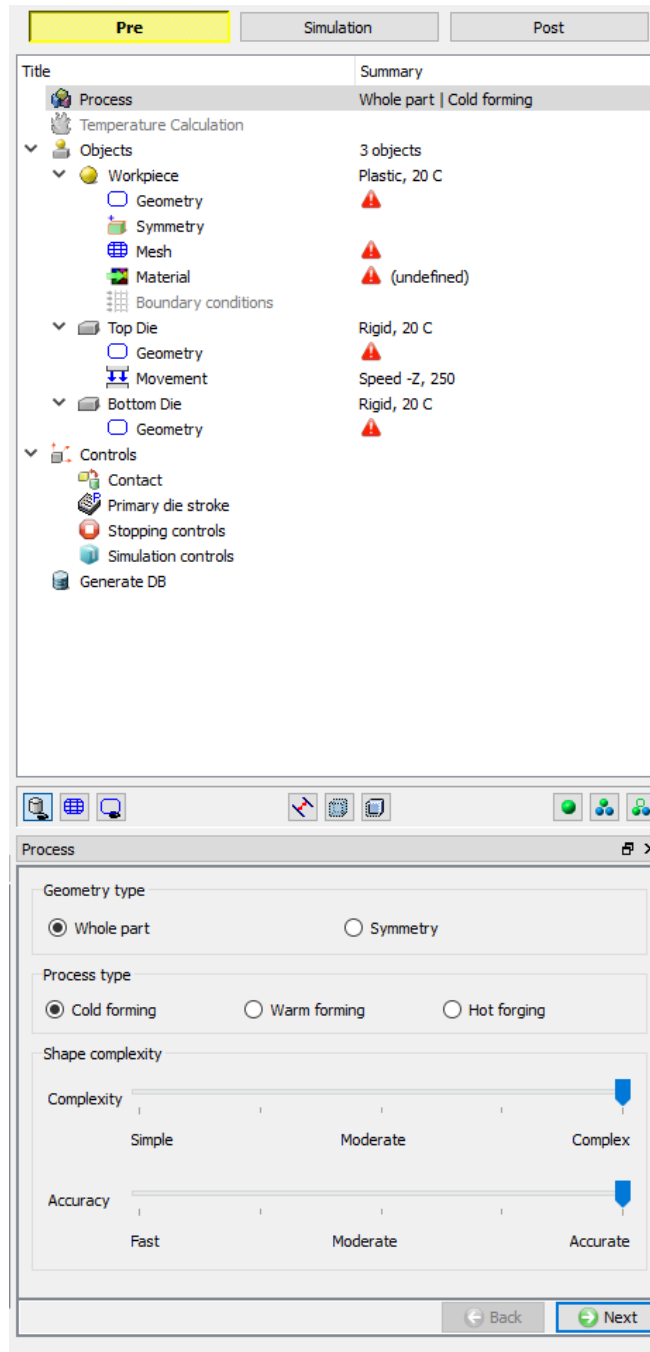
Figure 37: DEFORM 3D Forming Express settings

The first setting under the process tab, geometry type, was set to whole part.

Process type was set to cold forming which sets the temperature of the operation at 20°C.

Complexity and accuracy parameters were set to complex and accurate, respectively.

These parameters affect the number of points in the workpiece mesh along with other mesh parameters, which affect accuracy. The workpiece, top die, and bottom die geometries were set from an STL file created from the specific CAD part files. The mesh was generated with the suggested system settings which resulted in 86862 elements and 20198 nodes in the simulation of the bending operation of the machined bending punch and die set. The material of the workpiece was set to stainless steel 304 from the DEFORM materials library. No material properties are set for the punch and die as they are considered rigid in the forming analysis. The movement type of the top die was set as hydraulic, as all potential manufacturers of the rice transplanter claws intend to use hydraulic presses for the blanking and bending operations. The direction of the movement of the top die is set to the negative z-direction. The speed of the press is set to 10 for all operations. The total dwell time and number of steps is kept at zero. Figure 38 shows the top die movement settings used in the DEFORM simulations.
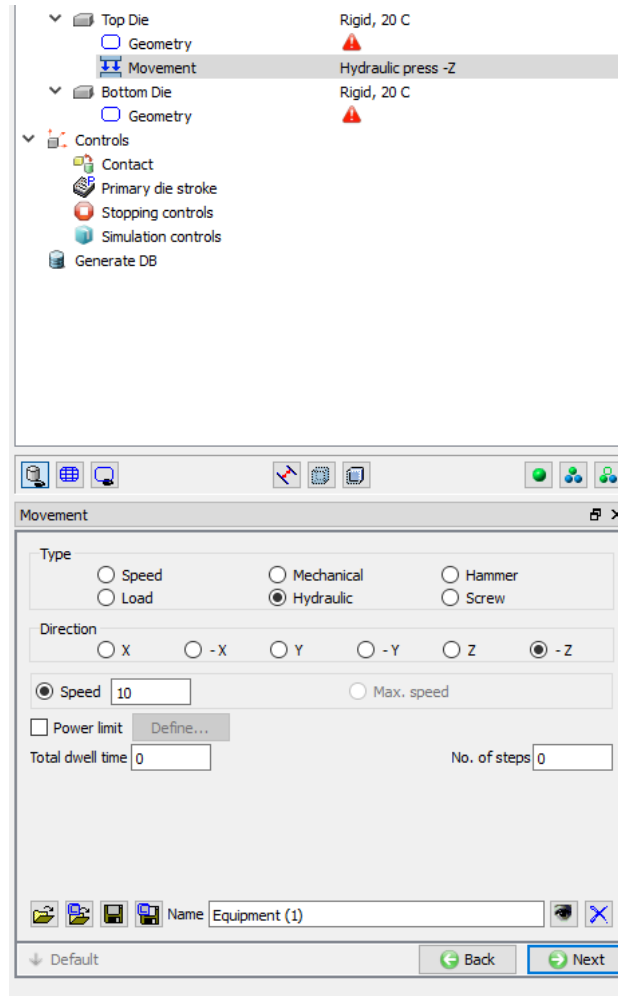
Figure 38: DEFORM 3D Forming Express top die movement settings

Finally, the controls settings were established. No changes were made to the setting under the contact tab. The primary die stroke was set to a rough estimate of the total die stroke expected and the exact amount box was left unchecked. In the stopping controls tab, the maximum load was set to 50 metric tons for the simulation of the prototype bending punch and die set and 150 metric tons for the simulation of the final design. Figure 39 shows the controls settings.
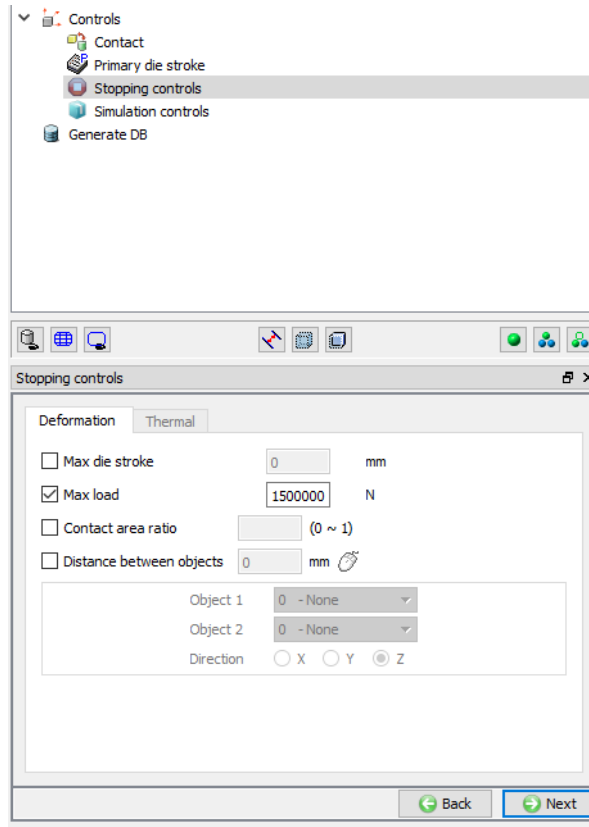
Figure 39: DEFORM 3D Forming Express controls settings

2.6.1 Section Summary

The DEFORM settings section discusses the finite element software used for the rice transplanter claw bending punch and die simulations. First, the background of the DEFORM-3D software is discussed along with the 3D Forming Express preprocessor which is used for all bending simulations. Finally, the process, geometry, and control settings within the 3D Forming Express preprocessor are discussed.

The next section presented the results and discussion of the material characteristic testing, experimental testing, and DEFORM-3D simulations.

2.7 Results and Discussion

2.7.1 XRF Results

The results for the x-ray fluorescence (XRF) spectroscopy are shown in Table 12. The Niton FXL Field XRF used does not detect the percentage of carbon in the sample. The XRF results for the original rice transplanter identifies the material as stainless steel 420, a martensitic stainless steel with high carbon content. The high carbon content and crystal structure of the martensitic stainless steel allow the material to achieve a very high hardness through effective heat treatment. The XRF of the casted rice transplanter claw was not able to identify the specific material used as the carbon content of the sample could not be identified. The significant elements registered by the XRF are shown in the right column of Table 12. The combination of significant elements found in the cast rice transplanter claw could not be matched to any known material composition. Therefore, it is assumed that the elemental composition of the material was not known during the manufacturing process.

The results of the XRF allowed for the easy identification of the material used in the manufacturing of the original rice transplanter claw. However, an XRF cannot determine the carbon content of a sample, which is important for determining proper heat treatment procedure. Optical emission spectroscopy (Spark OES) testing is a method of elemental analysis that can determine the carbon percentage of metals by analyzing the vaporized atoms created by an arc between the machine and the material (Acuren, 2019). It is recommended that a portable Spark OES system be purchased for elemental composition testing of scrap material in Bangladesh. Scrap material testing can be

provided by the local spare parts manufacturer or a private company looking to sell

known scrap materials to the local manufacturers. Elemental composition testing will

allow manufacturers to know that the carbon percentage of the stock material is high

enough for the part to be hardened through heat treatment thus reducing the wear and

increasing the tensile strength of the rice transplanter claws.

Table 12: Rice transplanter XRF Results (Material and Significant Elements)

Part	Suggested Material	Significant Elements (%)
Original Rice Transplanter Claw	Stainless Steel 420	Cr: 12 - 14 C: 0.15 - 0.4
Proposed material	Stainless Steel 304	Cr: 18 - 20 C: 0 - 0.08
Cast Rice Transplanter Claw	N/A	Fe: 98.129 P: 0.139 Si: 0.503 Cu: 0.154 Ni: 0.179

2.7.2 Hardness Testing Results

The second order polynomial regression equations used to estimate the tensile

strength with Rockwell C and B harnesses are shown below in Equations 24 and 25.

$$\sigma_{UTS} \text{ (psi)} = 88.67 * HRC^2 - 2031.6 * HRC + 119654$$

(24)

$$\sigma_{UTS} \text{ (psi)} = 17.425 * HRB^2 - 1327 * HRB + 71964$$

(25)

Table 13 contain the Rockwell hardness, Brinell hardness, and three tensile strength estimations of the original and casted rice transplanter claw as well as the stainless steel 304 material used in the prototype testing. The units have been converted from pounds per square inch in Equations 24 and 25 to megapascals in Table 13.

Table 13: Rockwell hardness and tensile strength estimation for rice transplanter claws

Part	Rockwell Hardness		Brinell Hardness	First Tensile Strength Estimation	Second Tensile Strength Estimation	Third Tensile Strength Estimation	Average Tensile Strength Estimation
	B Scale 100 kg	C Scale 150 kg		MPa	MPa	MPa	MPa
Original RTC		53	525	1811	1800	1950	1854
Cast RTC	64		114	393	403		398
SS 304	79		143	523	493	489	502

The high Rockwell hardness values of the original rice transplanter claws (HRC 53) indicate that the parts have been heat treated during their manufacturing process. In contrast, the hardness and tensile strengths of the cast rice transplanter claw (HRB 64) and austenitic stainless steel 304 (HRB 79) are significantly lower than that of the original rice transplanter claw due to the lower carbon content and inability to be heat treated.

The hardness of a material can also be related to the wear-rate constant of the material. The wear-rate of the rice transplanter claws is very important because the part is in repeated, dynamic contact with the rice mat and soil. Figure 40 displays the

relationship between hardness and the wear-rate constant. k_a, the wear-rate constant, is a measure of the wear rate experienced on a sliding surface. A larger wear-rate constant corresponds to more rapid wearing of the material at a specific pressure between the surfaces. The region for stainless steels encompasses hardness values of $1000 - 5000$ MPa and a dimensionless wear constant, K, of 10^{-4} indicated by the diagonal dashed line. The traditional dimensionless wear constant, K, considers the wear-rate, applied load, and the hardness of the material. However, the dimensionless wear constant in Figure 40 is equal to the wear rate constant times the material hardness. The hardness of the original rice transplanter claw, 5148 MPa, is determined by multiplying the Brinell hardness by the acceleration due to gravity as shown in Equation 26.

$$525 \ \frac{\text{kgf}}{\text{mm}^2} = 525 * 9.801 \ \frac{\text{N}}{\text{mm}^2} = 5148 \text{ MPa}$$

(26)

The hardness of the original rice transplanter claw is slightly above the range for stainless steels, due to heat treatment, and corresponds to a wear-rate constant, k_a, of approximately $0.1 \cdot 10^{-7} \ \frac{1}{\text{MPa}}$. The 304 stainless steel, which is proposed to use in the domestic manufacturing of rice transplanter claws, has a hardness of 1402 MPa, which corresponds to a wear-rate coefficient, k_a, of approximately $6.0 \cdot 10^{-7} \ \frac{1}{\text{MPa}}$. The larger wear-rate coefficient and tensile strength of the 304 stainless steel reveals that the tip of the rice transplanter claw is more likely to deform and wear under load when manufactured from stainless steel 304 in comparison to the heat-treated stainless steel 420 stock material of the original half-feed rice transplanter claw.
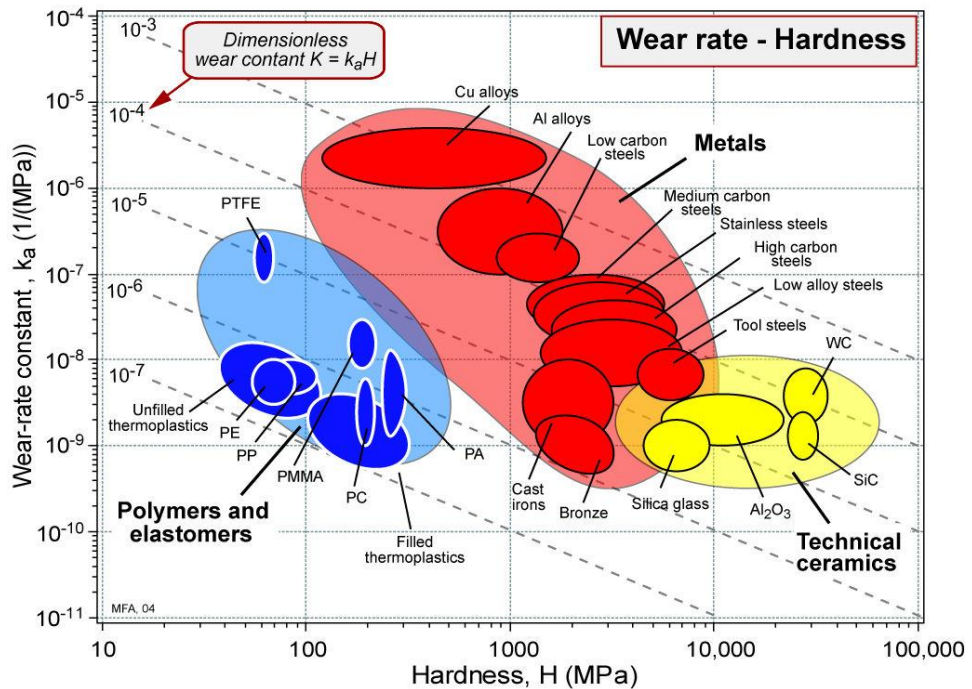
Figure 40: Wear-rate constant, k_a, to hardness. Reprinted from Granta CES 2009 EduPack Material and Process Selection Charts (p. 20), by Mike Ashby, 2009. Copyright 2009 by Granta Design Ltd.

The characterization of the hardness of the original rice transplanter claw and stainless steel 304 allows the potential manufacturers to understand the appropriate materials and heat treatment that are required to manufacture parts similar in quality to the OEM components. In Bangladesh, metals are separated by four main categories: aluminum alloys, mild steel alloys, stainless steel alloys, and cast irons without designation for specific material grades. Therefore, determining appropriate hardness values is an important parameter for selecting the correct stock material so that the final product has wear and strength properties similar to the original spare parts. It is recommended that the hardness of all scrap materials be tested prior to their use in manufacturing. Scrap material testing can be conducted by the manufacturer or a private

company looking to sell known scrap material to the local manufacturers. It is also recommended that manufacturers test the hardness of their finished products so that the hardness and wear rate coefficient can be compared to that of the original rice transplanter claw.

2.7.3 Experimental Testing Results

The testing of the bending punch and die set was performed with pressing forces of 25 tons/22.7 metric tons and 50 tons/45.4 metric tons. Figure 41 and Figure 42 show examples of the blanks after the experimental testing. A height difference is observed between the left and right sides of the bend. This is likely the result of the centerline of the blank and punch being offset.
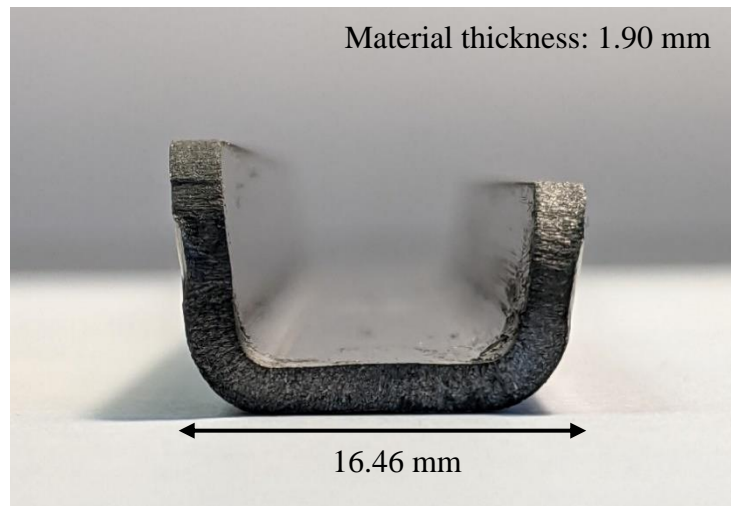
Figure 41: 25-ton test blank right side view
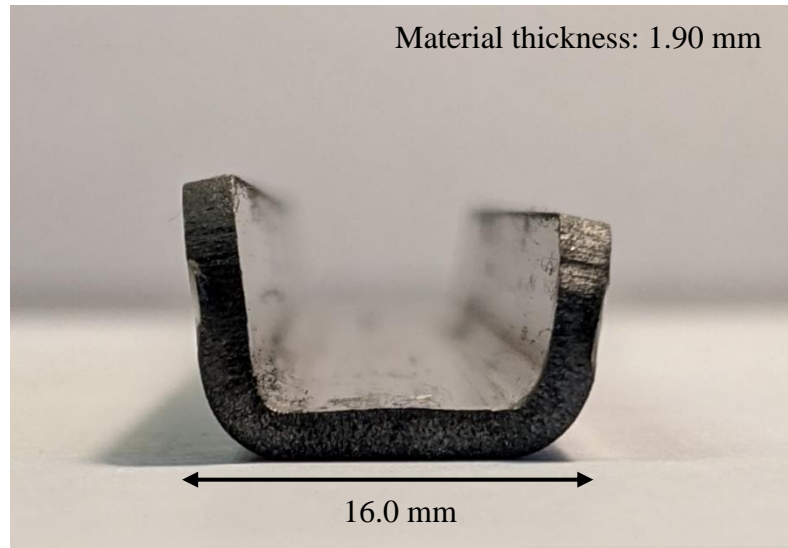
Figure 42: 50-ton test blank right side view

To further quantify the performance of the prototype bending punch and die set, width measurements were taken at both ends of the blanks as well as at the center of both the 25-ton and 50-ton blanks. Table 14 presents these width measurements compared with the width measurements of the original rice transplanter claws.

Table 14: Part width of test blanks versus original rice transplanter claw

Measurement	Original (mm)	25-ton Test Blank (mm)	50-ton Test Blank (mm)
Left Side	14.2	16.33	16.06
Center	14.3	16.48	16.05
Right Side	N/A	16.46	16.01

The results in Table 14 demonstrate that the prototype bending punch and die set failed to create a bend that adequately replicates the parameters of the original rice transplanter bend with pressing forces of 25 tons/22.7 metric tons and 50 tons/45.4 metric tons. The comparison of the 25-ton and 50-ton test blanks' width measurements reveals a difference in the width measurements however the differences are minimal when compared to the difference in width to the original rice transplanter claw. Therefore, it

can be surmised that the difference in width between the test blanks and original rice transplanter claw is not the results of a lack of pressing force but rather a design flaw in the bending punch and die set.

Due to the inability to bend the blank to the proper angle as well as the height difference between the two sides, changes were made to the design of the bending punch and die set to rectify these errors. The radius of the valley in the die block was increased from 1.5 mm to 3.0 mm after evaluation of the DEFORM model revealed that the blank was not contacting the valley corner at the bottom of the punch stroke. The results of this change are shown below in DEFORM simulation results.

2.7.4 DEFORM Simulation Results

After the validation of the DEFORM model by comparing results of the experimental testing and the prototype testing in DEFORM, further simulations were conducted to show the effects of the adjustment made to the die valley radius after the experimental testing revealed flaws in the previous design. Figure 43 and Figure 44 show top and side views of the left end of the blank from the DEFORM simulation of the updated punch and die set. A noticeable improvement in the angle between the bottom and side of the bend can be seen in Figure 44 when compared to the test blanks in Figure 42. The difference in the width measured in the DEFORM simulation of the updated punch and die set and the original rice transplanter has been reduced drastically by the design changes. The graph present in both figures shows the loading on the punch versus

the travel of the punch. The travel of the punch is kept constant for the comparison of the

performance of the bending punch and die set prototype and the updated/final design.
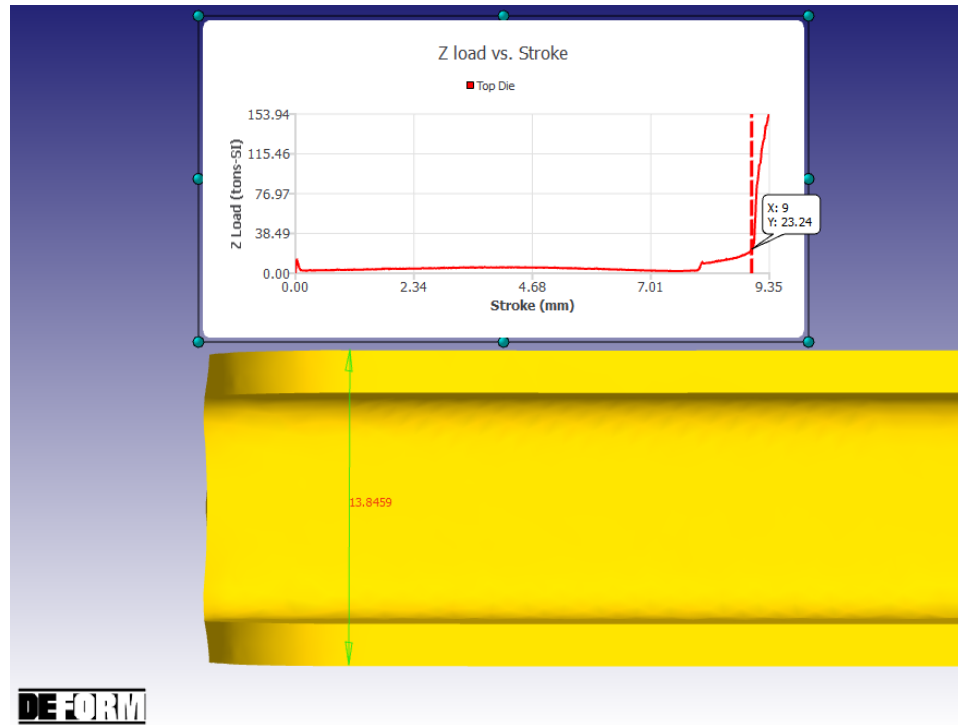
Figure 43: Top view of width measurement of updated DEFORM rice transplanter claw simulation
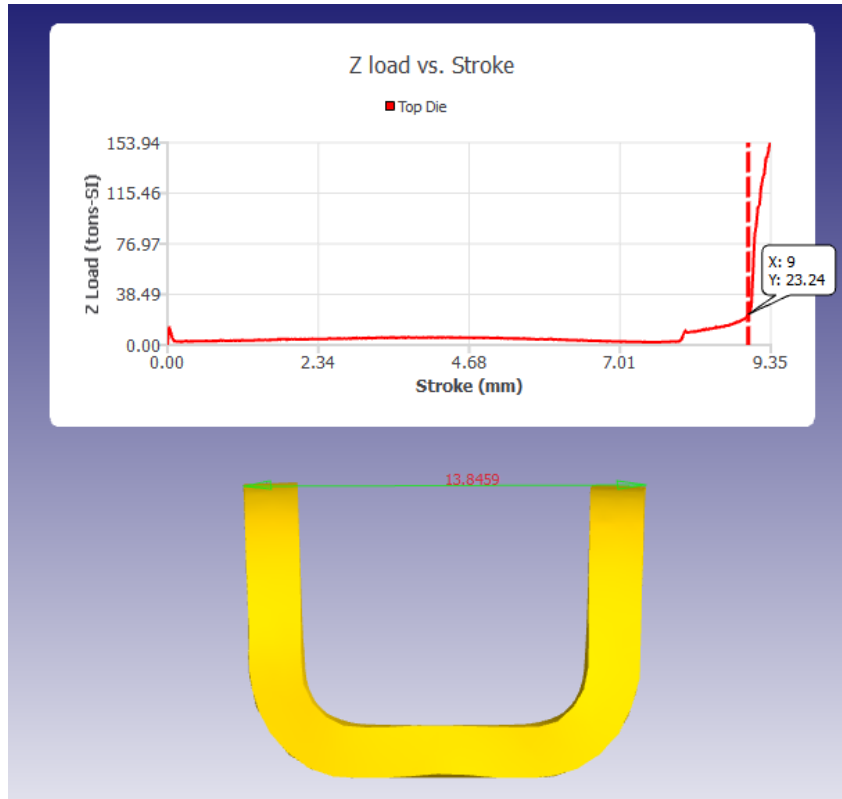
Figure 44: Side view of width measurement of updated DEFORM rice transplanter claw
simulation

Table 15 displays the width measurements computed during the DEFORM

simulation of the prototype testing and the final design simulation. These measurements

highlight the improvements in performance gained through the increase in the die block

valley radius from 1.5 mm to 3.0 mm.

Table 15: Comparison of DEFORM simulation width measurements of prototype and final bending punch and die set

Measurement	DEFORM Prototype Simulation (mm)	DEFORM Final Design Simulation (mm)	Original Rice Transplanter Claw (mm)
Left Side	16.15	13.85	14.17
Center	16.17	13.87	14.25
Right Side	16.13	13.81	N/A

The final design DEFORM simulation width methods do not account for the springback of the material due to the unloading of the punch. The springback was calculated using a sheet metal forming analysis that accounts for linear material strain hardening. Equation 27 shows the equation for calculating the final bend angle.

$$\alpha_{final} = \left(1 + \frac{\Delta\alpha}{\alpha_{punch}}\right)\alpha_{punch}$$

(27)

α_{punch} is set to 90 degrees. Substituting in values from Equation 23 the final angle of the part is calculated to be 90.64° (Equation 28)

$$\alpha_{final} = (1 + 0.009)90° = 90.81°$$

(28)

If the initial angle of the punch is subtracted from the final angle, the increase in part angle due to spring back is found to be 0.81° (Equation 29)

$$\alpha_{springback} = \alpha_{final} - \alpha_{punch} = 0.81°$$

(29)

Converting the angle of spring back to an increase in width due to spring back is accomplished by setting up a right triangle with the angle of spring back and the height of the rice transplanter claw. The height of the rice transplanter claw was found to be 10.56

mm in the DEFORM final design simulation. Therefore, the increase in width due to the springback of the material was found to be 0.24 mm (Equation 30)

$$w_{springback} \ = \ 2 \cdot 10.56 \text{ mm} \cdot \tan(0.81°) = 0.30 \text{ mm}$$

(30)

Table 16 shows the updated width measurements with the addition of the springback due to unloading. The average width difference between the updated DEFORM simulation + springback and the original rice transplanter claw is 0.05 mm.

Table 16: Comparison of DEFORM simulation width measurements of final bending punch and die set with springback due to unloading

Measurement	DEFORM Final Design Simulation (mm)	DEFORM Final Design Simulation + Springback (mm)	Original Rice Transplanter Claw (mm)
Left Side	13.85	14.15	14.17
Center	13.87	14.17	14.25
Right Side	13.81	14.09	N/A

Figure 9 shows the rice transplanter claw mounted to the rice transplanter assembly. The rice transplanter claw fits around the mounting block and is secured by two nuts and bolts going through the mounting holes. The seedling pusher is also seated within the bend of the rice transplanter claw. Therefore, the width of the rice transplanter claw is important so that it can be properly mounted to the rice transplanter arm assembly. The average width difference between the updated DEFORM simulation + springback and the original rice transplanter claw was found to be 0.05 mm. The width of the arm assembly mounting block and seedling pusher are unknown; however, the rice transplanter claw is mounted to the mounting block using two bolts and nuts which do

not allow for tight tolerances during mounting. Therefore, the design of the rice transplanter claw bending punch and die set is considered satisfactory. The tolerances of the bending punch and die set are also set such that any variation in machining results in a larger rice transplanter claw width as an increase in width allows for more clearance for the mounting block and seedling pusher.

2.7.5 DEFORM Bending Sensitivity Analysis

A sensitivity analysis was completed on the DEFORM model of the bending punch and die set to determine the effects of different grades of stainless steel on the ability of the bending punch to reach an adequate die stroke. The steel grades tested were AISI 304, AISI 316, AISI 410, and AISI 431. The material properties were set through the DEFORM-3D material library. As the elemental composition of stock material are not known in Bangladesh, the ability of the bending punch and die set to reach an adequate die stroke with a variety of stock material is important for the functionality of the rice transplanter claw bending process in Bangladesh.

In the previous comparison of the prototype, final DEFORM simulation, and original rice transplanter claw, a die stroke of 9 mm was found to be adequate at closely reproducing the width of the original rice transplanter claw. Table 17 displays the force required to reach a die stroke of 9 mm for the four stock materials tested (Annealed 316 Stainless Steel, 2020; Annealed 410 Stainless Steel, 2020; Tempered 431 Stainless Steel, 2020). The press force required to reach a die stroke of 9 mm for the materials with a yield strength of 520 – 580 MPa was found to be between 22.34 – 23.24 metric tons. An

increase in stock material yield strength to 890 MPa resulted in an increase in press force

to 31.10 metric tons. The results in Table 17 show that the pressing force required to

obtain a die stroke of 9 mm is sensitive to the ultimate tensile strength of the stock

stainless steel. However, it is not expected that AISI 410 or AISI 431 be used in the

manufacturing of rice transplanter claws due to its lack of availability in Bangladesh

(Inspira report). Therefore, the force required to complete the bending operation of the

rice transplanter claw manufacturing process is expected to be between 22.34 – 23.24

metric tons. Hydraulic and mechanical presses with maximum forces exceeding 25 metric

tons are prevalent in small machine shops throughout Bangladesh, therefore the creation

of a production line for rice transplanter claws would not require a high level of initial

capital investment for many manufacturers.

Table 17: Results of sensitivity analysis of rice transplanter claw bending punch and die set

Stock Material	σ_{UTS} (MPa)	Bending Press Force (metric tons)	Max Press Brake Force (metric tons)
AISI 304	580	23.24	1.05
AISI 316	570	22.23	1.03
AISI 410	520	23.24	N/A
AISI 431	890	31.10	N/A

2.7.6 DEFORM Validation

A mesh convergence study was completed on the DEFORM model of the

experimental testing to determine the initial of the accuracy of the DEFORM 3D Forming

Express preprocessor system defined mesh sizes. Table 18 displays number of mesh

elements and nodes and the corresponding die stroke at the press forces of 25 metric tons

and 50 metric tons. Figure 45 displays a graph of the die stroke versus the number of

83

mesh elements for pressing forces of 25 and 50 metric tons. The course, normal, and fine

mesh sizes predict a less accurate die stroke at both 25 and 50 metric tons, however the

very fine and extremely fine meshes predict very similar results at both 25 and 50 metric

tons pressing forces. Therefore, the very fine and extremely fine meshes are converged

with regards to die stroke (Mesh Convergence, 2017).

Table 18: Results of mesh convergence for DEFORM simulation of rice transplanter bending test

Mesh	Elements	Nodes	Die Stoke (25 metric tons) (mm)	Die Stroke (50 metric tons) (mm)
Course	6580	2041	8.93	9.18
Normal	13712	3669	9.04	9.17
Fine	22969	5962	8.95	9.12
Very Fine	38314	9586	9.00	9.06
Extremely Fine	86862	20198	9.02	9.05
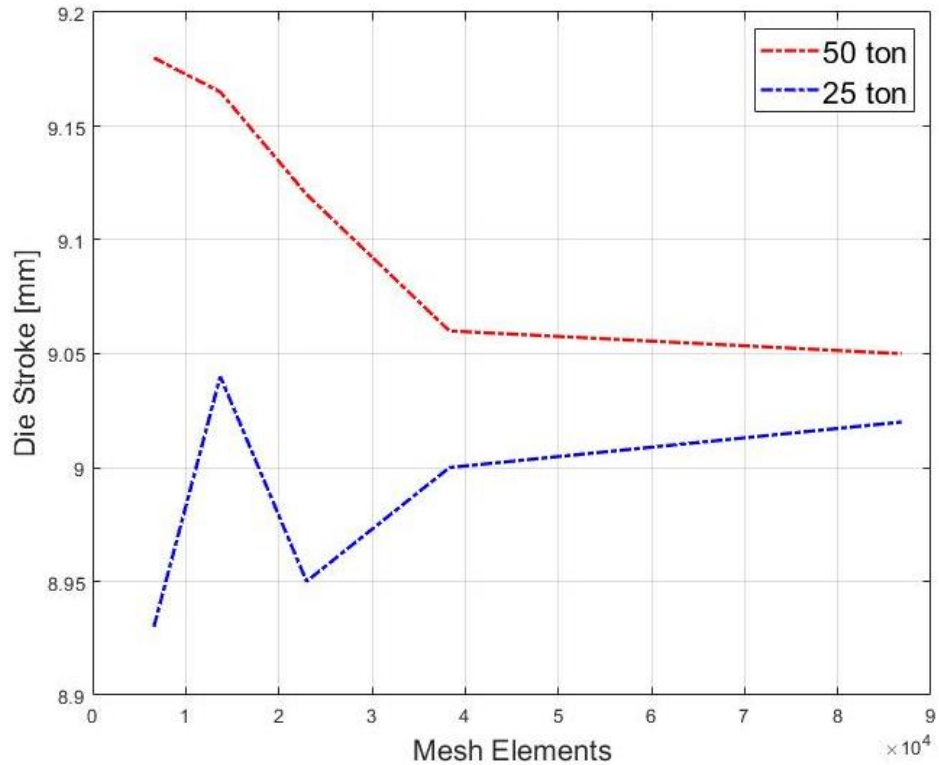
Figure 45: Mesh convergence of DEFORM simulation of rice transplanter claw bending test

The validation of the DEFORM model is performed by comparing the results of the experimental testing to the results of the DEFORM model of the experimental testing computed in the 3D Forming Express preprocessor. Various width measurements along the blanks are taken in DEFORM and compared to the results of the prototype testing to validate the accuracy of the model. The appearances of the blanks after bending are also compared between the physical testing and DEFORM simulations to aid in the validation of the model's ability to accurately predict the post operation appearance of the part. These results are presented in the section below.

Width measurements were taken at the center and at both ends of the blanks after the bending operations had been completed. The same width measurements were taken in the DEFORM model and are compared in Table 19.

Table 19: Part width of test blanks versus DEFORM simulation of prototype testing

Location	DEFORM 25 metric tons simulation (mm)	Experimental 25 metric ton test blank (mm)	25 metric tons percent difference (%)	DEFORM 50 metric tons simulation (mm)	Experimental 50 metric tons test blank (mm)	50 metric tons percent difference (%)
Left Side	16.29	16.33	0.25	16.09	16.06	0.19
Center	16.30	16.48	1.10	16.11	16.05	0.37
Right Side	16.24	16.46	1.35	16.06	16.01	0.31

The results in Table 19 show that the DEFORM model of the testing punch and die set resulted in small variations to that of the experimental testing. An average width difference of 0.16 mm and 0.05 mm was found between the DEFORM model and experimental testing at press forces of 25 tons/22.7 metric tons and 50 tons/45.4 metric tons. During the machining of the bending punch and die, machining tolerances of ±0.005" or ±0.125 mm were used. As the error between the DEFORM simulations and experimental testing are smaller than the machining tolerances, the error is considered negligible.

Next, visual comparisons are made between the experimental testing and DEFORM simulation. Figure 46 shows a transparent overlay of the left end of the blanks from the physical testing and simulation. The lower height of the left side of the blank can be seen in both the test blank and simulated blank however the difference in height is greater in the experimental testing. The difference in height between the left and right sides of the experimental blank and DEFORM simulation blank was found to be 0.96 mm

and 0.34 mm, respectively. Figure 47 shows the right end of the blanks. The lower height of the right side of the blank can be seen in the test blank and simulated blank. However, the DEFORM simulation has a greater difference in height between the left and right sides. The difference in height between the left and right sides of the experimental blank and DEFORM simulation blank were found to be 0.67 mm and 0.12 mm, respectively.

The height measurements taken along the left and right ends of the experimental testing and DEFORM simulation blanks reveal an average height difference of 0.52 mm. Standard machining tolerances of $\pm0.005''$ or ±0.125 mm were used during the machining of the prototype punch and die set. Therefore, machining tolerances cannot fully account for the height differences. The positioning of the blank into the recessed area of the bending die block and the positioning of the bending punch also contribute to the curvature of the bend as deviation from the centerline causes height differences between the left and rights sides of the blank. Therefore, due to the large height differences the DEFORM simulation cannot be validated to a high degree of accuracy regarding the height of the blanks. However, the average width differences of 0.1 mm (25 metric tons) and 0.05 mm (50 metric tons) between the experimental testing and DEFORM simulation validate the results of the DEFORM model up to the 50 metric tons press force limit with regard to the width measurements.
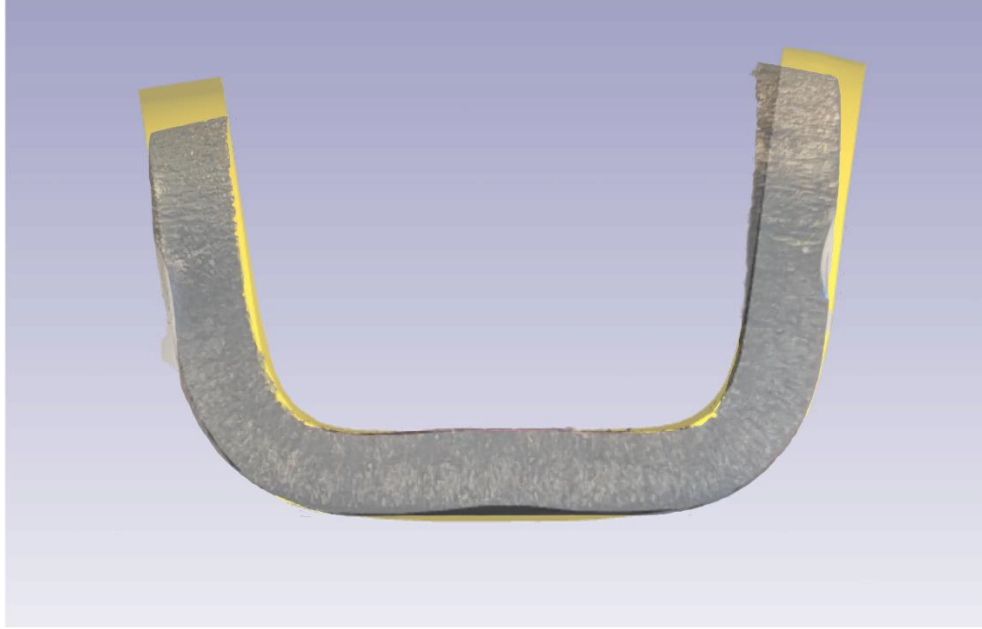
Figure 46: Visual comparison of DEFORM simulation and experimental testing blank left side profile
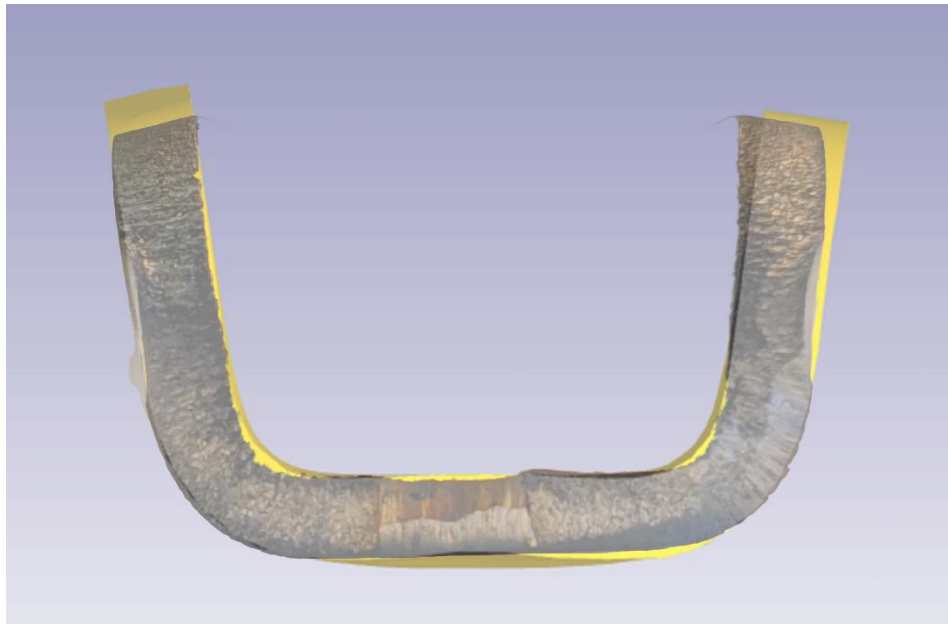
Figure 47: Visual comparison of DEFORM simulation and experimental testing blank right-side profile

2.7.7 Discussion and Recommendations

The cost analysis shown in Section 2.3 determines the cost per part for the low-, medium-, and high-volume manufacturing processes as between $0.22 and $0.57. The full breakdown of the cost per part for the three manufacturing methods is presented in Table 7. The dealer's sales price of the spare rice transplanter claws was found to be $2.15 through CSISA-MEA partners in Bangladesh. Assuming a 200% markup by the dealers, the production of spare rice transplanter claws in Bangladesh was found to be economically viable.

The DEFORM forging simulations shown in section 2.7.4 determined that the average width difference between the DEFORM simulation of the final bending die punch and die set + springback and the original rice transplanter claw is 0.05 mm. As shown in Figure 9, the rice transplanter claw is mounted to the rice transplanter arm assembly by two nuts and bolts going through the mounting holes of the claw with the seedling pusher seated within the bend of the claw. Therefore, the width of the rice transplanter claw is important to the operation of the part. The width of the mounting block and seedling pusher are unknown; however, the claw is mounted using two bolts and nuts which do not allow for very small positional tolerances. Therefore, the design of the rice transplanter claw bending punch and die set is considered satisfactory based upon the 0.05 mm difference in width when compared to the original rice transplanter claw.

The experimental testing of the prototype bending punch/die set failed to adequately recreate the outer width of the rice transplanter claw. However, the increase in valley die radius from 1.5 mm to 3.0 mm in the final design resulted in satisfactory bending of the claw during simulation. Therefore, it is recommended that the current

prototype bending die be machined to increase the valley die radius to 3.0 mm so that further experimental testing or production can be completed. Further machining can be conducted to remove the pocket from the bending die if a standard H frame hydraulic press is to be used for testing or production.

The sensitivity analysis of the four stock materials revealed a bending force of 31.10 metric tons required to reach a die stroke of 9 mm with a stock material of AISI 431. However, it is not recommended that AISI 431 be used in the manufacturing of rice transplanter claws due to low availability in Bangladesh. Therefore, it is recommended that a press with a maximum force of at least 50 metric tons is used for the blanking and bending of the rice transplanter claws as the final punch and die designs incorporate the blanking and bending of two rice transplanter claws. Hydraulic and mechanical presses with maximum forces exceeding 50 metric tons are prevalent in small machine throughout Bangladesh, therefore the creation of a production line for rice transplanter claws would not require a high level of initial capital investment. If a press brake is to be used for the bending of the rice transplanter claw the forces required for stock materials AISI 304 and AISI 316 were found to be 1.05 and 1.03 metric tons respectively. AISI 410 and AISI 431 are not suitable for the manufacturing of rice transplanter claws with a press brake due to their reduced elongation at break, which causes cracks to form along the edge of the bend. Therefore, it is recommended that a press brake with a maximum force of at least 2 metric tons be used in the manufacturing of rice transplanter claws.

The decision to complete the bending operation of the rice transplanter claw manufacturing process by mechanical/hydraulic press or press brake is primarily determined by the cost of the machinery. If the spare parts manufacturer does not own a

mechanical/hydraulic press or press brake, it is recommended that a mechanical/hydraulic press with a maximum force of at least 50 metric tons be purchased to complete the bending operation because mechanical/hydraulic presses were found to be less expensive than press brakes during the review of online marketplaces. However, if the spare parts manufacturer owns either a mechanical/hydraulic press or press brake with adequate maximum pressing force, it is recommended that the existing machinery be used to complete the bending operation.

2.7.8 Section Summary

The Results and Discussion section of Chapter 2 consists of seven main subsections: XRF Results, Hardness Testing Results, Experimental Testing Results, DEFORM simulation results, DEFORM bending sensitivity analysis, DEFORM validation, and Discussion and Recommendations. The XRF Results section presents the material composition results and comments on their application on selecting the appropriate stock materials for rice transplanter claw manufacturing in Bangladesh. The Hardness Testing Results section presents the results of the hardness testing conducted on the original and locally produced rice transplanter claws. The use of hardness testing in stock material selection and quality control testing are discussed. The Experimental Testing Results compares the results from the experimental testing of the bending punch and die set to that of the original rice transplanter claws. Differences in the experimental test and original claws are discussed along with the changes made to the design of the bending punch and die to alleviate these differences. Next, the DEFORM simulation results of the final design of the bending punch and die set are compared to the original

rice transplanter claws to determine the results changes from the experimental testing. Calculations for the springback of the claws due to the unloading of the press are also presented. The DEFORM Bending Sensitivity Analysis section presents the force required to reach a die stroke of 9 mm for four grades of stainless steel. The sensitivity analysis was completed to determine the effects of variation in material properties of the force required for bending. The DEFORM validation section presents the verification and validation of the DEFORM bending model through mesh convergence and experimental testing. Finally, the Discussion and Recommendations section discusses the potential of spare parts manufacturers in Bangladesh to manufacture spare rice transplanter claws accurately and at a profit. The recommended equipment the manufacturing of spare rice transplanter claws are also discussed.

2.8 Chapter Summary

Chapter 2 is divided into seven sections. Section 1 introduces the process of rice transplanting, operation of the rice transplanter, and the current state of the local rice transplanter claw manufacturing. Section 2 provides a literature review of published literature, video media, and online marketplaces regarding the manufacturing of rice transplanter claws. Section 3 describes the characterization of the original rice transplanter claws and the development of the manufacturing process through a combination of factory layout, cost, and market analysis. Section 4 provides a breakdown of the design of the required tooling for the manufacturing processes determined in Section 3. Section 5 provides a description of the experimental testing and procedures for

the bending punch and die set developed for the bending of the rice transplanter claws.

Section 6 describes the finite element analysis software setup which was used for all FEA

simulations. Section 7 provides the results and discussion of the characterization of the

original rice transplanter claw, experimental testing, and finite element simulations.

Finally, recommendations of equipment/machinery are made for the small machine shops

and CSISA-MEA staff in Bangladesh.

The next chapter presents the development of the combine harvester blade

manufacturing process which is broken down in seven sections.

CHAPTER 3

Development of Combine Harvester Blade Manufacturing Process

3.1 Introduction

3.1.1 Combine Harvester Cutter Bar Operation

Combine harvesters are agricultural machines that are used to reap, thresh, and winnow grains in a single continuous process. The use of a combine harvester greatly reduces the required labor to harvester both rice and wheat when compared to traditional manual processes and to mechanization of the individual harvesting steps (reaping, threshing, winnowing). Table 20 displays a comparison of the labor requirements for reaping, threshing, and winnowing rice for all three methods. The traditional and individual mechanization harvesting methods require approximately 28 and 15 times more labor compared to the use of combine harvester (Nath et al., 2022). The reduction in labor provides a farmer protection from the shrinking agricultural labor market and rising labor wages while reducing the drudgery and time required for manual harvesting.

Table 20: Comparison of labor required for rice harvesting

Harvesting Method	Traditional (manual)	Individual mechanization	Combine harvester
Labor, $\frac{\text{man hour}}{\text{ha}}$	283	154	9.87

The first step in the grain harvesting process is to reap or cut the stalks of the rice/wheat so that it can either be processed manually, through mechanized threshing and winnowing, or processed immediately within the combine harvester. Currently, there are three types of machinery that use cutter bar blades in Bangladesh: reapers, full-feed combine harvesters, and half-feed combine harvesters. Reaping is accomplished by a reciprocating cutter bar with blades that is attached along the bottom front edge of the combine harvester. Figure 48 shows a full-feed combine harvester. Figure 49 shows a half-feed combine harvester (Ansar Energy, 2013).

Figure 48: Full-feed combine harvester

Figure 49: Half-feed combine harvester operating in Bangladesh

Figure 50 shows a cutter bar of a half-feed combine harvester. The half-feed combine harvester cutter bar consists of top and bottom sets of blades. The bottom set of blades are attached to the bottom cutter bar base by press pins. The bottom cutter bar base is attached to the combine harvester through the mounting holes shown in Figure 50. The top set of blades are attached to top cutter bar base by press pins. The top cutter bar base attaches to reciprocating arms that provide the horizontal linear motion of the top set of cutter bar blades. The cutting force and shearing force between the top and bottom sets of blades acts to cut the crop stalks. The cutter bar binder bolts into the lower cutter bar base and sets the clearance between the top and bottom blades through a combination of spacers and shims.

Cutter bar
top base

Cutter bar
binder

Cutter bar
bottom base

Cutter bar
mounting holes
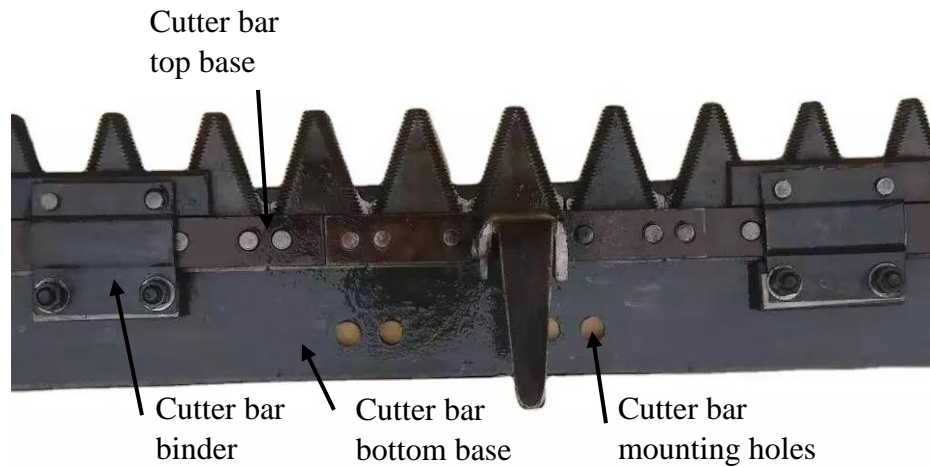
Figure 50: Half-feed combine harvester cutter bar

Figure 51 shows a cutter bar of a full-feed combine harvester. The full-feed combine harvester cutter bar consists of one set of blades attached to a cutter bar base using press pins. The cutter bar base is attached to a reciprocating arm, which creates the horizontal linear motion of the blades. The cutter bar base and blades move within a set of combine harvester tines, which act to hold the crop stalks so that shearing and cutting forces can be applied by the reciprocating blades. The operation of the full-feed combine harvester cutter bar is shown in the YouTube video by John Deer Harvester Repair (2020).

Figure 51: Full-feed combine harvester cutter bar

3.1.2 Combine Harvester Blade Manufacturing Introduction

The OEM combine harvester cutter bar blades provided with both full-feed and

half-feed combine harvester models wear down or break due to rapid and repeated

contact with the crop stalks and debris within the field (rocks, soil, etc.). The high

temperature and humidity within Bangladesh also contribute to the debris and rust

buildup on the combine harvester blades. The accumulation of rust and debris eventually

leads to premature failure of the cutter bar system due to increased friction between the

top and bottom sets of blades of the cutter bar. Figure 52 shows a full-feed combine

harvester cutter bar with a broken blade caused by contact with a brick while in

operation. Figure 53 shows a half-feed combine harvester cutter bar blade with debris

buildup and a broken blade.

Figure 52: Full-feed combine harvester cutter bar with broken blade

Figure 53: Half-feed combine harvester cutter bar with broken blade

The breaking of cutter bar blades and the buildup of rust and debris has created a

market for the manufacturing of spare combine harvester blades for both the full-feed and

half-feed combine harvesters. The full-feed cutter bar, shown in Figure 51, consists of

only one type of combine harvester blade shown in Figure 3. The half-feed combine

harvester cutter bar, shown in Figure 50, consists of three different types of blades shown

in Figure 4. The half-feed combine harvester blades are referenced by their location on

the cutter bar (top or bottom cutter bar) and their size as shown in Figure 4.

Table 21 lists the manufacturer and operator specified run times and prices for

imported and OEM cutter bars. The data were collected by CSISA MEA partners in

Bangladesh. Due to the limited run time of 200-300 hours for the average quality cutter

bar, the manufacturing of spare combine harvester blades has been established as a

needed advancement to continue the adoption of combine harvesters within Bangladesh.

Table 21: Combine Harvester Cutter Bar Run Times for Premium and Classic Quality

Cutter Bar	Manufacturer specified run time (hours)	Operator specified run time (hours)	Price (BDT)	Price (USD)
OEM	500-600	400-500	43,000	$500
Imported	200-300	150-200	15,000	$175

Small and medium sized machine shops have expressed interest in manufacturing

combine harvester blades in addition to the agricultural spare parts they currently

manufacture. However, the economic situation of the small and medium sized machine

shops has led to the manufacturing of combine harvester blades using manual processes

such as fabricating the individual teeth using an angle grinder. The reliance on manual

processes such as angle grinding does not allow for adherence to any tolerance standards

resulting in a complete lack of repeatability in the manufacturing process. The stock

materials used in the fabrication of the combine harvester blades often come from

dismantled, decommissioned ships that are cut into pieces in shipyards in southeastern

Bangladesh and sold as scrap material in the local markets throughout the country.

Therefore, the specific alloy of the metal used is not known to any degree of certainty as

the scrap materials are labeled as cast iron, mild steel, stainless steel, carbon steel, and

aluminum. This results in unpredictable mechanical properties such as hardness or tensile

strength. Figure 54 shows an example of a combine harvester blade fabricated by NRE, a

Bangladesh machine shop, with an OEM blade as reference.

Figure 54: Original combine harvester blade (left); NRE manufactured combine harvester
blade (right)

The goal of the work presented in this chapter is to improve the quality of

combine harvester cutter bar blade manufacturing by the small and medium sized

machine shops given the economic and skill constraints in Bangladesh. The ability to

manufacture high-quality combine harvester blades within Bangladesh will reduce the

need to import spare parts from the international markets. The domestic production of combine harvester blades will also result in the growth of the agricultural spare parts and machinery manufacturing industry, a main goal of Bangladesh's agricultural mechanization policy (Ministry of Agriculture, 2020). Domestically producing the parts will also reduce lead times and the logistical constraints of ordering and receiving shipments of foreign produced combine harvester blades.

The work presented in this chapter incorporates the development of a combine harvester blade manufacturing process that has been tailored to the conditions and machinery that is available to the small machine shops in Bangladesh. The first section contains a survey of published literature, video media, and online marketplaces regarding the current combine harvester blade spare parts market and the manufacturing of combine harvester blades. The second section presents the manufacturing method selection, which explains the process taken to characterize the original combine harvester blade, develop manufacturing process charts and cost analysis, and select the most appropriate manufacturing process for the agricultural spare parts manufacturers in Bangladesh. The third section contains the modeling, simulation, and experimentation used in the development of the blanking and forging die sets required to manufacture the combine harvester cutter bar blades. The fourth section presents the findings made during the characterization of the combine harvester blade, results from the experimental testing and FEM simulations, and validation of the FEM model.

3.2 Literature Review

A survey of literature, video media, online marketplaces, and the local Bangladesh market was completed regarding the current combine harvester blade spare parts market and the manufacturing of combine harvester blades. The survey of published literature revealed no published paper regarding the manufacturing of combine harvester blades. The survey of video media identified three videos showing the blanking, forging, and heat treatment steps of the combine harvester cutter bar blade manufacturing process. The survey of online marketplace such as Made-in-China (www.made-in-china.com) and indiamart (www.indiamart.com) identified the combine harvester spare parts currently available. The goal of the work presented in this section is to review the current products sold by dealers in Bangladesh as well as the video media and online marketplace listings found during the literature review so that an understanding of the current manufacturing processes and materials used in the combine harvester blade spare parts market can be developed.

Currently, almost all of the combine harvester spare cutter bar blades are imported from China into Bangladesh and sold through local spare parts dealers. As shown in Table 21, the imported blades are of lower quality than the original combine harvester blades, which leads to premature failure of the cutter bar. Figure 55 shows the imported half feed combine harvester blades currently sold in the Bangladesh spare parts market. Table 22 lists the dealer sales price for the full feed and half feed combine harvester blades in Bangladesh. Samples of the imported spare combine harvester cutter bar blades were not collected, therefore testing of the mechanical properties of the imported blades could not be conducted.

Figure 55: Spare half feed combine harvester blades in Bangladesh. From Left to Right: large bottom blade, top blade, half blade, and small bottom blade

Table 22: Prices of combine harvester blades from Bangladesh spare parts dealers

Blade	Price (USD)
Full feed	1.08
Half feed small bottom blade	1.51
Half feed large bottom blade	3.76
Half feed top blade	1.61

The survey of online marketplaces helped identify spare parts manufactured in both China and India. Common steel grades used in the manufacturing of combine harvester blade is 65Mn and En42J, which are high carbon manganese alloyed spring steel (JRS Farmparts, n.d.; Weifang, n.d.). The equivalent AISI grades for 65Mn and En42J were found to be AISI 1556 and AISI 1080 respectively. Table 23 lists the elemental composition the steels (Steel Grades, 2018; Grade 65Mn, 2022; SAE AISI 1080, 2019.; Aerospace Alloy, 2019).

Table 23: Elemental composition of imported combine harvester blade stock material

Chemical Composition, %						
Material	C	Mn	Si	Cr≤	Ni≤	Cu≤
65Mn	0.62 – 0.70	0.90 – 1.20	0.17 – 0.37	0.25	0.35	0.25
AISI 1566	0.6 – 0.71	0.85 – 1.15	0.07 – 0.6			
En42J	0.75 – 0.85	0.60 – 0.90	0.0 – 0.35			
AISI 1080	0.075 – 0.88	0.60 – 0.90				

The first video reviewed was published on YouTube by BESCO Machine Tool Limited headquartered in Shandong Province, China (BESCO, 2019). BESCOMT supplies machine tools and supporting equipment for the forging and stamping industries. The video presents the BESCO reaper blade making machine which consists of a blanking punch and die set and forging punch and die set. The blanking punch and die set fabricates two blanks and the mounting holes of the blanks in a single operation. The blades are blanked from a sheet of stock material that is held in place by a stock guide in front of the die set. Figure 56 shows the blanking punch and die set mounted to a press with the features labeled. The die is mounted on the top press plate with an internal stripper that eject the blanks from the die after the blanking operation. The punches are mounted under the base plate that acts to hold the stock material. Guide rods on the far side of press align the upper and lower dies so that the proper clearance between punch and die are maintained throughout the blanking process.
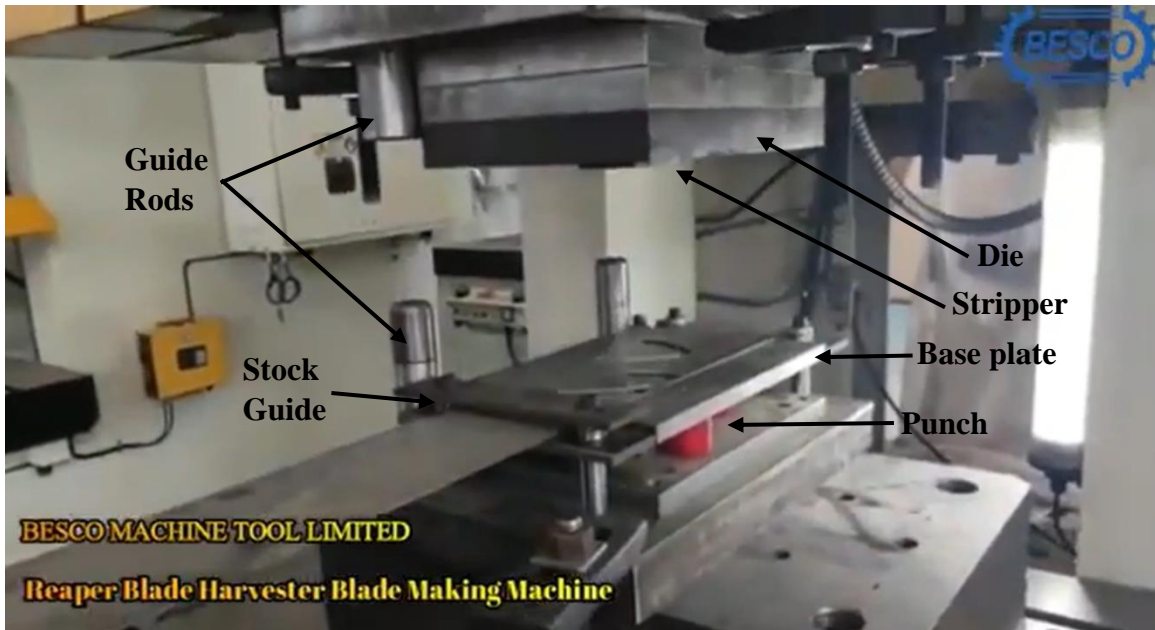
Figure 56: BESCO combine harvester blade blanking punch and die set

Figure 57 shows the forging punch and die set mounted to a press with features labeled. The punch is mounted on the top press plate and the die is mounted on the bottom press plate. The die contains two parts: a spring-loaded base plate that acts to hold the blank prior to forging and ejects the blank after the forging operation and the cavity that creates the serrated edge during the forging operation. Guide rods are mounted on either side of press to maintain clearance between the punch and die.

Figure 57: BESCO combine harvester blade serrated edge forging punch and die set

The second video reviewed was published on YouTube by Greenly Machinery headquartered in Zhejiang Province, China. Greenly Machinery supplies agricultural products such as flanges, chains, and hubs (Greenly Machinery, 2012). The video presents the Greenly manufacturing process for forging the teeth on the harvester cutter bar blades. Figure 58 shows the setup of the hydraulic press with labeled features. The punch is attached to the top press plate and the die is mounted on the bottom press plate. The cavity which forms the serrated edge of the combine harvester blade is in the upper punch as opposed to the BESCO forging punch and die set which positioned the cavity on the lower press plate. The die, as shown in Figure 59, has a protruding ledge that acts as a stripper to remove the blade from the punch after the forging operation. After the forging operation the loading arm pushes a blade blank onto the die that forces the forged

107

blade to slide into a storage container behind the press. Figure 60 shows the blades after the forging operation.
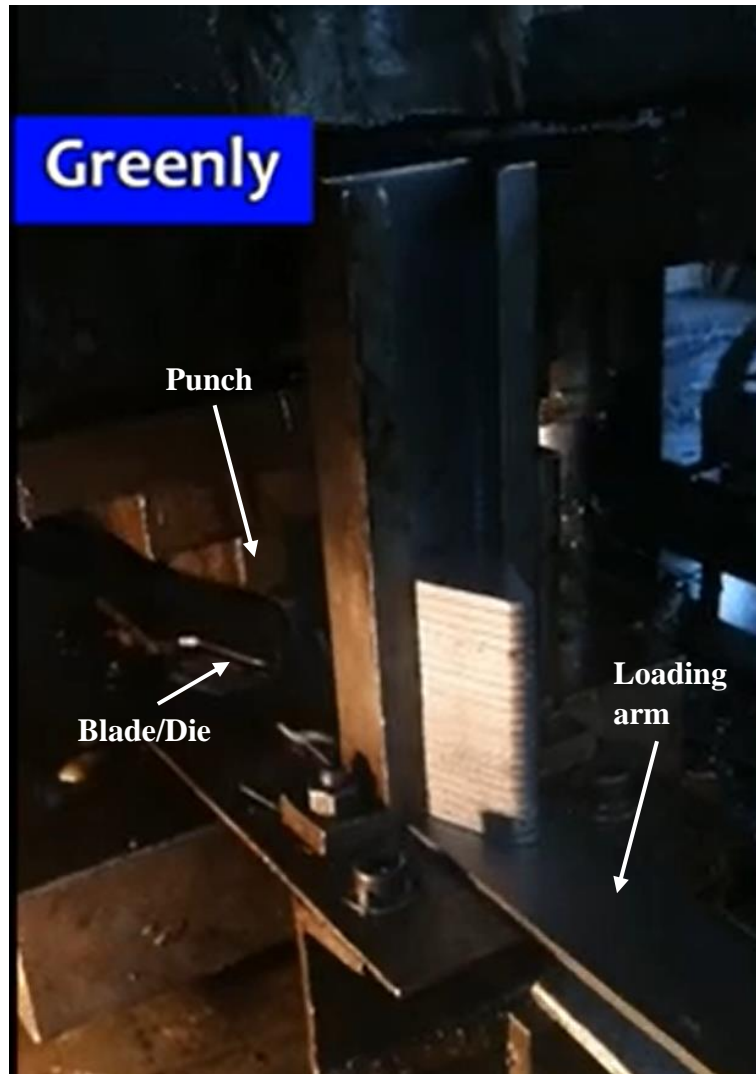
Figure 58: Greenly Machinery combine harvester blade serrated edge forging
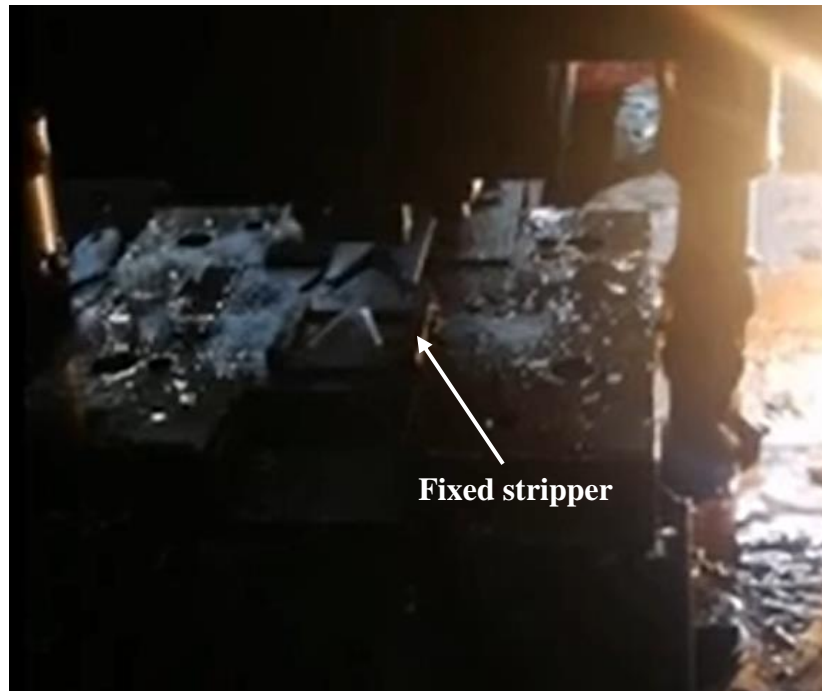
Figure 59: Rear view of Greenly Machinery combine harvester blade serrated edge forging

Figure 60: Post serrated edge forging combine harvester blades

The third video reviewed during the literature review was published on YouTube by Jatinder Singh Kundi (2013). The video demonstrates the heat treatment of the blade using electromagnetic induction. Figure 61 shows the induction heat treatment setup with labeled features. The induction coils are curved so that the edge of the blade is heated to ensure a proper heat treatment along the serrated edge of the blade. A blade locking mechanism is used to keep the blade locked into position throughout the heating process. Once the blade reaches the proper temperature for heat treatment, the operator releases the locking mechanism, which allows the blade to fall downwards presumably into an oil or water filled quench tank.
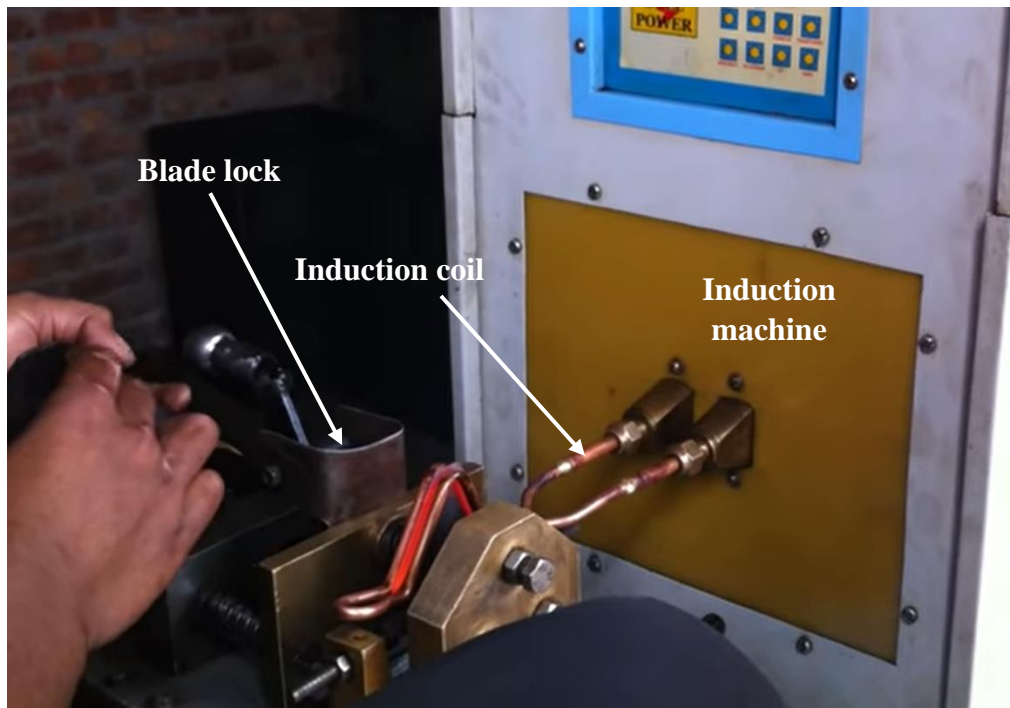
Figure 61: Heat treatment of combine harvester blades using electromagnetic induction

3.2.1 Section Summary

The Literature Review section of Chapter 3 presented the results of a survey of published literature, video media, and online marketplaces. The survey of published literature found no articles on the manufacturing of combine harvester blades. The survey of video media identified three videos showing the blanking, forging, and heat treatment steps of the combine harvester cutter bar blade manufacturing process. The survey of online marketplace such as Made-in-China (www.made-in-china.com) and indiamart (www.indiamart.com) identified the stock materials used for the manufacturing of spare combine harvester blades as well as the process of heat treatment using an induction furnace.

The next section describes the characterization of the original combine harvester blades using hardness and material composition testing, as well as an analysis of the manufacturing markers such as the witness marks found in the mounting holes. Next, the development of the manufacturing process is presented through a combination of manufacturing morphological charts, production cost analysis, and market analysis.

3.3 Manufacturing Method Selection

3.3.1 Material Characterization

The original combine harvester blades and scrap materials used to manufacture them in Bangladesh were tested for elemental composition and hardness using an x-ray fluorescence (XRF) spectrometer and Rockwell hardness tester using the same methods as described in Chapter 2 Section 2.3 Subsection 2.3.1 Material Characterization. The

determination of the elemental composition, hardness, and tensile strength of the original

and locally manufactured combine harvester blades allowed recommendations for various

material and material properties to be given to the CSISA-MEA partners in Bangladesh.

As most of the stock materials in Bangladesh are obtained through the ship breaking

market and specific materials grades are not known, the material characterization of the

original combine harvester blade established product quality testing metrics to determine

if materials in the scrap market are suitable for the manufacturing of combine harvester

blades. Characterization of the original combine harvester blades also establishes

production quality checks for locally manufactured parts.

3.3.2 Manufacturing Method Selection

The first step taken in developing an effective manufacturing process for

producing combine harvester blades in Bangladesh was an inspection of the original

combine harvester for manufacturing marks. The evaluation of the various manufacturing

marks allowed for the 'reverse engineering' of the original manufacturing processes,

which would then be adjusted for the constraints faced by local manufacturers in

Bangladesh. Next, a morphological chart of possible manufacturing processes for each

product feature were created ranging from the least to most capital investment needed for

the process. Manufacturing methods that were determined to be unfeasible in Bangladesh

were eliminated from the morphological chart. The remaining manufacturing methods are

then sorted into three possible manufacturing processed based upon production volume.

Collaboration with CSISA-MEA members in Bangladesh on suitable manufacturing

methods provided additional information on available machine tools and the amount of

capital owners are willing to invest in the creation of a new manufacturing process. Cost analyses including machinery, labor, and material costs are then performed on the proposed manufacturing processes to determine the cost of production of a single part based upon a variety of factors. Once the appropriate manufacturing processes are chosen, the tooling required for the blanking and forging operations are developed using design references, finite element analysis, and experimental testing. After conducting the experimental testing, the results are analyzed, and the appropriate adjustments were made to the design of the tooling.

Manufacturing marks on the original combine harvester blades were analyzed to determine the manufacturing process used by the original manufacturer so that adjustments could be made to satisfy the constraints faced by machine shops in Bangladesh. The initial step was to identify the features of the combine harvester blade. Figure 62 shows the original half-feed combine harvester small bottom blade with reference dimensions and Figure 63 shows the blade with the features labeled. The features are the general shape, ground top and bottom, mounting holes, and serrated edge. The general shape of the combine harvester blade is defined as the shape of the blade before the operations that create the mounting holes, serrated edge and ground surfaces (i.e., the combine harvester blade blank).
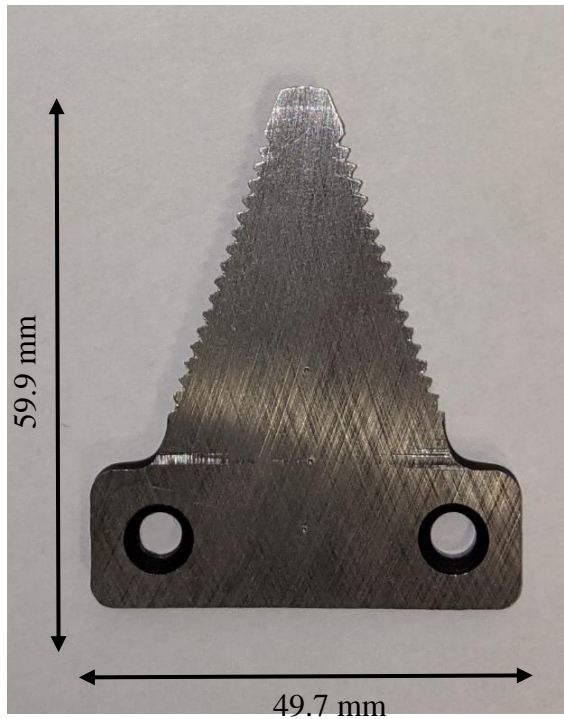
Figure 62: Half-feed combine harvester blade with basic size dimensions
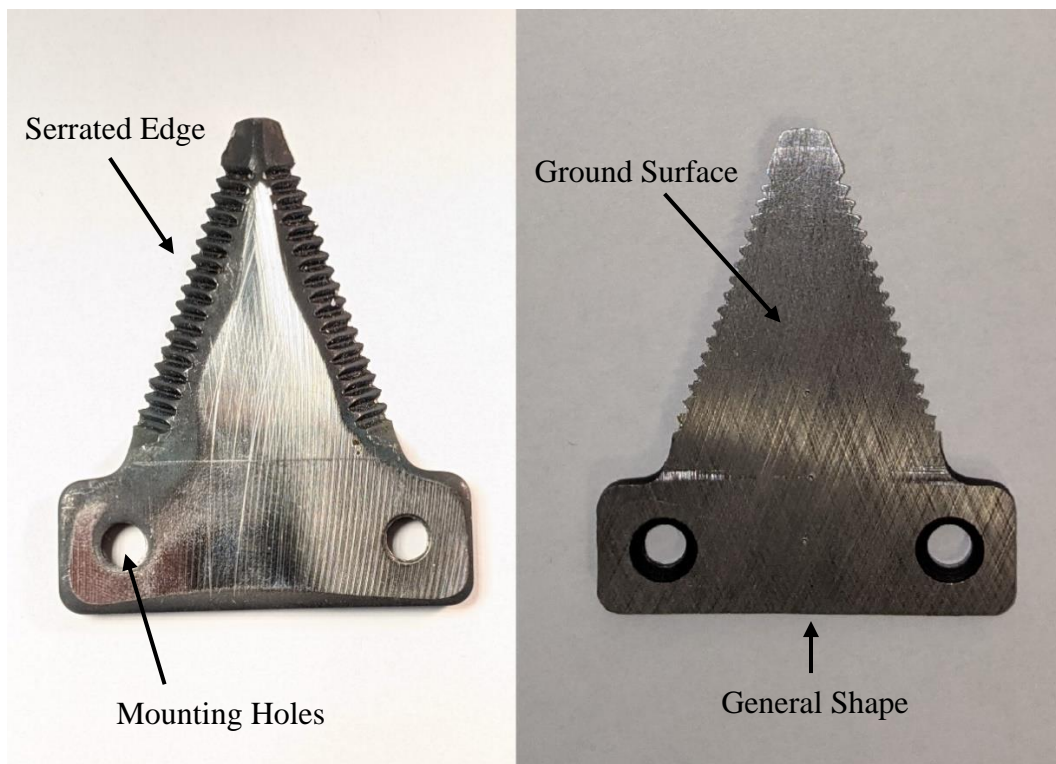
Figure 63: Half-feed combine harvester small bottom blade with labeled features

Visual analysis of the inside of the mounting holes reveals witness marks from a piercing operation. Similar witness marks are found along the outside of the edge of the blade therefore the general shape of the blade was likely blanked from a larger sheet of material. Figure 64 and Figure 65 show closeup images of the combine harvester mounting holes and outside edge witness marks.

Figure 64: Piercing witness marks on inside of mounting holes
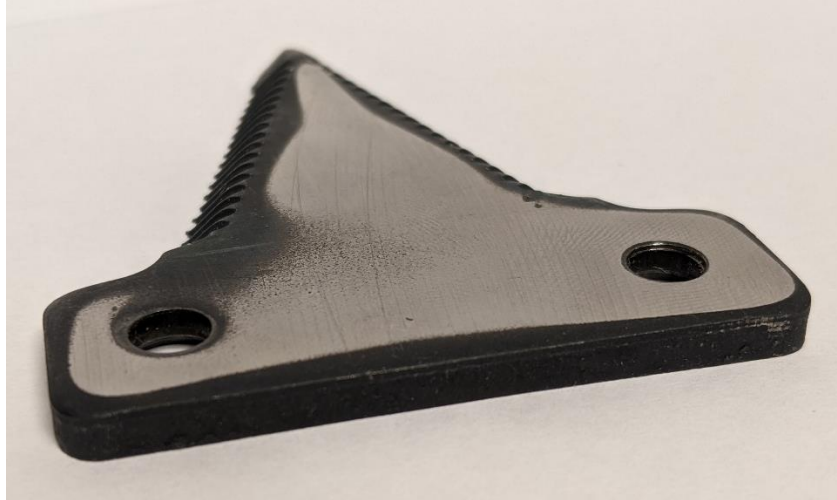
Figure 65: Blanking witness marks on outside edge of original half-feed combine
harvester blade

The serrated edges along the sides of the blade shows no grinding marks, therefore the

serrations were likely created through closed die forging of the blade edge. Figure 66

shows an up-close view of the serrated edge.
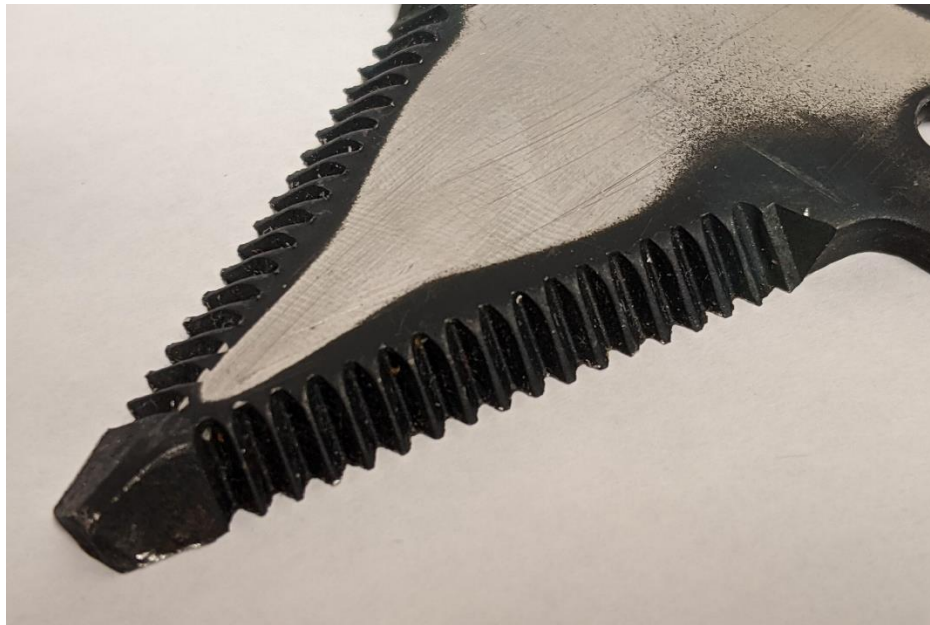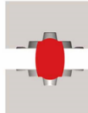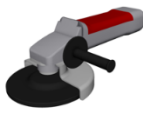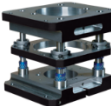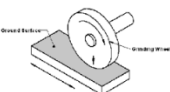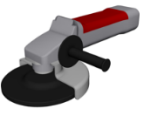
Figure 66: Serrated edge of original half-feed combine harvester blade

The initial characterization of the original manufacturing process led to the creation of a morphological chart of possible manufacturing techniques. Morphological charts are traditionally used for product ideation sessions by listing the product functions on the left most column and possible solutions across the rows (Boeijen et al., 2020). Table 24 shows the initial manufacturing morphological chart that lists the product features on the left most column and the proposed manufacturing techniques to create the feature to the right.
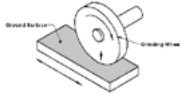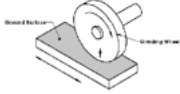
Table 24: Morphological chart of combine harvester blade manufacturing process

Feature	Solution #1	Solution #2	Solution #3
General Shape	Blanking	Bandsaw	
Serrated Edge	Forging	Angle grinding	
Mounting Holes	Drilling	Blanking	Piercing
Parallel sides	Surface grinding	Angle grinding	

Once the most appropriate manufacturing techniques were finalized based on the cost and availability constraints in Bangladesh, three manufacturing processes were

established based on the volume of production labeled as low, medium, or high. Table 25 shows the manufacturing processes for each feature for all three manufacturing processes.

Table 25: Combine harvester blade manufacturing processes by production volume

Feature	Low Volume	Medium Volume	High Volume
General Shape	Bandsaw	Blanking	Blanking
Serrated Edge	Forging	Forging	Forging
Mounting Holes	Drilling	Drilling	Piercing
Parallel sides	Angle grinding	Surface grinding	Surface grinding

The low-volume manufacturing process, shown in the second column from the left, relies more on manual labor therefore decreasing the initial capital cost of manufacturing process. The lower initial cost of the low-volume manufacturing is attributable to differences in the forming of the general shape, mounting holes, and parallel sides. The low-volume manufacturing method differs from both the medium- and high-volume manufacturing processes as it forms the initial shape of the blade using a band saw instead of blanking. The lack of a mechanical press as well as a punch and die

set reduces the initial cost of the machinery over the medium- and high-volume methods. The mounting holes are formed using a drill press further reducing cost over the high-volume method that creates the mounting holes by piercing using an additional mechanical press. The top and bottom the blades are then made parallel by a manual process with an angle grinder as opposed to a surface grinding used in the medium- and high-volume manufacturing. The initial capital investment of the low-volume manufacturing process is the lowest of the three methods because it relies more heavily on manual labor rather than the inclusion of higher priced machine tools. However, the reliance on manual labor contributes to this option having the lowest product quality because the effects of human error are amplified in processes such as grinding of the top and bottom of the blades.

The medium-volume approaches improve both the production and quality of the product by introducing the blanking punch and die set for forming the blade blanks and surface grinding to maintain flat top and bottom surfaces. The adoption of the blanking process significantly increases the initial capital investment due to the manufacturing of a punch and die set and the purchasing of a press that a higher maximum force. However, the addition of the blanking operation improves the product quality by replacing the imprecise manufacturing of the blanks on a bandsaw with the highly repeatable blanking process. The other addition in the medium-volume manufacturing process is the surface grinder for maintaining the proper thickness and flatness across the top and bottom surfaces of the blade. The surface grinder machine tool can be set to maintain a specific thickness as compared to the angle grinding used in the low-volume manufacturing. The implementation of the surface grinder greatly increases the accuracy and repeatability of

119

the thickness and flatness of the top and bottom blade surfaces, which are important for maintaining proper clearance between the blades. The production rate is also increased as the addition of the blanking and surface grinding significantly reduce the amount of time for their respective processes.

The high-volume manufacturing process further increases the production rate of manufacturing processes by replacing the drilling of the mounting holes with piercing using a mechanical press. The piercing punch can form both mounting holes simultaneously unlike a drill press which forms the two mounting holes independently. Although the use of a piercing operation increases the production rate of the manufacturing process, the use of a piercing operations requires the purchasing of appropriate punches and holders for the piercing of the mounting holes. These additional costs further increase the initial cost of the high-volume manufacturing process when compared to the low- and medium-volume approaches. Along with cost of purchasing the appropriate punches, the addition of two piercing operations increases the number of operations that require a mechanical press thereby forcing the machine shops to either invest in additional presses or swap punch and die sets more frequently. Due to these factors, the high-volume approach further increases the needed capital investment to purchase machinery and punches over that of the low- and medium-volume approaches.

Process charts, factory layouts, and cost analysis were done for the low-, medium-, and high-volume manufacturing process so that the economic differences of the processes could be studied quantitatively. Figure 67 shows a potential factory layout for the low-volume manufacturing process. The numbers associated with each machine tool indicate the number of workers in each area. The number of workers at each area was

kept to one for the low-, medium-, and high-volume manufacturing processes as increasing the number of workers artificially increases the production output. The production rate [$\frac{parts}{minute}$] of each manufacturing process is determined by dividing the time taken for the slowest operation of the manufacturing process by the number of workers performing the operation. For example, if a drilling operation takes 2 minutes to complete, a single operator is expected to complete 0.5 $\frac{parts}{minute}$ while two operators (on separate drill presses) would be expected to complete 1 $\frac{parts}{minute}$. Therefore, the number of workers at each area is set to one so that an objective comparison of the low, medium, and high-volume manufacturing process can be made.
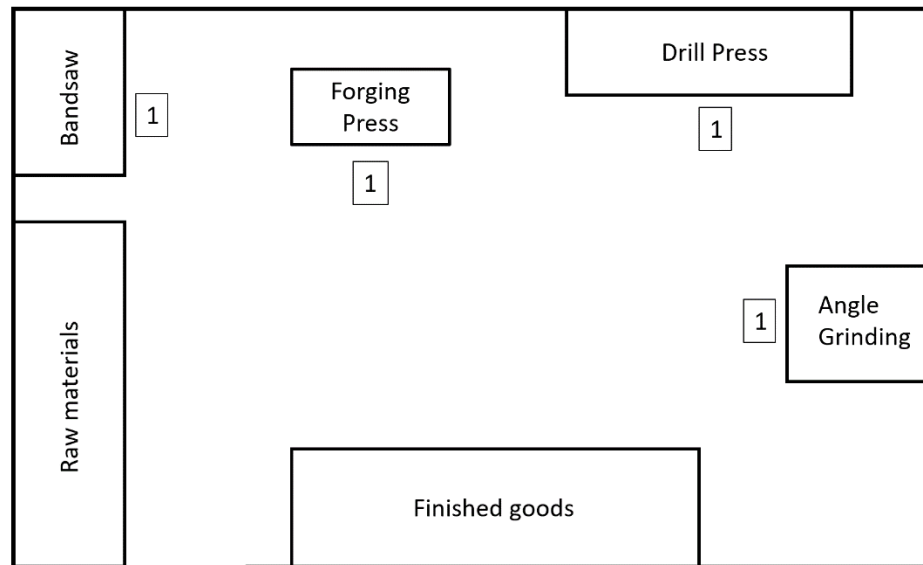
Figure 67: Proposed factory layout for low-volume production of combine harvester blades

The process flow chart, shown in Figure 68, displays the steps of the low-volume combine harvester blade manufacturing process. A description of each activity is provided on the left side of the process chart. The two columns to the right of the activity

description show the time required to complete the activity and the distance traveled for each activity. The time required for the heat treatment and cooling of the blades are left blank in Figure 68 as the parameters of the heat treatment process are determined by the specific grade of steel used in the manufacturing process. The distances are intentionally left blank in Figure 68 because the layout of the individual factories are not known. Next, each activity is identified as either an operation, transport, inspection, delay, or storage by placing an "X" under the specified column. The total time for each activity type is summed under each column. Finally, each activity is classified as either value added (VA) or non-value added (NVA). Operation and inspection activities are value added while transport, delay, and storage activities are non-value added. The number and time of all VA and NVA operations are shown at the bottom of the chart.

Step #	Activity description	Time (minutes)	Distance (meters)	Operation O	Transport ⇨	Inspection □	Delay D	Storage V	Value Category
1	Metal stored in storage							X	NVA
2	Move metal to cutting tool	2			X				NVA
3	Cut metal to form blanks	0.56-0.88		X					VA
4	Inspect blank for imperfections	0.1				X			VA
5	Move blanks to hydraullic press	0.25			X				NVA
6	Create serrated edge with press	0.15						X	NVA
7	Inspect serrated edge	0.05						X	NVA
8	Move to drill press	0.25					X		NVA
9	Create mounting holes with drill press	0.2		X					VA
10	Move to angle grinder	0.25			X				NVA
11	Grind top and bottom of blade until flat	0.5		X					VA
12	Move to heat treatment	0.5			X				NVA
13	Heat treat blades			X					VA
14	Cool blades			X					VA
15	Store finished part	0.25						X	NVA
16									
17									
18									
19									
20									
	Count:			5	4	1	1	4	
	Time per process step:			0.7	3	0.1	0.25	0.45	

Total VA	6	
VA Time	0.8	Minutes
Distance traveled	0	Meters

Total NVA	9	
NVA Time	3.7	Minutes
Lead Time	5	Minutes

Total ENVA	0	
ENVA Time	0	
VS Ratio	17.778%	

Figure 68: Process chart for low-volume manufacturing process of combine harvester blades

122

The times required for each operation of the process charts were determined through collaboration with CSISA MEA partners in Bangladesh as well as the analysis of the manufacturing operation for steps 3 and 9. The time required for step 3, cut metal to form blanks, was determined using recommended cutting speeds for carbon steel on a bandsaw. The recommended cutting speed was found to be 5-7 squared inches per minute (SIPM) (Sawblade, 2015). The square inches required to create the largest and smallest blanks were found to be 0.846 in^2 and 1.36 in^2 respectively. These values were determined by multiplying the blank's thickness by the blank's perimeter. The time required to complete each operation was then determined using a cutting speed of 6 SIPM resulting in cutting times of 0.14 min and 0.22 min. These cutting times then were multiplied by a factor of four due to the complexity of the blanks shape resulting in the range of $0.56 - 0.88$ minute shown in Figure 68.

The time required to complete step 9, which is to create mounting holes with the drill press, was calculated by determining the appropriate speeds and feeds for the specified diameter and material. The mounting hole diameters were found to be 5.0 mm and the material chosen for the analysis was AISI 1035. A feed rate of 0.003" per revolution and a speed of 60 surface feet per minute (SFPM) were determined (Viking Drill and Tool, 2015). The revolutions per minute (RPM) for the specified speed was found to be 1163 RPM (Equation 31).

$$\frac{60 \text{ SPM}}{\pi * \frac{1}{12} * 0.197 \text{ inch}} = 1163 \text{ RPM}$$

(31)

Given the feed rate of 0.003 inch per revolution and a material thickness of approximately 0.16 inches, the number of revolutions in the drilling operation was determined to be 53 revolutions. Therefore, the time to complete the drilling of one mounting hole was determined to be 0.05 minutes (Equation 32)

$$53 \text{ rev} \cdot \frac{1}{775 \frac{\text{rev}}{\text{min}}} = 0.05 \text{ min}$$

(32)

The time value in Equation 32 was multiplied by a factor of four to determine the time required for the drilling operation of 0.2 min. A multiplication factor of four was used due to the drilling of the two mounting holes and the time necessary to position the blade for each drilling operations.

Finally, a cost analysis was performed on the low-volume production method to determine the selling price of the combine harvester blades so that the initial equipment costs are recouped in 18 months of operation. It is assumed that a loan for the entire cost of the machinery is borrowed by the spare parts manufacturers with a length of 18 months and an interest rate of 9%. Payments for the loan are made monthly. The loan length, interest rates, and payment plan are the average for loans provide to ABLEs in Bangladesh. The loan information was provided by CSISA-MEA staff in Bangladesh. Other factors such as the required factory size for each manufacturing method are not considered in the cost analysis. Table 26 shows the cost analysis breakdown for the proposed low-volume production factory. The first step in determining the selling price was to determine the cost of the initial capital investment. Equipment prices were determined through online sellers within Bangladesh as well as from listings on

indiamart.com because the prices of larger machinery are difficult to determine within Bangladesh due to import duties and other regulations. Table C1 in Appendix C lists the individual machinery costs and links for purchasing. Next, the total monthly costs were determined by calculating the monthly loan payments and multiplying by 18 months, the length of the loan. Equation 33 shows the equation for the total machinery cost.

$$Total\ Machinery\ Cost = 18 \cdot Base\ Machinery\ Cost \cdot \left[\frac{0.09(1 + 0.09)^{18}}{(1 + 0.09)^{18} - 1}\right]$$

(33)

Next, the wage rates for the factory are calculated using an hourly wage for one employee. The cost of both the blanking and forging die sets were determined by combining the cost of the tool steel and machining of the punch and die sets. The cost of the tool steel in Bangladesh was determined using the Bangladesh Industrial Technical Assistance Centre's material price list (BITAC, n.d.). The hourly wages for a factory worker in the agricultural spare parts industry was established by converting and averaging the daily and monthly wages of medium skilled workers throughout three cities in Bangladesh. Worker's salary data were established through contact between members of the CSISA-MEA project in Bangladesh and individual factory managers. Material cost per part then was determined by multiplying the price of mild steel plate per kg by the weight of a single blank, which was calculated by multiplying the blank volume by the density of mild steel. The parts produced per minute were estimated by determining the parts per minute for the slowest operation on a single part within the manufacturing process. As shown in the low-volume process control chart in Figure 68, the operation that requires the longest time is the cutting of the blanks by the bandsaw at $0.56 - 0.92$ minutes per operation. For the low-volume cost analysis, the average bandsaw cutting

time for the four combine harvester blades was used resulting in 1.33 parts per minute. Finally, the cost per part is calculated using Equation 34.

$$\frac{Total\ Machinery\ cost\ +\ 1.5\ [yr]\left[\frac{Parts}{yr}\cdot\frac{Material\ cost}{part}(1-Downtime[\%])+\frac{Wages}{yr}\right]}{\frac{Parts}{yr}\cdot(1-Downtime[\%])\cdot 1.5\ [yr]}$$

(34)

The yearly material and wage costs as well as the yearly production are established by converting from a per minute or hourly basis to a yearly basis using the 2400 working hours per year. The 2400 working hours per year is based on the standard work week in Bangladesh which is a 6-day work week with 8 working hours per day. The production line downtime of 20% is set for machine tool failures, maintenance, power outages and other events which result in production line being nonoperational. The base cost per part refers to the cost per part if no money is borrowed by the spare parts manufacturer. The cost per part with loan refers to the cost per part if all the money for the machinery is borrowed through an 18-month loan with a 9% interest rate. The cost per part required to recoup the initial investment in 18 months is $0.27 if a loan is borrowed. If the spare parts manufacturer purchases the machinery without a loan the cost per part required to recoup the initial investment in 18 months is $0.24.

Table 26: Low-volume combine harvester manufacturing process cost analysis

Manufacturing Method:	Low Volume	
Equipment Costs		
Feature	Equipment	Price [USD]
General shape	Bandsaw	523
Serrated edge	300 ton press	6827
	Forging punch/die set	470
Mounting Holes	Drill press	140
Parallel top and bottom sides	Angle grinder	43
Base Price		8003
Total Price		16453
Labor Costs		
# of workers		4
Hourly rate		0.84
Total wages per hour		3.36
Material Costs		
Mild steel per kg		1.32
Material cost per part		0.15
Manufacturing Time Analysis		
Parts per minute		1.33
Parts produced per day		511
Cost per part		
Hours per year		2400
Payback period [yrs.]		1.5
Downtime		20%
Process cost per part (no loan)		0.24
Process cost per part (loan)		0.27

Factory layouts, process charts, and cost analysis were also created for the medium- and high-volume manufacturing processes. Figure 69 and Figure 70 show the factory layout and process chart for the medium-volume production process. The factory layout and process charts have been modified to reflect the additional mechanical press used in the blanking operation and the surface grinder.
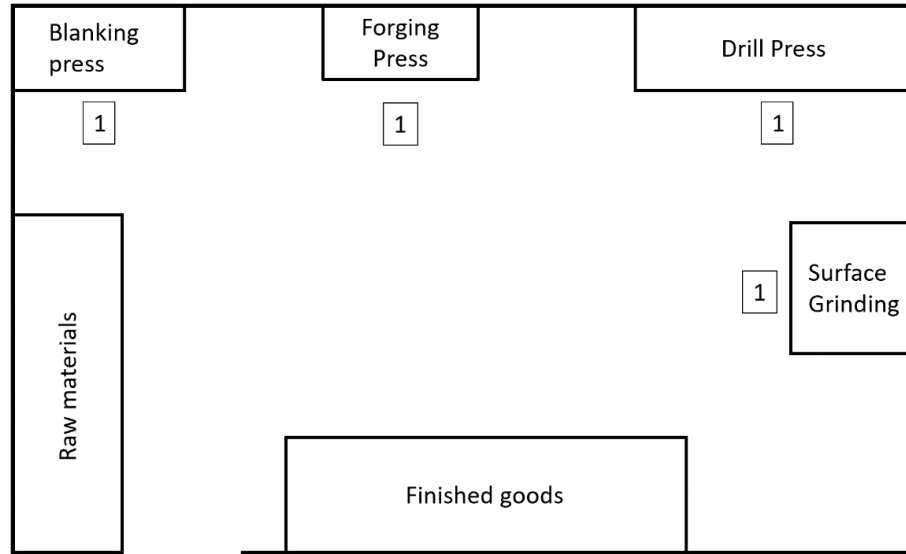
Figure 69: Proposed factory layout for medium-volume production of combine harvester blades

Step #	Activity description	Time (minutes)	Distance (meters)	Operation O	Transport ⇨	Inspection ☐	Delay D	Storage V	Value Category
1	Metal stored in storage							X	NVA
2	Move metal to cutting tools	2			X				NVA
3	Cut metal to size to fit in blanking die	0.5		X					VA
4	Move metal strips to press	0.25			X				NVA
5	Create blanks using press	0.1		X					VA
6	Inspect blanks	0.1				X			VA
7	Move blanks to hydraulic press	0.25			X				NVA
8	Create serrated edge	0.1		X					VA
9	Inspect serrated edge	0.1				X			VA
10	Move blanks to drill	0.25			X				NVA
11	Create holes using drill	0.2		X					VA
12	Move pickup forks to surface grinder	0.25			X				NVA
13	Grind top and bottom of blade flat	0.25		X					VA
14	Move to heat treatment	0.5			X				NVA
15	Heat treat blades			X					VA
16	Cool blades			X					VA
17	Store finished part	0.25						X	NVA
18									
	Count:			6	6	2	0	1	
	Time per process step:			1.15	3.5	0.2	0	0	

Total VA	8		Total NVA	7		Total ENVA	0
VA Time	1.35	Minutes	NVA Time	3.5	Minutes	ENVA Time	0
Distance traveled	0	Meters	Lead Time	5	Minutes	VS Ratio	27.835%

Figure 70: Process chart for medium-volume manufacturing process of combine harvester blades

Table 27 below shows the cost analysis for medium-volume production process of combine harvester blades. As shown in the bottom of the far-right column the cost per part required to recoup the initial investment within one year is $0.18 without a loan and $0.19 with a loan. Relative to the low-volume process the medium-volume production process reduces the cost per part by an average of $0.07 while tripling the number of parts produced in each time period. The reduction in production cost per part is due to the increased rate of production from 1.33 parts per minute to 4.0 part per minute. The addition of the blanking process eliminates the fabrication of the blanks as the slowest operation and the addition of the surface grinder reduces the amount of time required to grind the top of bottom of the blades flat. Therefore, the slowest operation of the medium-volume production process is the grinding of the top and bottom of the blade which has a time of 0.25 minutes per part.

Table 27: Medium-volume manufacturing process cost analysis for combine harvester blades

Manufacturing Method:	Medium Volume	
Equipment Costs		
Feature	Equipment	Price [USD]
General Shape	Mechanical press	1300
	Blanking punch/die set	512
Serrated edge	300 ton press	6827
	Forging punch/die set	470
Mounting Holes	Drill press	140
Parallel top and bottom sides	Surface grinder	1550
Base price		10,799
Total Price		19528
Labor Costs		
# of workers		4
Hourly rate per worker [USD]		0.84
Total wages per hour		3.36
Material Costs		
Mild steel per kg		1.32
Material cost per part		0.15
Manufacturing Time Analysis		
Parts per minute		4
Parts produced per day		1536
Cost per part		
Hours per year		2400
Payback period [yrs.]		1.5
Downtime		20%
Process Cost per part (no loan)		0.18
Process Cost per part (loan)		0.19

Figure 71 and Figure 72 display the example factory layout and process charts for the high-volume manufacturing process. The factory layout in Figure 71 shows the additional presses used to fabricate the mounting holes. The process chart in Figure 72 shows the change in the manufacturing process and corresponding operation times with the replacement of the drilling the mounting holes with the piercing operation.
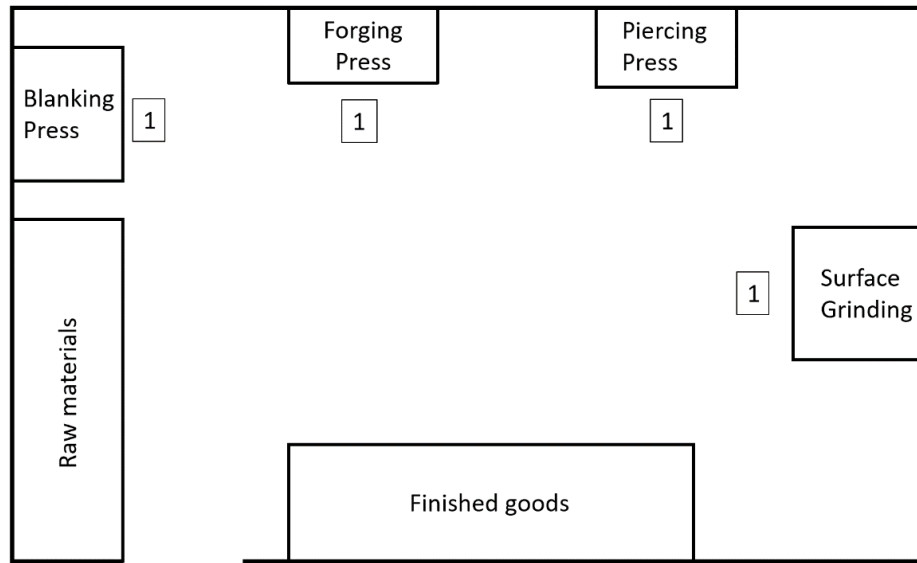
Figure 71: Proposed factory layout for high-volume production of combine harvester blades

Step #	Activity description	Time (minutes)	Distance (meters)	Operation O	Transport ⇒	Inspection ☐	Delay D	Storage V	Value Category
1	Metal stored in storage							X	NVA
2	Move metal to cutting tools	2			X				NVA
3	Cut metal to size to fit in blanking die	0.5		X					VA
4	Move metal strips to press	0.25			X				NVA
5	Create blanks using press	0.1		X					VA
6	Inspect blanks	0.1				X			VA
7	Move blanks to hydraulic press	0.25			X				NVA
8	Create serrated edge	0.1		X					VA
9	Inspect serrated edge	0.1				X			VA
10	Move blanks to piercing press	0.25			X				NVA
11	Create holes using press	0.1		X					VA
12	Move pickup forks to surface grinder	0.25			X				NVA
13	Grind top and bottom of blade flat	0.25		X					VA
14	Move to heat treatment	0.5			X				NVA
15	Heat treat blades			X					VA
16	Cool blades				X				VA
17	Store finished part	0.25						X	NVA
18									
	Count:			6	6	2	0	1	
	Time per process step:			1.05	3.5	0.2	0	0	

Total VA	8		Total NVA	7		Total ENVA	0	
VA Time	1.25	Minutes	NVA Time	3.5	Minutes	ENVA Time	0	
Distance traveled	0	Meters	Lead Time	5	Minutes	VS Ratio	26.316%	

Figure 72: Process chart for high-volume manufacturing process of combine harvester blades

Table 28 displays the cost analysis for the combine harvester blade high-volume manufacturing process. The production cost of producing the combine harvester blades to recoup the initial investment in one year is $0.16 without a loan and $0.17 with a loan. This represents a reduction in cost per part of $0.09 and $0.02 from the low- and medium-volume production methods. The production rate is increased to 10 parts per minute due to the fabrication of the mounting holes with piercing operations as opposed to the drilling medium-volume manufacturing processes. Therefore, the cost per part is reduced despite the increase in initial equipment cost of $4457 and $1382 over the low- and medium-volume manufacturing processes.

Table 28: High-volume manufacturing process cost analysis for combine harvester blades

Manufacturing Method:	High Volume	
Equipment Costs		
Feature	Equipment	Price [USD]
General Shape	Mechanical press	1300
	Blanking punch/die set	512
Serrated edge	300 ton press	6827
	Forging punch/die set	470
Mounting Holes	Mechanical press	1300
	Piercing punch/die	24
Parallel top and bottom sides	Surface grinder	1550
Base price		11983
Total Price		20910
Labor Costs		
# of workers		4
Hourly rate per worker [USD]		0.84
Total wages per hour		3.36
Material Costs		
Mild steel per kg		1.32
Material cost per part		0.15
Manufacturing Time Analysis		
Parts per minute		10
Parts produced per day		3840
Cost per part		
Hours per year		2400
Payback period [yrs.]		1.5
Downtime		20%
Process cost per part (no loan)		0.16
Process Cost per part (loan)		0.17

Table 29 shown below lists the cost per part (loan) for the low-, medium-, and high-volume manufacturing processes as well as the current dealer sales price for the full feed and half feed combine harvester blades. If it is assumed that the dealers apply a 200% mark up on the sales price, the cost per part low, medium, and high-volume

manufacturing methods are low enough to provide profit for the spare parts manufacturers. Therefore, according to the cost per parts presented for the low-, medium-, and high-volume manufacturing process, the manufacturing of spare combine harvester blades within Bangladesh is economically viable.

Table 29: Comparison of cost of manufacturing versus dealer sales price

Blade	Cost per part (USD)			
	Low Volume	Medium Volume	High Volume	Dealer
Full feed	0.27	0.19	0.17	1.08
Half feed small bottom blade	0.27	0.19	0.17	1.51
Half feed large bottom blade	0.27	0.19	0.17	3.76
Half feed top blade	0.27	0.19	0.17	1.61

The results shown in Table 29 indicate that the production of spare combine harvester blades in Bangladesh is economically viable through all three manufacturing processes shown in this thesis. The differences of the low-, medium-, and high-volume production process cost analyses show that, as the production of harvester blades increases, the cost per part required to recoup the initial investment decreases despite the increase in the initial cost of the machinery. However, this relationship between higher production rates and low cost per part is predicated on the assumption that there is sufficient market demand such that all parts which are produced are sold. Therefore, increasing a machine shop's rate of production may not be the best option as the market size for combine harvester blades within Bangladesh and the surrounding area may not be large enough to handle a high-volume production process. Therefore, the market size along with other factors such as shop floor size and initial capital investment must be considered when determining the most appropriate manufacturing process for spare parts

manufacturers in Bangladesh. Table 30 shows the total machinery cost, cost per part and

production rates for the low-, medium-, and high-volume production rates combine

harvester blade manufacturing processes.

Table 30: Total machinery cost, part cost, and production rate for combine harvester manufacturing

	Low Volume	Medium Volume	High Volume
Machinery cost (USD)	7,627	10,048	11,232
Cost per part (USD)	0.27	0.19	0.17
Production rate $\frac{parts}{day}$	511	1536	3840

As of 2021, an estimated 3020 combine harvesters are in operation throughout

Bangladesh (Alam, 2022). The half-feed combine harvester cutter bar blade contains of

52 blades and the full-feed model contains 38 blades. Assuming that the market is evenly

split between full-feed and half-feed models the average number of blades per combine

harvester is 45. Therefore, if it is assumed that all combine harvester blades are replaced

once per year then the current market size for combine harvester blades per year is

estimated to be 135,900, as shown in Equation 35.

$$\frac{\text{Market Size}}{\text{yr.}} = 3020 \text{ CH} \cdot 45 \frac{\text{blades}}{\text{CH}} \cdot 1 \frac{\text{replacement}}{\text{yr.}} = 135,900 \frac{\text{blades}}{\text{yr.}}$$

(35)

Table 31 shows the daily and yearly production rates for the low-, medium-, and

high-volume manufacturing processes. The yearly production rate is based on an 8-hour

6-day a week work week which is standard in Bangladesh. The standard work week

equates to 300 working days per year. From the results presented in Table 31, the yearly

production of the low volume manufacturing method most closely matches the current

estimated market size. The yearly production rate of the medium-volume manufacturing

method is approximately 3.5 times that of the current combine harvester blade market

size in Bangladesh. Therefore, it is recommended that the low-volume manufacturing

process be implemented if the local manufacturers plan to produce combine harvester

blades constantly throughout the year. However, if the local manufacturers plan to

fabricate the combine harvester blades based upon orders from local dealers, then the

medium-volume manufacturing process is recommended. The increased production rate

of the medium-volume manufacturing process will help reduce lead times between the

spare parts manufacturers and customers. The production rate of the high-volume

manufacturing process is approximately nine times higher than the estimated combine

harvester blade market size. The high-volume manufacturing process is not

recommended for local spare parts manufacturers unless the spare parts are to be

exported in large quantities.

Table 31: Production rates for low-, medium-, and high-volume combine harvester manufacturing processes

Process	Low	Medium	High
Daily Production	511	1536	3840
Yearly Production	153,300	460,800	1,152,000

A sensitivity analysis was conducted on the effect of batch size on part cost using

the part cost estimator in Ansys Granta EduPack 2021 published by Ansys, Inc.

(Canonsburg, Pennsylvania). Figure 73 shows the part cost estimation as a function of

batch size from one hundred parts to one million parts for two closed die forging

operations on annealed AISI 1060 steel. AISI 1060 was used in the part cost estimator because AISI 1070, the material proposed for the local manufacturing of combine harvester blades, is not available in the part cost estimator. AISI 1070 was chosen as the proposed material for local manufacturing of combine harvester blades due to its high strength, wear resistance, and high carbon content which allow for hardening of the serrated edge of the blade (1070 Carbon Steel, 2020).

The part length and mass were set to 0.233 ft. and 0.165 lb. The load factor was set to 50% and the overhead rate was set to $3.36 \frac{\text{USD}}{\text{hr}}$. The remaining parameters of the rice transplanter part cost estimator can be found in Table B2 in Appendix B.

The part cost, shown in Figure 73, follows an exponential decay as the batch size increases. The decrease in part cost is because an increase in batch size results in a larger number of parts to spread the fixed cost over, therefore the cost per part is inversely related to the batch size. In Equation 34, the fixed costs are the machinery and labor costs which do not change relative to the production rate. The current estimated market size of 135,900 blades per year corresponds to an estimated cost per part of approximately $0.25. As shown in Figure 73, a batch size of at least 10,000 parts is needed to maintain a low part cost over a large range of batch sizes. Therefore, at the current market size of 135,900 $\frac{\text{parts}}{\text{yr.}}$, the cost per part is not sensitive to fluctuations in market size.
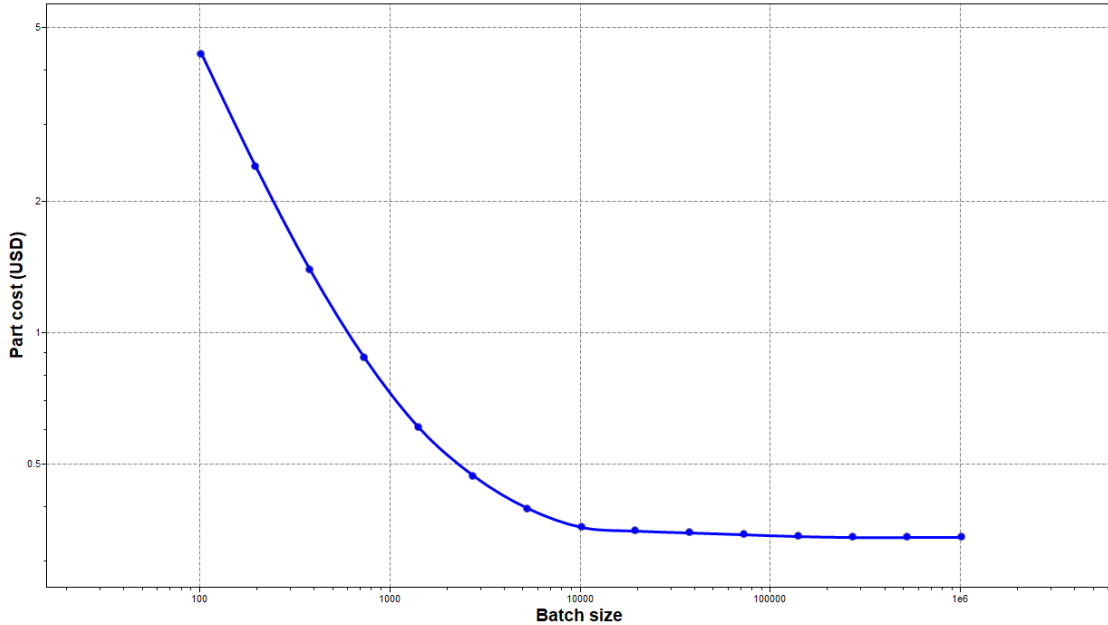
Figure 73: Part cost versus batch size for closed die forging operations

3.3.3 Section Summary

The Manufacturing Method Selection section of Chapter 3 consists of two subsections: material characterization and manufacturing method selection. The material characterization section provides an overview of the XRF material composition testing and Rockwell hardness tests performed on the original and locally produced combine harvester blades. Next, the original combine harvester blades were inspected for manufacturing markers such as the grinding pattern shown along the top and bottom sides of the blade as shown in Figure 63. Next, in the manufacturing method selection section, a list of possible manufacturing methods for each feature of the combine harvester blade is presented. Three manufacturing processes were then chosen based on a low, medium, and high volumes of production. Factory layouts, process charts, and cost analysis then are presented for all three manufacturing processes. The manufacturing costs per part for

the low-, medium-, and high-volume manufacturing processes were determined to be $0.27, $0.19, $0.17, respectively. The costs per part for the three manufacturing methods were then compared to the dealer sales prices of the full-feed and half-feed combine harvester blade and it was determined that the manufacturing of spare combine harvester blades in Bangladesh is economically viable. Next, a market size analysis was performed based upon the number of half-feed and full-feed combine harvesters in Bangladesh. The three manufacturing processes were then compared to the estimated market size. The low and medium volume manufacturing process was determined to be the recommended method for locally producing rice transplanter claws based upon the current estimated market size. Finally, a sensitivity analysis was performed using the Granta EduPack part cost estimator. The results of the part cost estimator revealed that the cost per part is not sensitive to changes in market size due to the large estimated market size.

The next section presents the design of the blanking and forging punch and die sets for the combine harvester blade manufacturing process.

3.4 Design of Tooling

3.4.1 Development of Combine Harvest Blade CAD Models

The design of the tooling for the blanking and forging operations began with the modeling of the original four combine harvester blades in SolidWorks 2020 (Dassault Systemes, Velizy-Villacoublay, France). Initial measurements were taken across all four combine harvester blades to create the CAD models. Table 32 shows the basic measurements taken for both the full-feed and half-feed blades.

Table 32: Combine harvester blade basic dimensions

Dimension	Full-feed blade	Half-feed small bottom blade	Half-feed large bottom blade	Half-feed top blade
Thickness (mm)	1.80	3.69	3.70	3.46
Width (mm)	75.85	49.73	69.85	49.75
Length (mm)	83.95	59.90	60.79	79.26

The dimension listed in Table 32 along with additional measurements were used to create a SolidWorks model of all four combine harvester blades. Figure 74 shows a SolidWorks rendering of all four combine harvester blades.
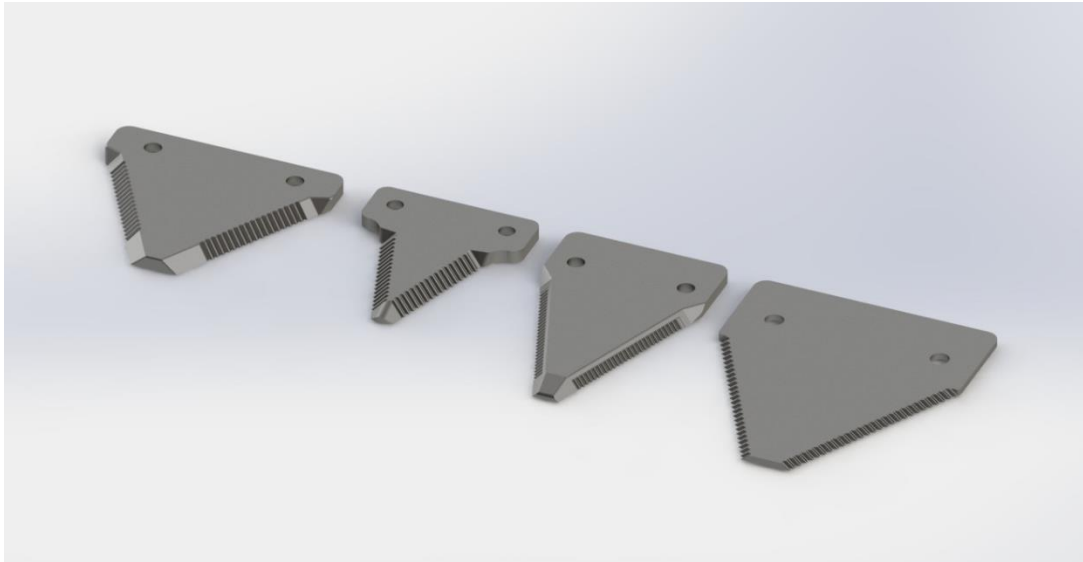
Figure 74: SolidWorks rendering of full-feed and half-feed combine harvester blades

Once the SolidWorks models for the full-feed and half-feed combine harvester blades were finalized, then the blanks were designed such that they encompassed the appropriate size and shape for each of the four blades. Figure 75 shows a rendering containing all four blade blanks.
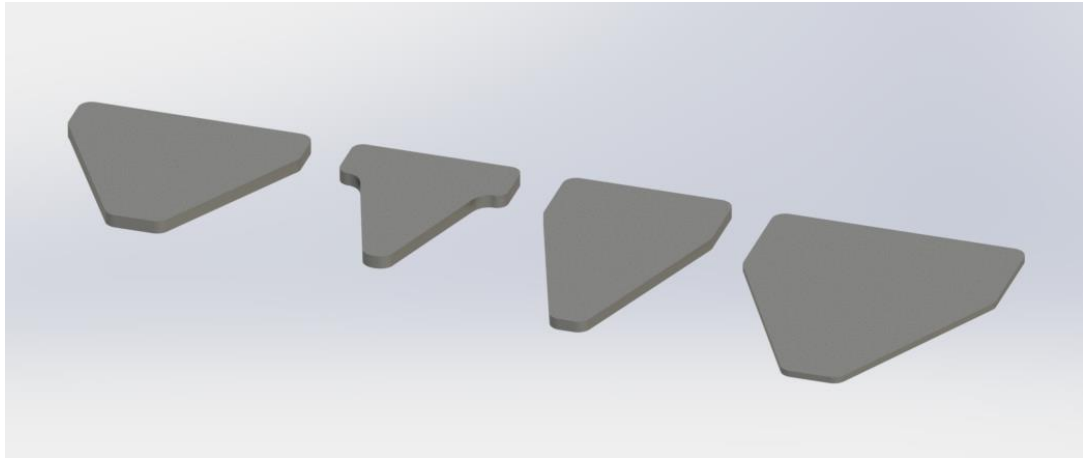
Figure 75: SolidWorks rendering of combine harvester blanks

3.4.2 Design Theory for Blanking and Forging Punch and die Sets

Next, the blanking dies for each of the combine harvester blades were developed. The depth of the initial blanking die opening was set to be the thickness of the stock material, which is 2.00 mm for the full-feed harvester blade and 4.00 mm for the three-half-feed combine harvester blades. These values are greater than the thicknesses found in Table 32 because additional material is removed during grinding. Beneath the initial die openings, a 0.5° taper is applied to the bottom of the die to allow for easy release of the blank from the die (Boljanovic & Pacquin, 2006, p. 92).

The minimum thickness of the die blocks was determined using Equation 36 found in Suchy's Handbook of Die Design, where P_{max} is the maximum cutting force in metric tons (p. 196).

$$T_{die\ block} \geq \sqrt[3]{P_{max}}$$

$$(36)$$

P_{max} was approximated using F_{shear} shown in Equation 37, where σ_{UTS} is the ultimate tensile strength of AISI 1070 (1070 Carbon Steel, 2020).

$$F_{shear} = 0.7\sigma_{UTS} * \text{perimeter} * \text{thickness}$$

(37)

Table 33 shows the F_{shear} for the full-feed and half-feed combine harvester blades determined using Equation 37.

Table 33: Blanking shear force for combing harvester blades

Blade	F_{shear} (metric tons)
Full-feed blade	27.5
Half-feed – small bottom blade	37.5
Half-feed – large bottom blade	43.3
Half-feed – top blade	44.1

Table 34 shows the die block thickness for the combine harvester blades based on Equation 36.

Table 34: Blanking die thickness for combine harvester blades

Blade	$t_{die\ block}$ (mm)
Full-feed blade	30.2
Half-feed – small bottom blade	33.5
Half-feed – large bottom blade	35.1
Half-feed – top blade	35.3

The final thickness of the full-feed blade die block was rounded to 30 mm and the half-feed blade die blocks were rounded up 35 mm. Finally, the distance from the die block openings to the edge of the die block were determined using the guide shown in Figure 76 (Boljanovic & Paquin, 2006, p. 94).

Figure 76: Recommended minimum distances from die block opening to outside edge. Adapted [reprinted] from *Die Design Fundamentals* (p. 94), by V. Boljanovic and J.R. Paquin, 2006, Industrial Press Inc. Copyright 2006 by Industrial Press.

Starting with column A, the strip thickness for the full-feed combine harvester blade falls within $\frac{1}{16}$" $-\frac{1}{8}$" or $1.59 - 3.175$ mm and the half-feed combine harvester blade strip thickness falls within $\frac{1}{8}$" $-\frac{3}{16}$" or $3.175 - 4.76$ mm. Under column B, an estimated die block thickness of approximately $1\frac{1}{8}$" ~ 28.6 mm and $1\frac{3}{8}$" ~ 34.9 mm were found for the full-feed and half-feed combine harvester blade die blocks, respectively. The thickness of the full-feed blade die block found using Figure 76 is 0.5 % smaller than the minimum die block thickness found in Table 34 derived from Suchy's formula for minimum die block thickness in Equation 36. The thickness of the

half-feed blade die block found using Figure 76 is 2.5 % larger than the average

minimum die block thickness found in Table 34.

To determine the minimum distance between the die opening and edge of the die

block, the proper die contour was selected from options 1, 2, and 3 under column C. Due

to the more complex shape of the blanks and rounded edges the inside corners contour,

option 2, was chosen. The values are listed under column C in section 2 are die block

thickness multiplication factors which determine the minimum distance from the die

openings to the edge of the die block. In the row corresponding to a strip thickness of

$\frac{1}{16}$" $- \frac{1}{8}$", the multiplication factor was found to be 1.6875. The full-feed blade die block

thickness was found to be a minimum of 30.2 mm in Table 34. Therefore, the minimum

distance from the die opening to the edge of the die block was calculated to be 51 mm, as

shown in Equation 38.

$$1.6875 * t_{min} = 1.6875 * 28.9 \text{ mm} = 51 \text{ mm}$$

(38)

For strip thicknesses of $\frac{1}{8}$" $- \frac{3}{16}$", the multiplication factor was found to be 2.0625. The

minimum distances from the die openings for the three half-feed blades are shown in

Table 35.

Table 35: Minimum distance from die opening to edge of die block for blanking die blocks

Blade	d_{min} (mm)
Half-feed – small bottom blade	66.2
Half-feed – large bottom blade	69.3
Half-feed – top blade	69.9

Figure 77 shows the die block for the full-feed combine harvester blades with reference dimensions.
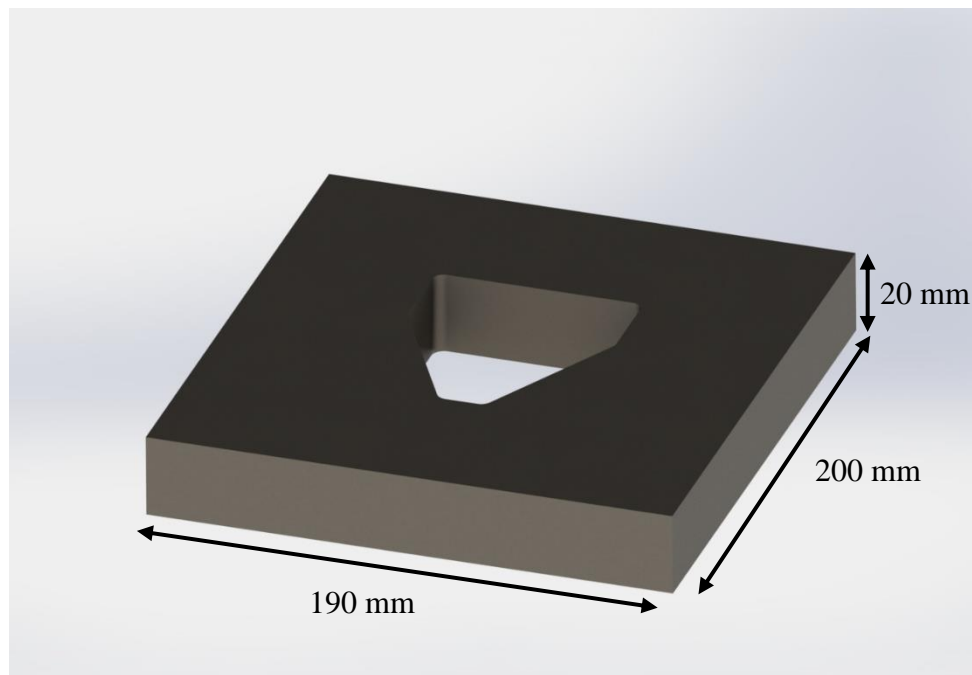
Figure 77: Full-feed combine harvester blade die block

Figure 78, Figure 79, and Figure 80 show the die blocks for the half-feed combine harvester blades.
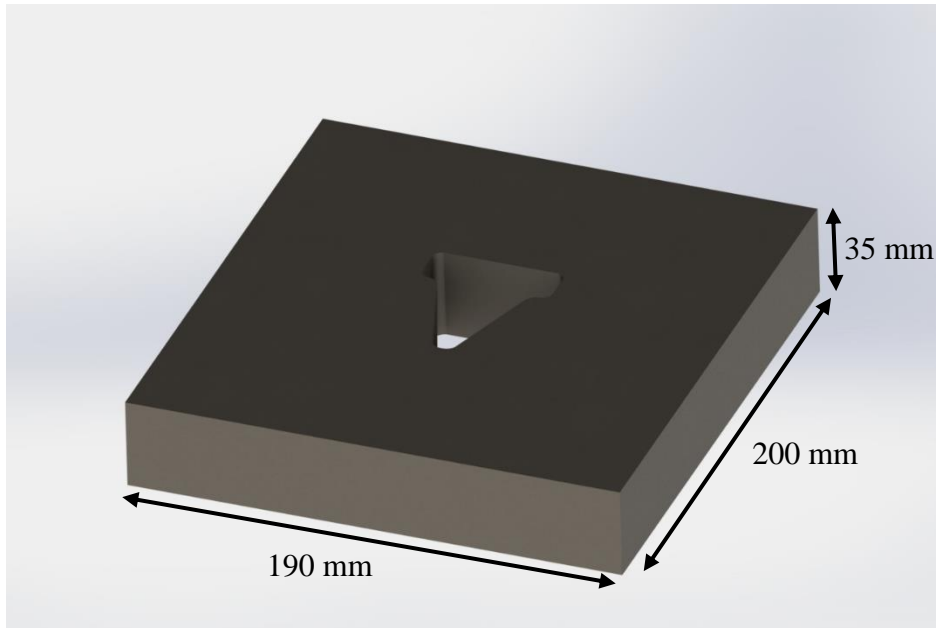
Figure 78: Half-feed combine harvester small bottom blade die block
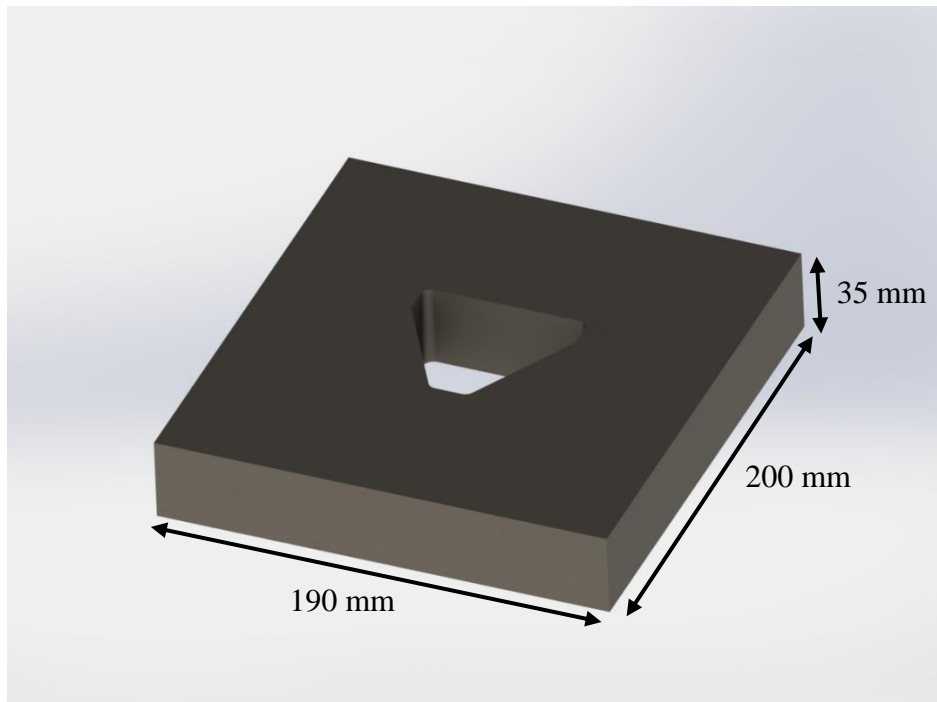
Figure 79: Half-feed combine harvester large bottom blade die block
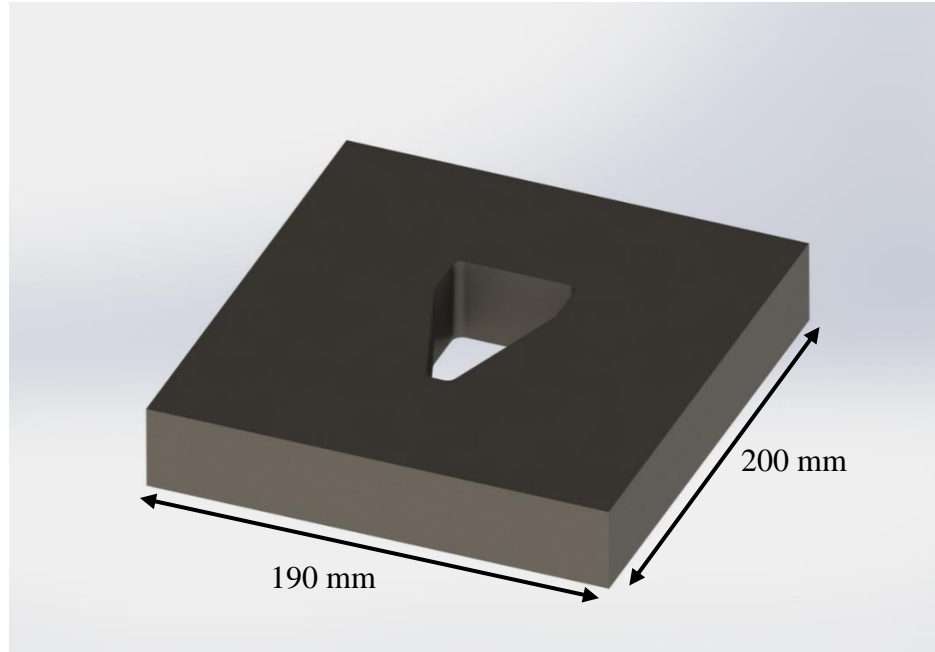
Figure 80: Half-feed combine harvester top blade die block

Next, the punches for both the full-feed and half-feed combine harvester blade punch and die sets were designed. The blanking punch for the full-feed blade has a clearance of 18% of stock thickness or 0.36 mm between the edge of the punch and the opening of the die block as recommended for blanking of steel with a thickness of 2 mm. The blanking punches for the three half-feed combine harvester blades have a clearance of 22% of stock thickness or 0.88 mm between the edge of the punches and the opening of the die blocks as recommended for blanking steel with a thickness of 4.0 mm (Clearance Calculation, 2019). The clearance ensures proper function of the punch as well as reduced wear and tear during repeated blanking of the stock material. The height of the punches was set to half of the respective die block thickness. Therefore, the height of the punch for the full-feed blade is 15 mm and the heigh of the punches for the half-feed blades are 17.5 mm. Figure 81 shows the punch for the full-feed combine harvester blades.
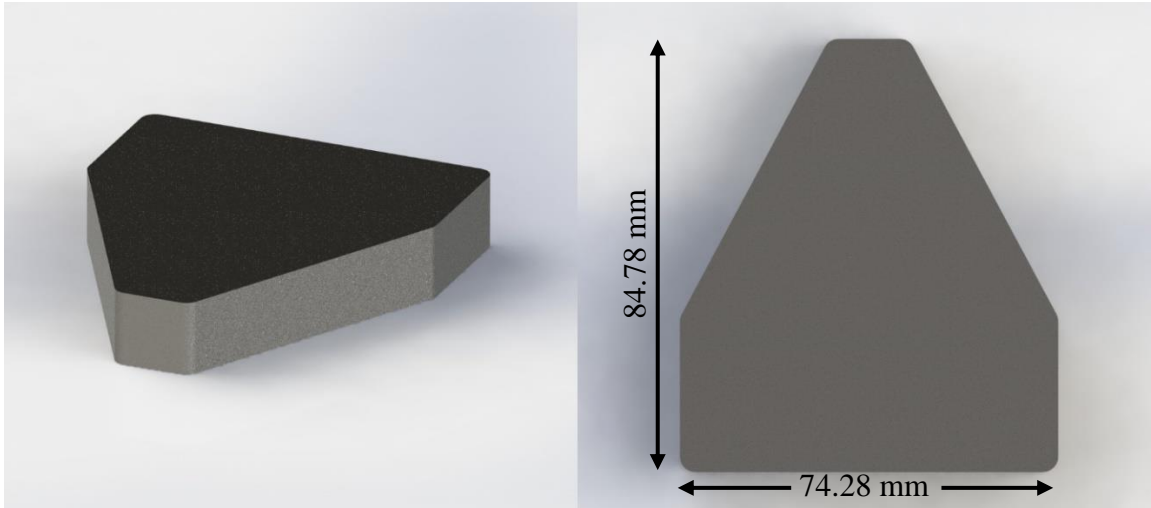
Figure 81: SolidWorks rendering of full-feed combine harvester blanking punch

Figure 82, Figure 83, and Figure 84 show the small bottom blade, large bottom blade, and top blade punches for the half-feed combine harvester blades.
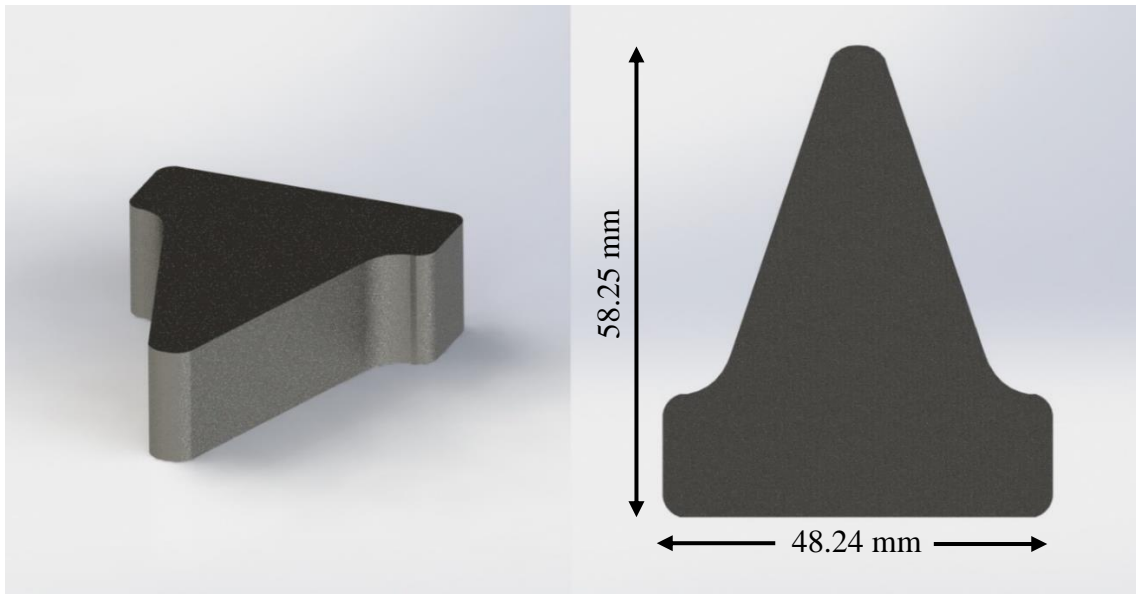
Figure 82: SolidWorks rendering of half-feed combine harvester small bottom blade blanking punch
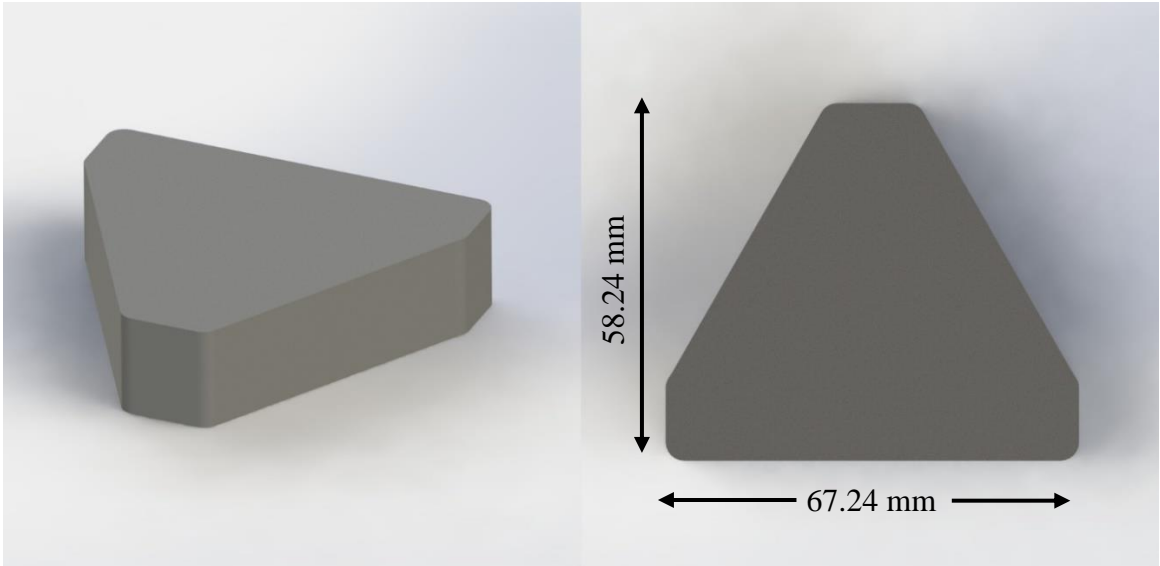
Figure 83: SolidWorks rendering of half-feed combine harvester large bottom blade blanking punch
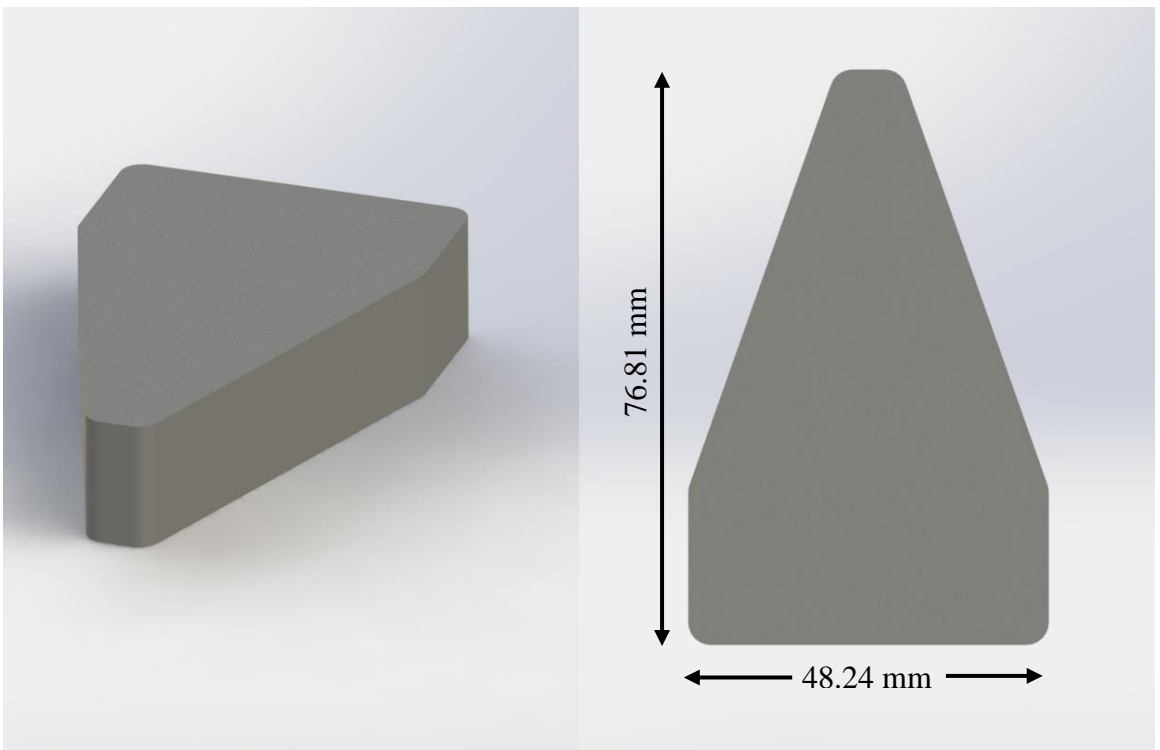
Figure 84: SolidWorks rendering of half-feed combine harvester top blade blanking punch

The design of the punches for both the full-feed and half-feed blades do not

include any mounting plates or holes because the presses used by the machine shops in

Bangladesh are not standardized. Therefore, the mounting holes and plates used to mount

the punches to a mechanical or hydraulic press will need to be developed independently.

Next, forging punch and die sets were developed for the full-feed and half-feed

combine harvester blades. Figure 85 shows the forging die block. The forging die block

was designed with a raised portion along the bottom edge and lower left corner. The

raised section allows the press operator to quickly lineup the full-feed and half-feed blade

blanks in the correct location by placing the corner of the blade into the corner of the die

block. The addition of the raised portion on the forging die block decreases the time

required to lineup the blade blank in the proper position for the forging punch when

compared to positioning the blade blanks by hand without any aides. The raised section

running along the bottom of the die block also provides a backstop for the blade blank

during the forging operation. The direction of the teeth on the half-feed combine

harvester blade serrated edge are not horizontal but angled as shown in Figure 74. The

angle in the serrated edge forces the blank backwards during the forging process, which

can result in misalignment of the part.
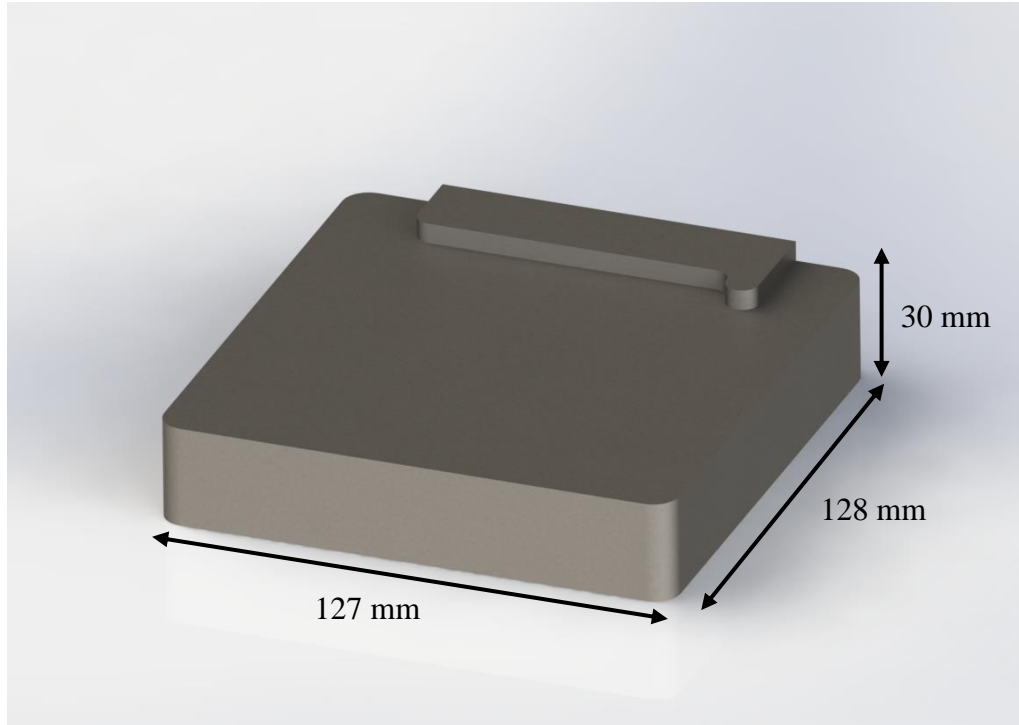
Figure 85: Combine harvester blade forging die block

The forging punch for the full-feed and half-feed blades is split into two parts: the punch base and punch plates. The punch base acts as a backing to the punch plates and consists of flat machined tool steel surface with four threaded holes in the corners for attaching the individual punch plates. Figure 86 shows a rendering of the punch base.
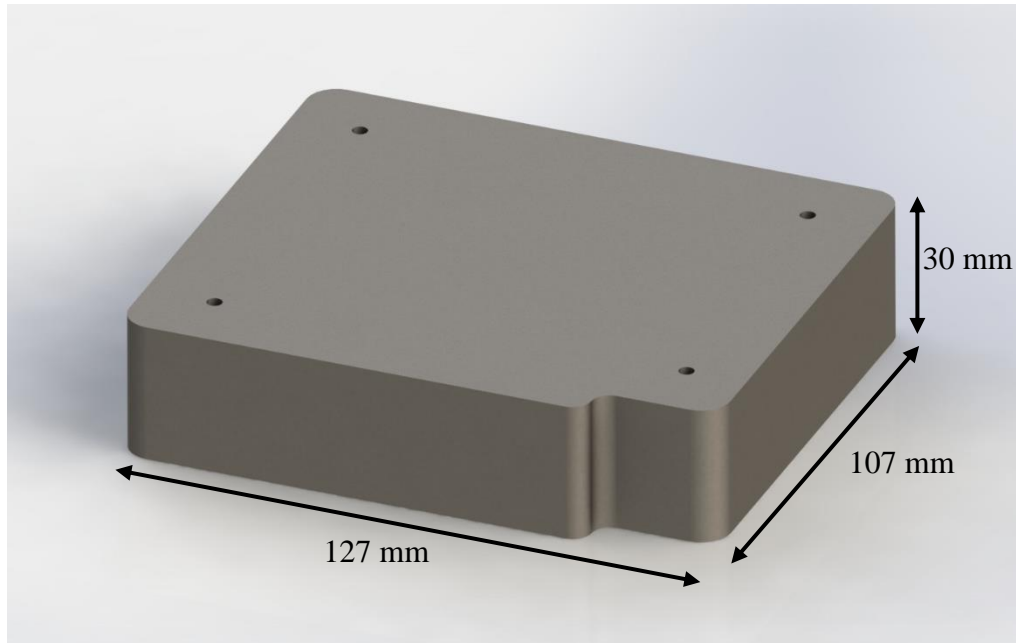
Figure 86: Combine harvester forging punch base

The punch plates are designed for the individual combine harvester blades and created the serrated edges of the combine harvester blades in the forging process. Figure 87 shows a SolidWorks rendering of the full-feed blade punch plate. The split punch design allows for the machine shops easily swap between manufacturing different combine harvester blades by removing four screws from the punch. If the punch were machined from a single piece of tool steel the process of swapping between punches would require the removal of the entire punch from the press. Therefore, a split punch reduces the amount of time require to swap punches to manufacture a different combine harvester blade. The split punch also allows for the punch to be machined on a 3-axis mill as opposed to the 5-axis mill, which would be required if the punch were to be machined from a single piece of tool steel. Therefore, the split punch reduces both the material and machining costs of the forging punch and die sets. Additional adjustments were made to the punch plates to maintain a single blade angle of 45° across the full-feed and half-feed

combine harvester blades. The blade angle of the full feed combine harvester blade and half-feed combine harvester top blade were adjusted from approximately 30° to 45°. A single blade angle further reduces the machining cost as only a single fixture is needed to properly position the punch plates during the machining of the serrated edge of the punch plate cavity.
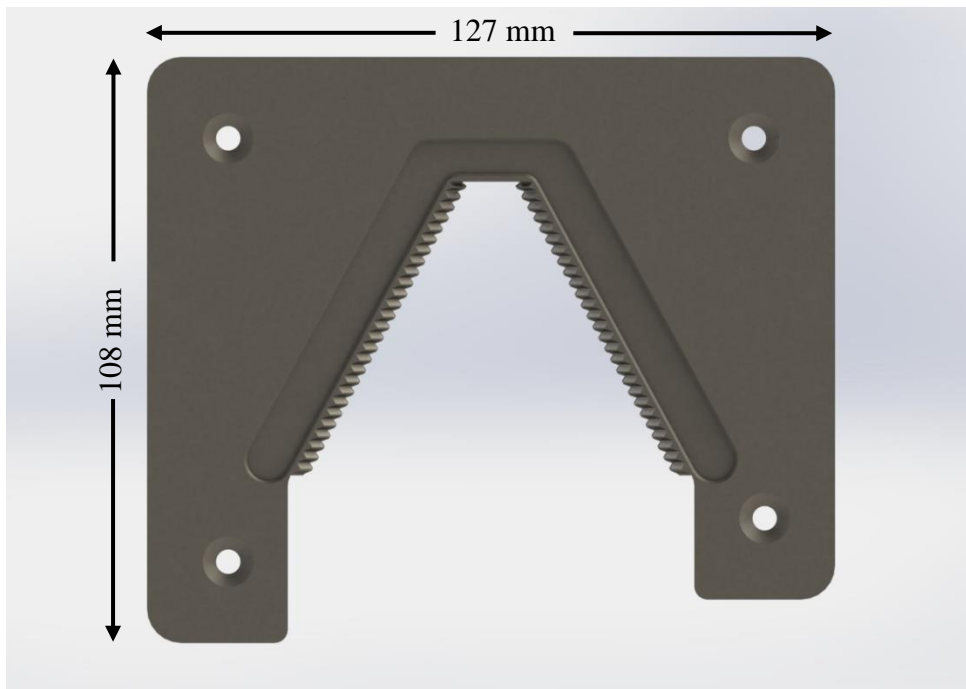
Figure 87: Full-feed combine harvester forging punch plate

The punch plates were designed individually for each of the four combine harvester blades. Figure 88 Figure 89, and Figure 90 show the punch plates for the full-feed and combine harvester blades. The thickness of the punch plates is equal to the stock material thickness of the corresponding blade. The cavities of the punch plates were designed to match the pattern of the combine harvester blades serrated edges. The recessed area, or gutter, outside of the blade cavity is designed to hold excess material or

flash, which is created during the forging process. The creation of flash during the forging process acts to regulate the pressure so that all cavities of the die are filled properly. The addition of a gutter to the punch plate reduces the force needed in the forging operation and acts to prevent a very thin and wide flash.
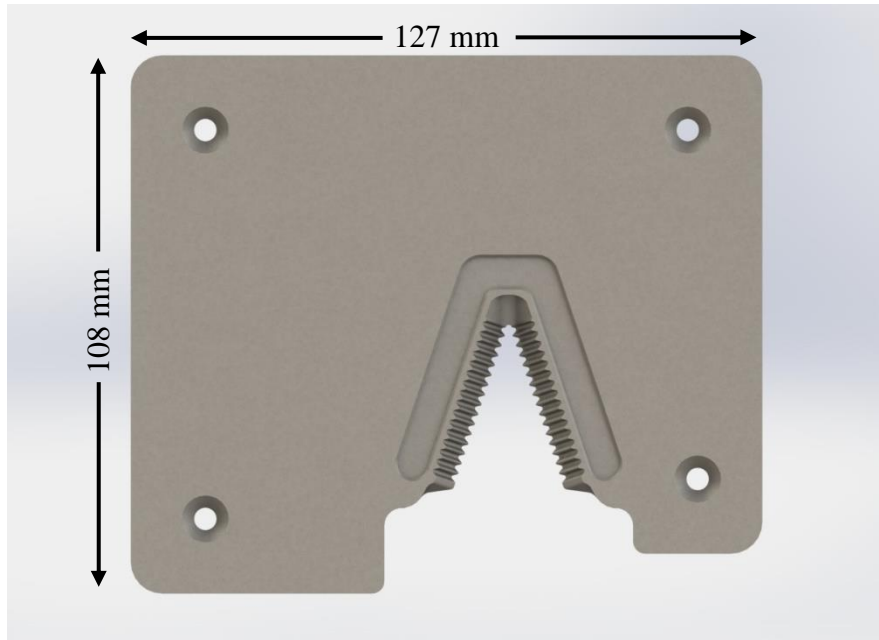
Figure 88: Half-feed combine harvester small bottom blade forging punch plate
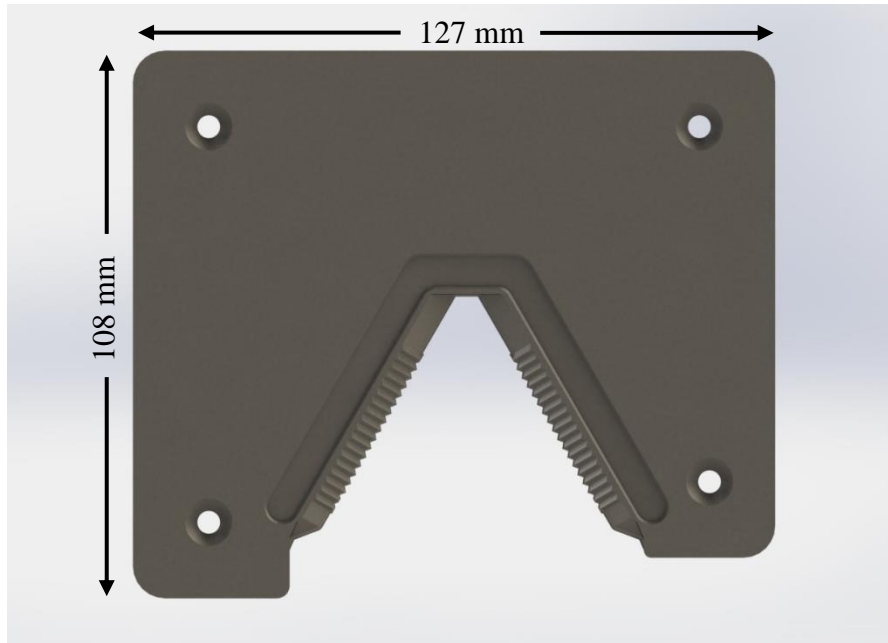
Figure 89: Half-feed combine harvester large bottom blade punch plate
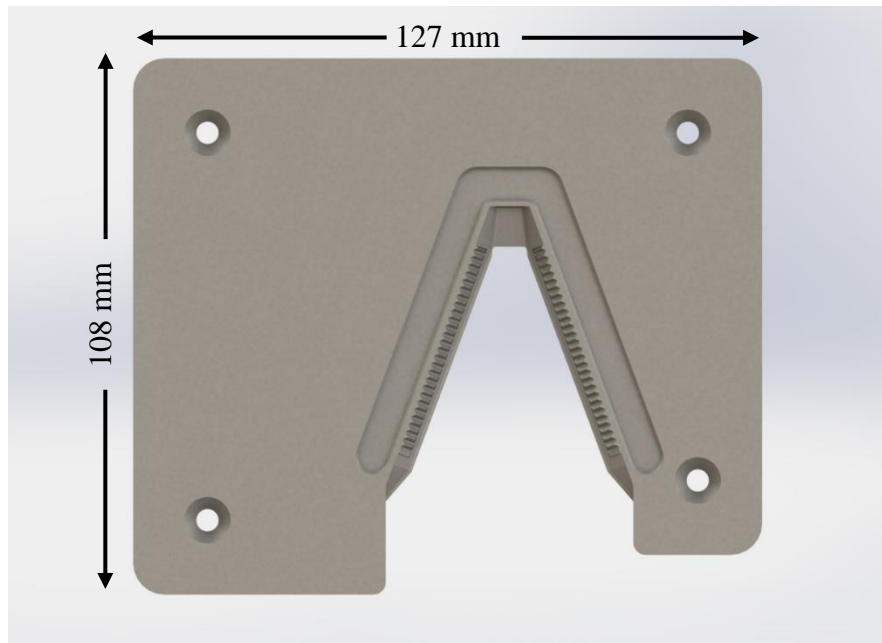
Figure 90: Half-feed combine harvester top blade punch plate

The dimensions of the gutter were developed through finite element simulations

using DEFORM 3D (Version 11.1 published by Scientific Forming Technologies

Corporation in Columbus, Ohio). Simulations were performed with varying gutter sizes and adjusted according to force and punch stroke results obtained in DEFORM 3D. Similar to the design of the blanking punchs, the design of the forging punch base plates do not include any mounting plates or mounting holes. Therefore, the mounting holes and plates used to mount the punches to hydraulic press will need to be developed in tandem with the machine shops.

3.4.3 Section Summary

The Design of Required Tooling section of Chapter 3 is composed of two subsections: the development of the combine harvester CAD models for the full-feed and half-feed blades and the design theory for blanking and forging punch and die sets. The first subsection displays the SolidWorks renderings of the full-feed and half-feed combine harvester blades. The second subsection provides the design theory background for the development of the blanking and forging dies. First, the blanking punch and die set is discussed with relevant equations for punch and die clearances and die block thickness. Finally, the final design of the blanking and forging punch and die sets are discussed and examined.

The next section presents the experimental methods and procedures for the prototype forging punch and die testing. First the design of the forging punch and die set is presented followed by the testing conditions. Finally, the testing procedure is listed.

3.5 Experimental Methods and Procedures

Prototypes of the half-feed combine harvester small bottom blade forging punch and die set were machined out of A2 tool steel at Georgia Tech's Montgomery Machining Mall. Figure 91, Figure 92, and Figure 93 show the forging punch base, plate, and die block.
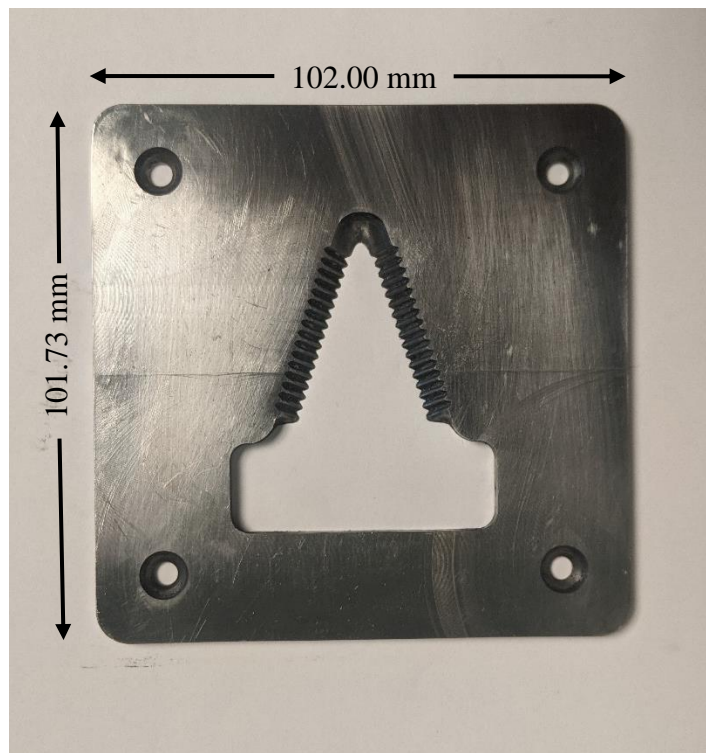
Figure 91: Machined half-feed combine harvester small bottom blade forging punch plate

101.6 mm

Height: 24.4 mm
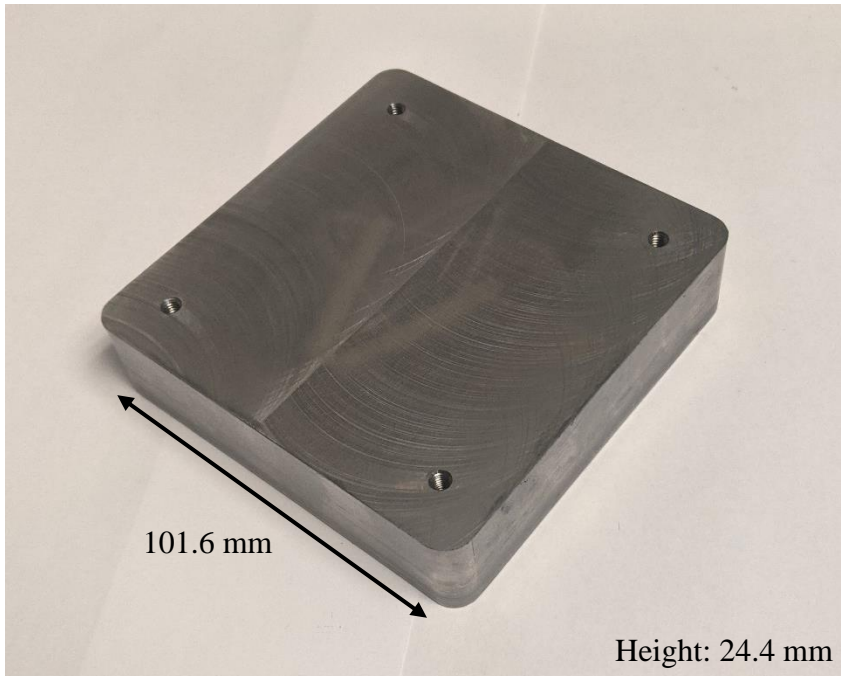
Figure 92: Machined half-feed combine harvester small bottom blade forging punch base

152.87 mm

Height: 34.80 mm
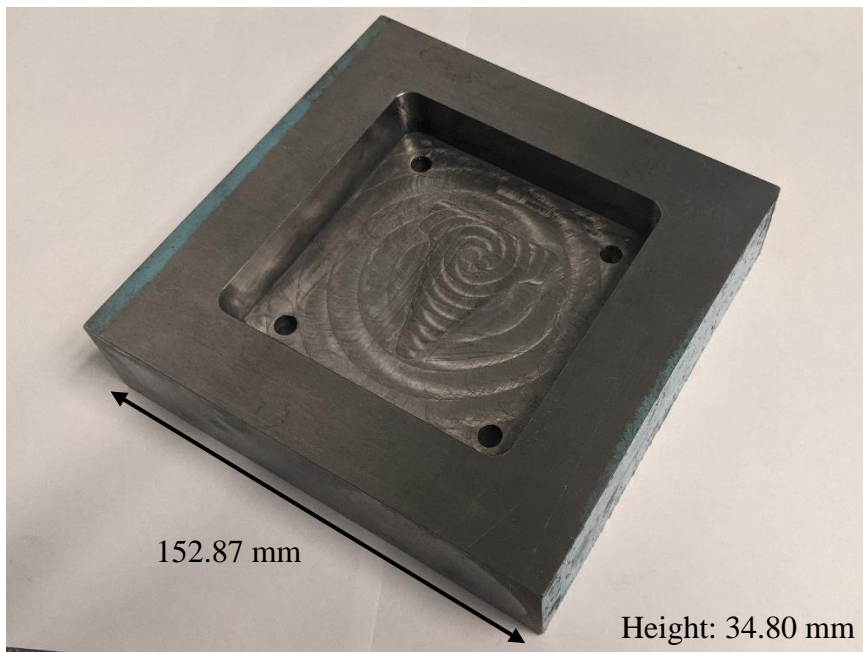
Figure 93: Machined half-feed combine harvester small bottom blade forging die block

Testing of the bending punch and die set was performed on the Wabash 50-ton hot press shown in Figure 31. All tests were conducted at room temperature. During operation of the hydraulic press the entire bottom platen moves up, therefore the use of a die set with static guide rods was not possible because the rods would contact the platen before the punch reached the die block. An example of a standard die set as mentioned is shown in Figure 32.

Due to this height restriction, the design of the punch and die block were altered to allow for operation in the hydraulic press. The design of the forging punch and die set was altered such that the die block contains a pocket which centers the punch without the need for any guide rods, which are traditionally used to position the punch in the proper position over the die block. Other changes made to the design of the prototype include the addition of holes in the die block to ensure that both the punch base, punch plate, and blank could be removed from the die block if jammed. A very slight recessed area was machined into the die block to aid in lining up the blade blank relative to the punch.

The blanks used during the tests were fabricated using a water jet from 4.10 mm thick aluminum 6061-T6 sheet metal. Aluminum 6061-T6 was used due to the 50-ton force limit on the hydraulic press used for prototype testing. The blanks were lubricated using molybdenum disulfide to prevent the possibility of the blank getting stuck during the bending operation.

The testing procedure used in the testing of the combine harvester blades forging punch and die set is as follows:

1. Lubricate the blank with a thin layer of molybdenum disulfide on both sides

2. Set blank into the center of the die block

3. Lower punch into cavity until contact with blank

4. Place bending punch and die set onto bottom platen of press

5. Close hydraulic press until contact is made between the punch and top platen

6. Slowly increase hydraulic press force to 50 tons/45.35 metric tons

7. Unload hydraulic press

8. Remove punch and die set from press and remove punch from punch and die set

9. Remove blank from die block.

3.5.1 Section Summary

The Experimental Methods and Procedures section presents background information regarding the setup for the experimental testing of the forging punch and die set. The 50-ton hydraulic press used for testing is discussed along with the necessary changes to the design of the forging punch and die set to allow for proper alignment of the punch and die. Finally, the testing procedure is listed.

The next section presents the DEFORM-3D Forming Express setup used for the finite element simulations of the forging punch and die set.

3.6 DEFORM Setup

DEFORM 3D is a process simulation system which uses the finite element method to simulate manufacturing processes such as open and closed die forgings (Scientific Forming Technologies Corporation). As mentioned earlier, DEFORM 3D was

used to simulate the forging operations to study the effects of changes to various design

parameters made prior to and after the machining and testing of the physical prototypes.

This setup of the DEFORM 3D settings are discussed in this section with the results of

the simulation are presented in the results section.

The settings used during the simulation of operations with DEFORM 3D were

constant for all forging simulations. The DEFORM 3D preprocessor used was 3D

Forming Express. 3D Forming Express sets many of the constraints to allow for ease of

use when conducting studies on cold or hot forming operations. An example of a

constraint set by the preprocessor is the constraint of the punch and die as rigid bodies.

This sets the punch and die as unable to be deformed, which reduces the computing

power needed as the internal compressive forces experienced by the punch and die are

not calculated. Figure 94 below shows the settings of the 3D Forming Express

preprocessor.
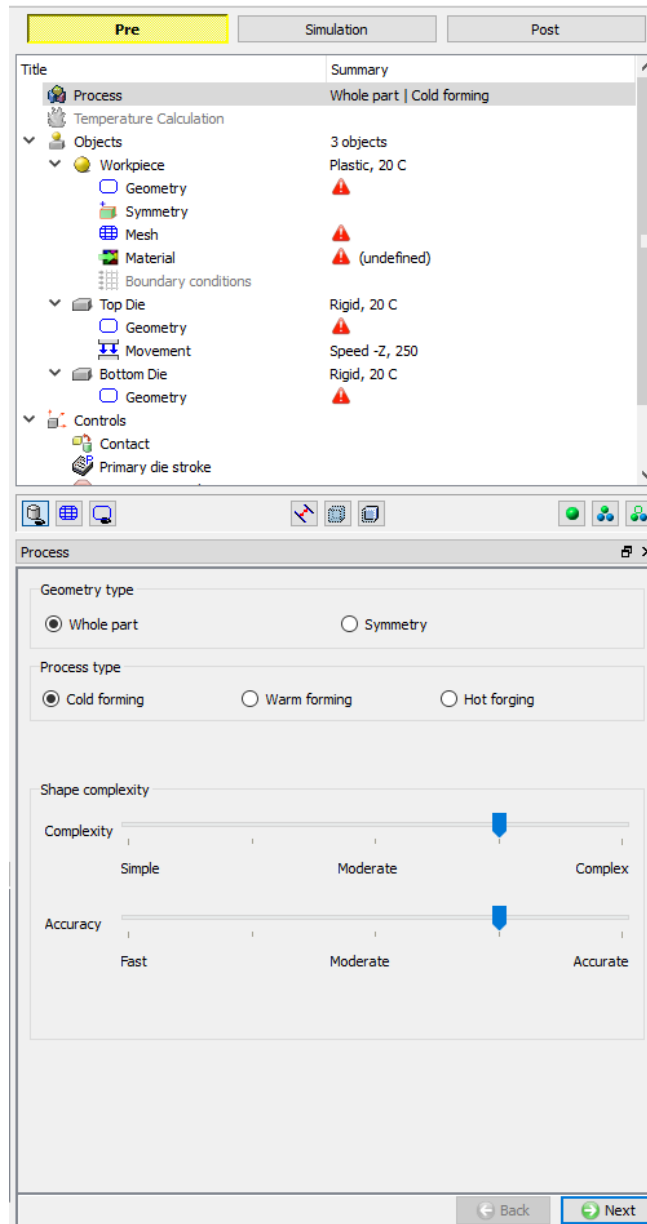
Figure 94: DEFORM 3D Forming Express settings

The first setting under the process tab, geometry type, was set to whole part.

Process type was set to cold forming which sets the temperature of the operation at 20°C.

Complexity and accuracy parameters were set to complex and accurate respectively, due

to the geometric complexity of the serrated edge. These parameters affect the number of

points in the workpiece mesh along with other mesh parameters, which affect accuracy.

The workpiece, top die, and bottom die geometries were set from an STL file created from the specific CAD part files. The mesh was generated with the suggested system settings which resulted in 51703 elements and 11970 nodes in the simulation of the bending operation of the machined bending punch and die set. The material of the workpiece was set to AISI 1070 COLD from the DEFORM materials library to replicate the proposed stock material. Material properties for the punch and die are not set as they are considered rigid in the forming analysis. The movement type of the top die was set as hydraulic, as all potential manufacturers of the combine harvester blades intend to use hydraulic presses for the blanking and bending operations. The direction of the movement of the top die is set to the z-direction. The speed of the press is set to 10 for all operations. The total dwell time and number of steps are kept at zero (0). Figure 95 shows the top die movement settings used in the DEFORM simulations.
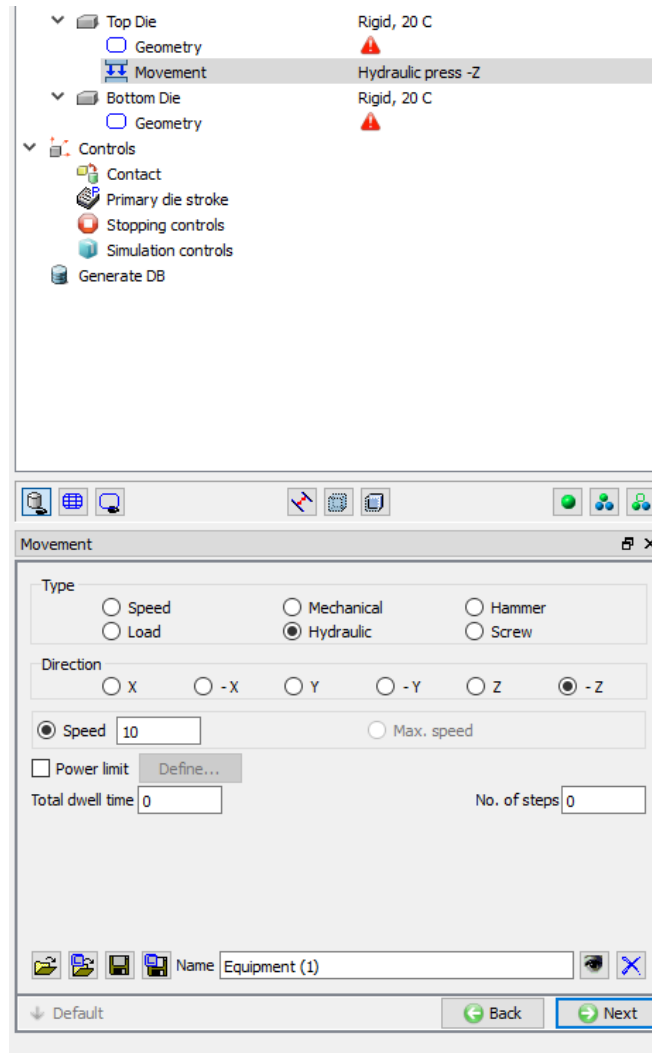
Figure 95: DEFORM 3D Forming Express top die movement settings

Finally, the controls settings were established. No changes were made to the setting under the contact tab. The primary die stroke was set to a rough estimate of the total die stroke expected and the exact amount box was left unchecked. In the stopping controls tab the max load was set to 50 metric tons for the simulation of the prototype forging punch and die set and 300 metric tons for the simulation of the final forging punch and die set design. Figure 96 shows the controls settings.

164
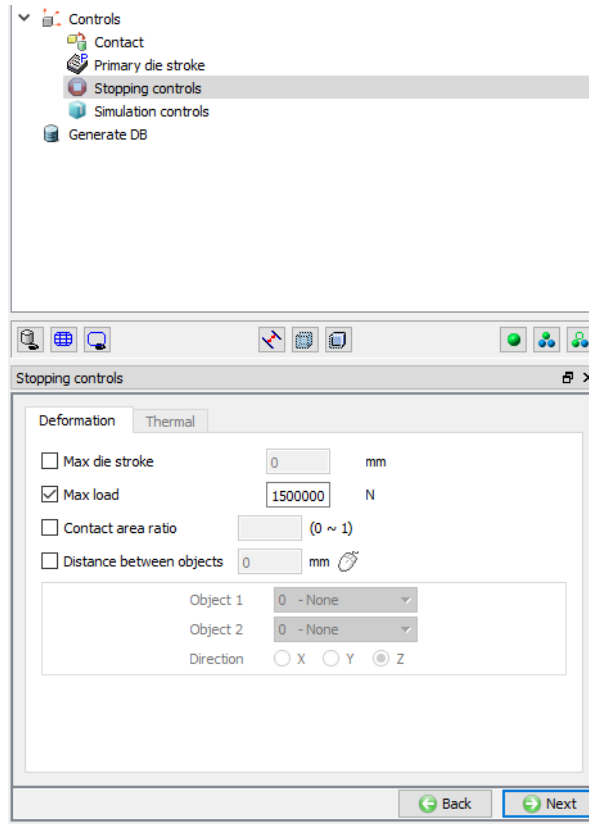
Figure 96: DEFORM 3D Forming Express controls settings

3.6.1 Section Summary

The DEFORM settings section discusses the finite element software used for the combine harvester blade punch and die simulations. First, the background of the DEFORM-3D software is discussed along with the 3D Forming Express preprocessor. Finally, the process, geometry, and control settings within the 3D Forming Express preprocessor are discussed.

The next section presented the results and discussion of the material characteristic testing, experimental testing, and DEFORM-3D simulations of the forging punch and die set.

3.7 Results and Discussion

3.7.1 XRF Results

The results for the x-ray fluorescence (XRF) spectroscopy are shown in Table 36 below. The Niton FXL Field XRF used does not detect the percentage of carbon in the sample. The XRF results for the original half-feed combine harvester small bottom blade was not able to identify the specific material used. However, six significant elements were identified and are listed in Table 27. The XRF results of the combine harvester blade fabricated by NRE identified the material as wrought iron. Wrought iron is not able to be hardened through heat treatment due to a lack of carbon. Therefore, the material is unsuitable for the manufacturing of combine harvester blades.

Table 36: Combine harvester blade XRF results (Material & Significant Elements)

Part	Suggested Material	Significant Elements (%)
Half-feed small bottom blade	N/A	Fe: 98.129 Mn: 0.441 P: 0.139 Si: 0.503 Cu: 0.154 Ni: 0.179
Proposed Material	AISI 1070	C: 0.65-0.75 Mn: 0.6-0.9
NRE blade	Wrought iron	Fe: 99.78 Mn: 0.086

The results of the XRF allowed for the easy identification of the material used in the local production of combine harvester blades. However, an XRF cannot detect the

percentage of carbon within a sample. Carbon content is important for determining the specific grade of low, medium, and high carbon steel and the selection of proper heat treatment procedure for hardening. Optical emission spectroscopy (Spark OES) is a method of elemental analysis that can determine the carbon percentage of metals by analyzing the vaporized atoms created by an arc between the machine and the material (Acuren, 2019). It is recommended that a portable Spark OES system be purchased for material composition testing of scrap material in Bangladesh. Scrap material testing can be provided by the local spare parts manufacturer or a private company looking to sell known scrap materials to the local manufacturers. Spark OES testing will allow manufacturers to determine the carbon percentage of the stock material therefore reducing the probability that they receive stock materials not suitable for the manufacturing of combine harvester blades. A minimum carbon percentage of 0.30% is recommended for stock materials used in the manufacturing of the combine harvester blades so that the blades can be properly hardened.

3.7.2 Hardness Testing Results

The second order polynomial regression equations for tensile strength estimation using Rockwell C and B hardness are shown in Equations 39 and 40.

$$\sigma_{UTS} \, (psi) = 88.67 * HRC^2 - 2031.6 * HRC + 119654$$

(39)

$$\sigma_{UTS} \, (psi) = 17.425 * HRB^2 - 1327 * HRB + 71964$$

(40)

Table 37 contain the Rockwell hardness, Brinell hardness, and three tensile strength estimations of the original and locally manufactured combine harvester blades. The units have been converted from pounds per square inch in Equations 39 and 40 to megapascals in Table 37.

Table 37: Rockwell hardness and tensile strength estimation for combine harvester blades

Part	Rockwell Hardness		Brinell Hardness	First Tensile Strength Estimation	Second Tensile Strength Estimation	Third Tensile Strength Estimation	Average Tensile Strength Estimation
	B Scale 100 kg	C Scale 150 kg		MPa	MPa	MPa	MPa
Small bottom blade		55	560	1904	1932	2090	1975
Large bottom blade		53	525	1800	1811	1956	1856
Top blade		56	577	1958	1991	2160	2036
NRE blade			29		100		

The high Rockwell hardness of the original half-feed combine harvester blades indicates the blades had been heat treated during the manufacturing process. In contrast, the hardness and tensile strength of the combine harvester blade produced by NRE is low in comparison to most unheat-treated carbon steel. Therefore, the serrated edge of the locally produced part will deform or wear under load in comparison to the original half-feed combine harvester blades.

The hardness of a material can also be related to the wear-rate constant of the material. The wear-rate of the combine harvester blades is very important as the part is in repeated contact with the crop stalks. Figure 97 displays the relationship between hardness and the wear-rate constant. k_a, the wear-rate constant, is a measure of the wear experienced on a sliding surface. A larger wear-rate constant corresponds to more rapid wearing of the material at a specific pressure between the surfaces. The region for high carbon steels encompasses hardness values of $1000 - 5000$ MPa and a dimensionless wear constant, K, of 10^{-4} indicated by the diagonal dashed line. The traditional dimensionless wear constant, K, considers the wear-rate, applied load, and the hardness of the material. However, the dimensionless wear constant in Figure 97 is equal to the wear rate constant times the material hardness. The average hardness, in megapascals, of the original half-feed combine harvester blades is determined by multiplying the average Brinell hardness by the acceleration due to gravity. The average hardness was found to be 5433 MPa, as shown in Equation 41.

$$554 \ \frac{\text{kgf}}{\text{mm}^2} = 554 * 9.801 \ \frac{\text{N}}{\text{mm}^2} = 5432 \ \text{MPa}$$

(41)

The average hardness of the half-feed combine harvester blades is at the top end of the high carbon steel range, likely due to the heat treatment. From the Ashby chart, a hardness of 5433 MPa corresponds to a wear-rate constant, k_a, of approximately $0.5 \cdot 10^{-7} \ \frac{1}{\text{MPa}}$. The locally produced combine harvester blade has a hardness of 284 MPa which corresponds to a wear-rate constant, k_a, of approximately $3.0 \cdot 10^{-6} \ \frac{1}{\text{MPa}}$. The annealed AISI 1070, proposed to use in the domestic manufacturing of combine harvester

blade, has a hardness of 1832 MPa which corresponds to a wear-rate coefficient, k_a, of

approximately $5.0 \cdot 10^{-7} \; \frac{1}{\text{MPa}}$. The large wear-rate coefficient of the locally produced

blade shows that the wrought iron blade will wear more rapidly than both the AISI 1070

and the original combine harvester blades. The wear-rate coefficient of the AISI 1070 is

also larger than the original combine harvester blades and therefore will wear more

quickly than the OEM blades. Therefore, heat treatment is needed to increase the

hardness of the blades to reduce the wear of the part under normal operation conditions.
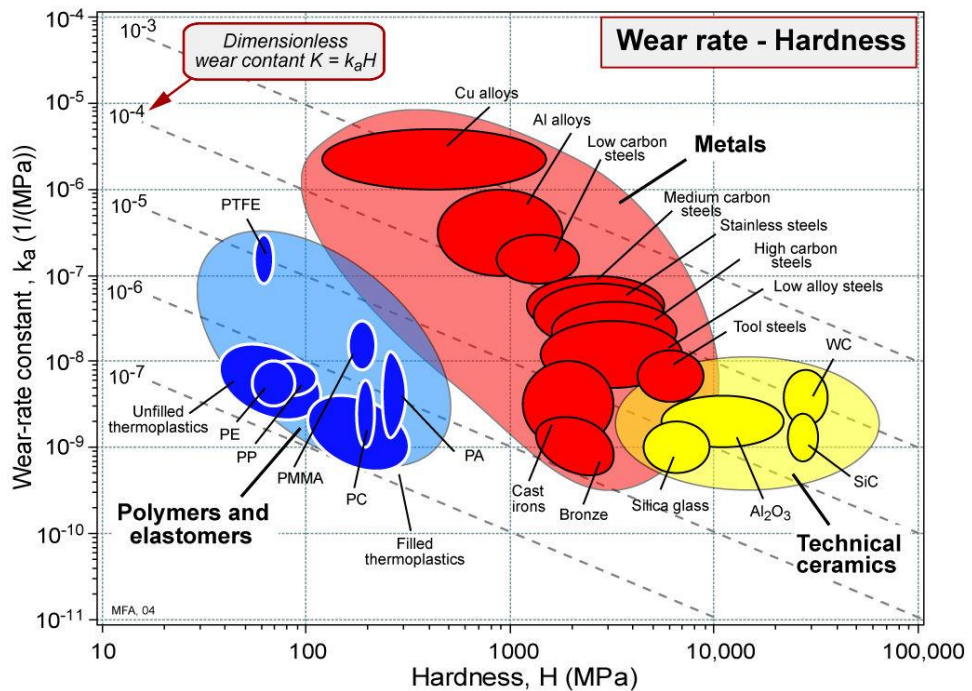
Figure 97: Wear-rate constant, k_a, to hardness. Reprinted from Granta CES 2009
EduPack Material and Process Selection Charts (p. 20), by Mike Ashby, 2009. Copyright
2009 by Granta Design Ltd.

The characterization of the hardness of the original and locally produced combine

harvester blades as well as the proposed material allows the potential manufacturers of

the combine harvester blades to understand the appropriate materials and heat treatment that are required to manufacture parts similar in quality to the OEM components. Due to the difficulty and expense of importing steel into Bangladesh, the scrap market is used to source stock material. However, in the scrap market the specific grades of metals are often unknown leaving companies to produce products without knowledge of the material properties or composition. Therefore, it is recommended that the hardness of scrap materials be tested in conjunction with material composition testing prior to their use in the manufacturing of combine harvester blades. Scrap material characterization can be completed by the individual manufacturers or a private company looking to sell known scrap material to the local manufacturers. A minimum Brinell hardness of 180, corresponding to AISI 1030, is recommended for stock materials used in the manufacturing of the combine harvester blades. However, material hardness can be affected by other factors such as the heat treatment of the metal or surface treatments. Therefore, material composition testing is recommended over hardness testing for the characterization of scrap material prior to their use in the manufacturing process. It is also recommended that manufacturers test the hardness of their finished products so that the hardness and wear rate coefficient can be compared to that of the original combine harvester blades.

3.7.3 Experimental Testing Results

The testing of the forging punch and die set was performed with a maximum pressing force of 50 tons/45.35 metric tons. Figure 98 shows examples of the blanks after the experimental testing. Flash, which is excess material, can be seen around the bottom

edge of the serrated edge as well as along the rear edge of the blade. The flash along the rear edge is due to misalignment of the blank with the punch in addition to the rearward force exerted on the blade during the forging process. As mentioned earlier, the final design of the forging punch and die alleviated this issue by incorporating a backstop for the blade which is incorporated into the die block. The forging of the serrated edge caused the center of the blade between the serrated edge to dome raising both the top and bottom of the blade. Therefore, the top and bottom of the half-feed combine harvester small bottom blade must be ground flat to adhere to proper tolerances between the top and bottom cutter bar blades. The average deformation of the center of the blade was found to be 0.50 mm.

Figure 98: Top view of test half-feed combine harvester small bottom blade

The average thickness of the flash around the edge of the test blanks was found to be 0.54 mm. The thickness of the aluminum 6061-T6 used was 4.10 mm therefore the

average total die stroke during testing was found to be 3.56 mm. The thickness of the

original half-feed small bottom blade is 3.70 mm; therefore, an additional pressing force

is needed to achieve a die stroke equal to that of the original half-feed combine harvester

small bottom blade. As the testing blanks were fabricated from aluminum 6061-T6 and

the press used had a maximum force of 50 tons/45.35 metric tons, an objective

comparison of the resulting dimensions of the experimental testing blades and the

original half-feed combine harvester small bottom blade cannot be made. However, the

testing was conducted to test the viability of creating the serrated edge using forging as

well as validation of the forging DEFORM simulations. Figure 99 shows a closeup shot

of the serrated edge of the test blade and the original half-feed blade.

Figure 99: Comparison of test blade and original half-feed combine harvester small
bottom blade

3.7.4 DEFORM Simulation Results

After the validation of the DEFORM model by comparing results of the

experimental testing and the prototype testing in DEFORM, further simulations were

conducted to determine the effects of the addition of a flash gutter into the punch plate design. Conducting simulations using DEFORM also allowed the testing of the full-feed and two other half-feed combine harvester blades without having to machine the punch plates and conduct experimental testing. Figure 100 shows a graph of the force versus die stroke for the DEFORM simulations of the full-feed blade punch plate with and without the flash gutter. As seen in Figure 100, the performance of the full-feed punch plate is improved throughout the die stroke with the addition of the flash gutter because less force is required to obtain a specified die stroke. At a force of 200 metric tons, the die stoke without the gutter is found to be 1.69 mm, whereas the die stroke with the addition of the gutter is found to be 1.89 mm. At a force of 300 metric tons, the die stoke without the gutter is found to be 1.79 mm, whereas the die stroke with the addition of the gutter is found to be 1.90 mm. The maximum forging die stroke for the full-feed combine harvester blade is 2 mm, therefore the addition of the gutter increases the total die stroke by 10% at a force of 200 metric tons and 5.5% at a force of 300 metric tons. Table 38 displays these results. The thickness of the original full-feed combine harvester blade was found to be 1.86 mm. Therefore, a pressing force of 200 – 300 metric tons is recommended to obtain an adequate die stroke during the forging of the serrated edge.
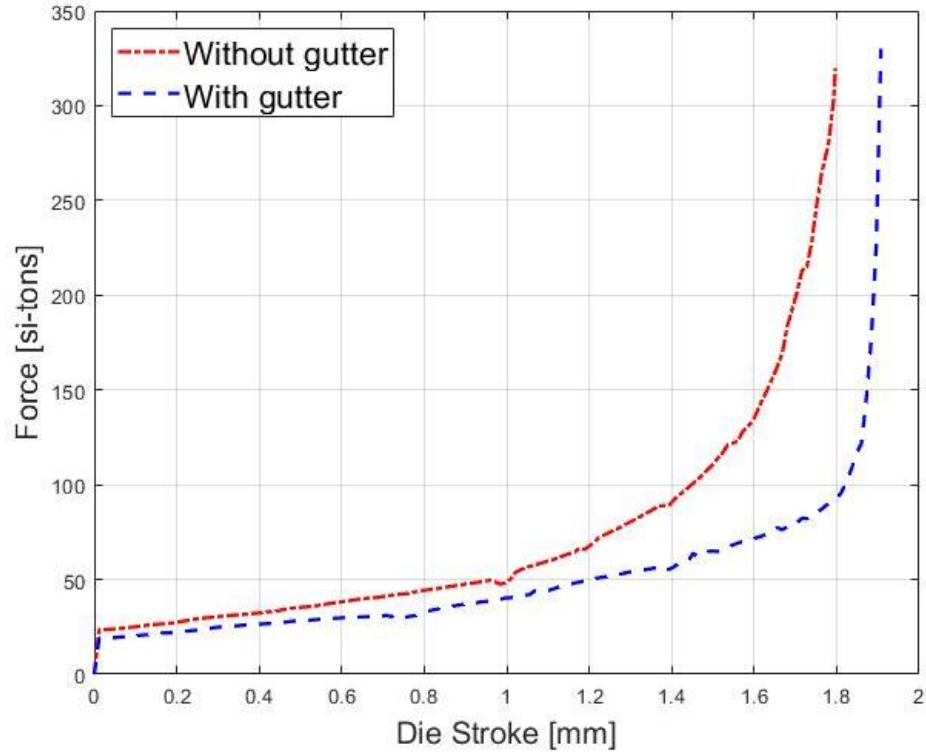
Figure 100: Force versus die stroke for DEFORM forging simulation of full-feed combine harvester blade

Table 38: Comparison of full-feed combine harvester forging punch performance

Punch Plate	Die stroke – 200 metric tons (mm)	Die Stroke – 300 metric tons (mm)
No gutter	1.69	1.79
Gutter	1.89	1.90
Increase (% of max die stroke)	10%	5.5%

Figure 101 shows the graph of the force versus die stroke for the DEFORM simulations of the half-feed small bottom blade punch plate with and without the flash gutter. The performance of the half-feed small bottom blade punch plate is slightly improved with the addition of the flash gutter after a die stroke of approximately 3.0 mm. At a force of 200 metric tons, the die stoke without the gutter is found to be 3.42 mm, whereas the die stroke with the addition of the gutter is found to be 3.52 mm. At a force

of 300 metric tons, the die stoke without the gutter is found to be 3.55 mm, whereas the die stroke with the addition of the gutter is found to be 3.71 mm. The maximum forging die stroke for the half-feed combine harvester small bottom blade is 4 mm therefore the addition of the gutter increases the total die stroke 2.5% at a force of 200 metric tons and 4.0% at a force of 300 metric tons. These results are shown in Table 38. The thickness of the original half-feed combine harvester small bottom blade was found to be 3.69 mm. Therefore, a pressing force of approximately 300 metric tons is recommended for the forging of the serrated edge of the half-feed small bottom blade.
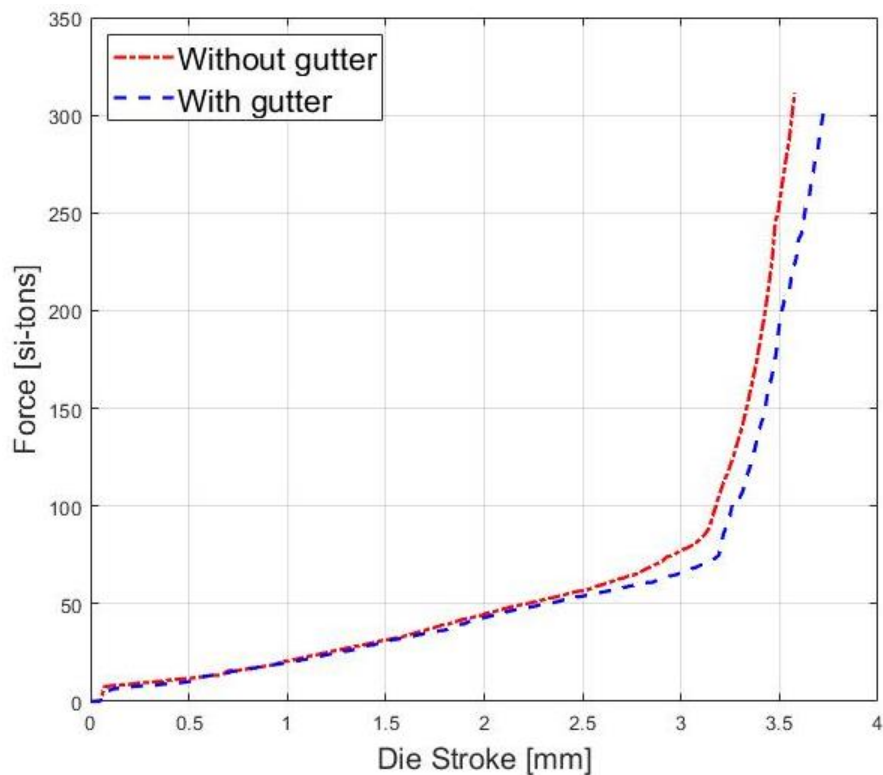
Figure 101: Force versus die stroke for DEFORM forging simulation of half-feed combine harvester small bottom blade

Table 39: Comparison of half-feed combine harvester small bottom blade forging punch performance

Punch Plate	Die stroke – 200 metric tons (mm)	Die Stroke – 300 metric tons (mm)
No gutter	3.42	3.55
Gutter	3.52	3.71
Increase (% of max die stroke)	2.5%	4.0%

Figure 102 shows the graph of the force versus die stroke for the DEFORM simulations of the half-feed large bottom blade punch plate with and without the flash gutter. The performance of the half-feed large bottom blade punch plate is improved throughout the die stroke range with the addition of the flash gutter. At a force of 200 metric tons, the die stoke without the gutter is found to be 3.49 mm, whereas the die stroke with the addition of the gutter is found to be 3.62 mm. At a force of 300 metric tons, the die stoke without the gutter is found to be 3.58 mm, whereas the die stroke with the addition of the gutter is found to be 3.68 mm. The maximum forging die stroke for the half-feed combine harvester large bottom blade is 4 mm therefore the addition of the gutter increases the total die stroke by 3.3% at a force of 200 metric tons and 2.5% at a force of 300 metric tons. These results are shown in Table 40. The thickness of the original half-feed combine harvester small bottom blade was found to be 3.70 mm. Therefore, a pressing force of approximately 300 metric tons is recommended for the forging of the serrated edge of the half-feed large bottom blade.
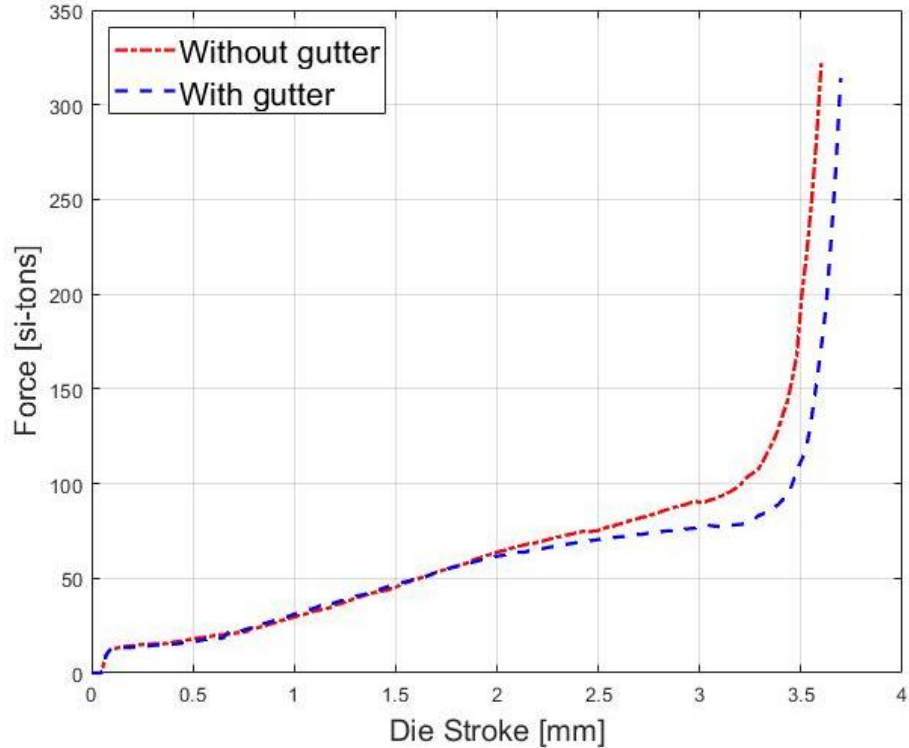
Figure 102: Force versus die stroke for DEFORM forging simulation of half-feed combine harvester large bottom blade

Table 40: Comparison of half-feed combine harvester large bottom blade forging punch performance

Punch Plate	Die stroke – 200 metric tons (mm)	Die Stroke – 300 metric tons (mm)
No gutter	3.49	3.58
Gutter	3.62	3.68
Increase (% of max die stroke)	3.3%	2.5%

Figure 103 shows the graph of the force versus die stroke for the DEFORM simulations of the half-feed top blade punch plate with and without the flash gutter. The performance of the half-feed large bottom blade punch plate is improved throughout the die stroke range with the addition of the flash gutter. At a force of 200 metric tons, the die stoke without the gutter is found to be 3.43 mm, whereas the die stroke with the addition of the gutter is found to be 3.53 mm. At a force of 300 metric tons, the die stoke without

the gutter is found to be 3.56 mm, whereas the die stroke with the addition of the gutter is

found to be 3.68. The maximum forging die stroke for the half-feed combine harvester

top blade is 4.0 mm; therefore, the addition of the gutter increases the total die stroke by

3.8% at a force of 200 metric tons and 3.8% at a force of 300 metric tons. These results

are summarized in Table 40. The thickness of the original half-feed combine harvester

small bottom blade was found to be 3.49 mm. Therefore, a pressing force of

approximately 200 – 300 metric tons is recommended for the forging of the serrated edge

of the half-feed top blade.
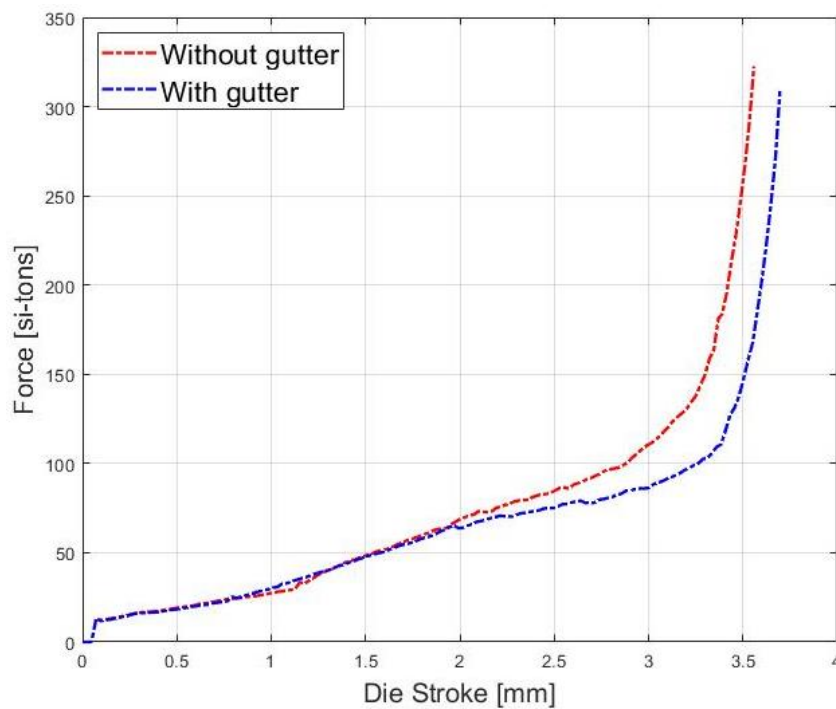
Figure 103: Force versus die stroke for DEFORM forging simulation of half-feed
combine harvester top blade

Table 41: Comparison of half-feed combine harvester top blade forging punch performance

Punch Plate	Die stroke – 200 metric tons (mm)	Die Stroke – 300 metric tons (mm)
No gutter	3.43	3.53
Gutter	3.58	3.68
Increase (% of max die stroke)	3.8%	3.8%

Table 42 shows a comparison of the original combine harvester blade thickness and the die strokes for the DEFORM forging simulations at pressing forces of 100, 200, and 300 metric tons. The recommended pressing forces for the full-feed and half-feed combine harvester blades are summarized in Table 42 based upon the original combine harvester blade thicknesses.

Table 42: Comparison of DEFORM forging simulation results to original combine harvester blade thickness

Blade	OEM Blade Thickness (mm)	Die-stroke (100 metric tons) (mm)	Die-stroke (200 metric tons) (mm)	Die-stroke (300 metric tons) (mm)
Full-feed	1.80	1.82	1.89	1.90
Half-feed small bottom blade	3.69	3.26	3.52	3.71
Half-feed large bottom blade	3.70	3.46	3.62	3.68
Half-feed top blade	3.46	3.27	3.58	3.68

3.7.5 DEFORM Forging Sensitivity Analysis

A sensitivity analysis was completed on the DEFORM model of the forging punch and die set with gutter to determine the effects of different grades of steel on the ability of the forging punch to reach an adequate die stroke. The steel grades tested were

AISI 1008, AISI 1035, AISI 1043, AISI 1045, and AISI 1070. The material properties were set through the DEFORM-3D material library. As the elemental composition of stock material are not known in Bangladesh, the ability of the forging punch and die set to reach an adequate die stroke with a variety of stock material is important for the functionality of the serrated edge forging process in Bangladesh.

Table 43 displays the dies stroke of the DEFORM-3D full-feed combine harvester forging simulation at pressing forces of 50, 100, 200, and 300 metric tons for the five stock materials tested (1008 Carbon Steel, 1035 Carbon, 1043 Carbon Steel, 1045 Carbon Steel, and 1070 Carbon Steel, 2020). Figure 104 shows the force versus die stroke graph for AISI 1070 in red with the blue horizontal error bars corresponding to the range of die strokes for the stock materials listed in Table 43. The largest measured range of the die strokes between the five stock materials is 0.75 mm, which occurs at a press force of 50 metric tons. As the press force increases the range of the die strokes decreases to 0.12 mm, 0.04 mm, and 0.04 mm for press forces of 100, 200, and 300 metric tons. As the yield stresses of the five stock materials range from 310-590 MPa, the full-feed forging punch and die set is not sensitive to deviations in stock material yield stress at high pressing forces. The thickness of the original full-feed combine harvester blade was found to be 1.80 mm, therefore pressing forces of 100-300 metric tons are recommended.

Table 43: Sensitivity analysis results for full-feed forging punch and die set

Material	σ_{UTS} (MPa)	Die Stoke (mm)			
		50 metric tons	100 metric tons	200 metric tons	300 metric tons
AISI 1008	370	1.81	1.88	1.91	1.92
AISI 1035	620	1.19	1.85	1.90	1.93
AISI 1043	710	1.15	1.82	1.88	1.91
AISI 1045	660	1.11	1.78	1.87	1.89
AISI 1070	640	1.21	1.82	1.89	1.90
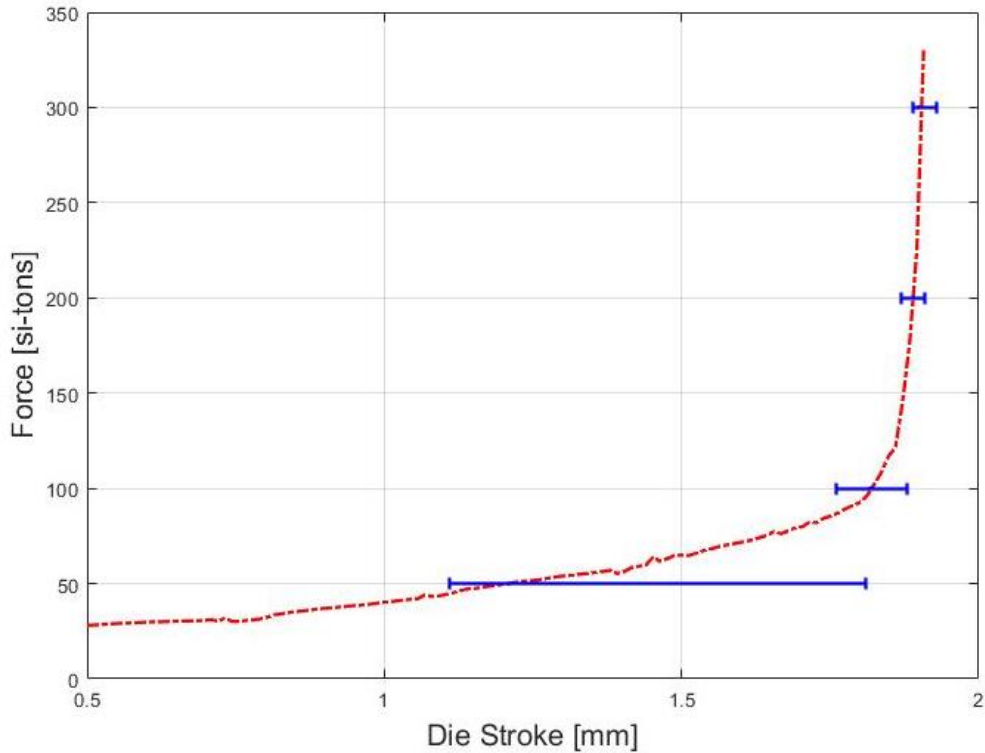
Figure 104: Force versus die stroke with error bars for sensitivity analysis of full-feed forging punch and die set

Table 44 displays the dies stroke of the DEFORM-3D half-feed combine harvester small bottom blade forging simulation at pressing forces of 50, 100, 200, and 300 metric tons for the five stock materials tested. Figure 105 shows the force versus die stroke graph for AISI 1070 in red with the blue horizontal error bars corresponding to the range of die strokes for the five stock materials tested. The largest measured range of the

die strokes between the five stock materials is 1.23 mm, which occurs at a press force of 50 tons. The range of the die strokes for press forces of 100, 200, and 300 metric tons were 0.19 mm, 0.28 mm, and 0.11 mm, respectively. Therefore, at a press force of 300 metric tons, the die stroke is not sensitive to changes in yield stress between 500 – 590 MPa. The thickness of the original half-feed small bottom blade was found to be 3.69 mm; therefore, a press force of 300 metric tons is required to reach an adequate die stroke during the forging process.

Table 44: Sensitivity analysis results for half-feed small bottom blade forging punch and die set

Material	σ_{UTS} (MPa)	Die Stroke (mm)			
		50 metric tons	100 metric tons	200 metric tons	300 metric tons
AISI 1008	370	3.16	3.44	3.75	3.79
AISI 1035	620	2.34	3.28	3.52	3.73
AISI 1043	710	2.18	3.25	3.47	3.68
AISI 1045	660	2.44	3.25	3.52	3.72
AISI 1070	640	2.33	3.26	3.52	3.71
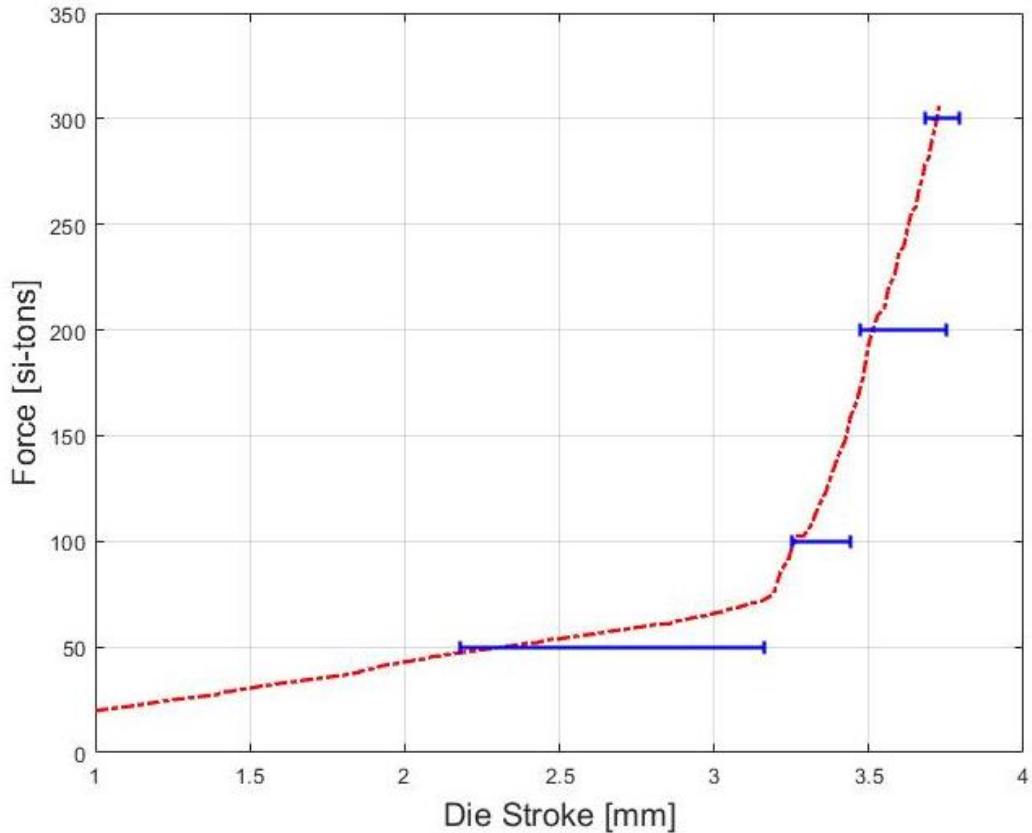
Figure 105: Force versus die stroke with error bars for sensitivity analysis of half-feed small bottom blade forging punch and die set

Table 45 displays the dies stroke of the DEFORM-3D half-feed combine harvester large bottom blade forging simulation at pressing forces of 50, 100, 200, and 300 metric tons for the five stock materials tested. Figure 106 shows the force versus die stroke graph for AISI 1070 in red with the blue horizontal error bars corresponding to the range of die strokes for the five stock materials tested. The largest measured range of the die strokes between the five stock materials is 1.90 mm, which occurs at a press force of 50 metric tons. As the press force increases, the range of the die strokes decreases to 0.13 mm, 0.07 mm, and 0.06 mm for pressing forces of 100, 200, and 300 metric tons. Therefore, at pressing forces above 100 metric tons, the half-feed large bottom forging

punch and die is not sensitive to varying yield stresses in the range of 500 – 590 MPa.

The original half-feed large bottom blade was found to be 3.70 mm so a press force of

300 metric tons is recommended so that an adequate die stroke is reached during the

forging process.

Table 45: Sensitivity analysis results for half-feed large bottom blade forging punch and die set

Material	σ_{UTS} (MPa)	Die Stoke (mm)			
		50 metric tons	100 metric tons	200 metric tons	300 metric tons
AISI 1008	370	3.40	3.57	3.68	3.74
AISI 1035	620	1.65	3.48	3.63	3.69
AISI 1043	710	1.50	3.44	3.61	3.67
AISI 1045	660	1.72	3.48	3.62	3.68
AISI 1070	640	1.63	3.46	3.62	3.68
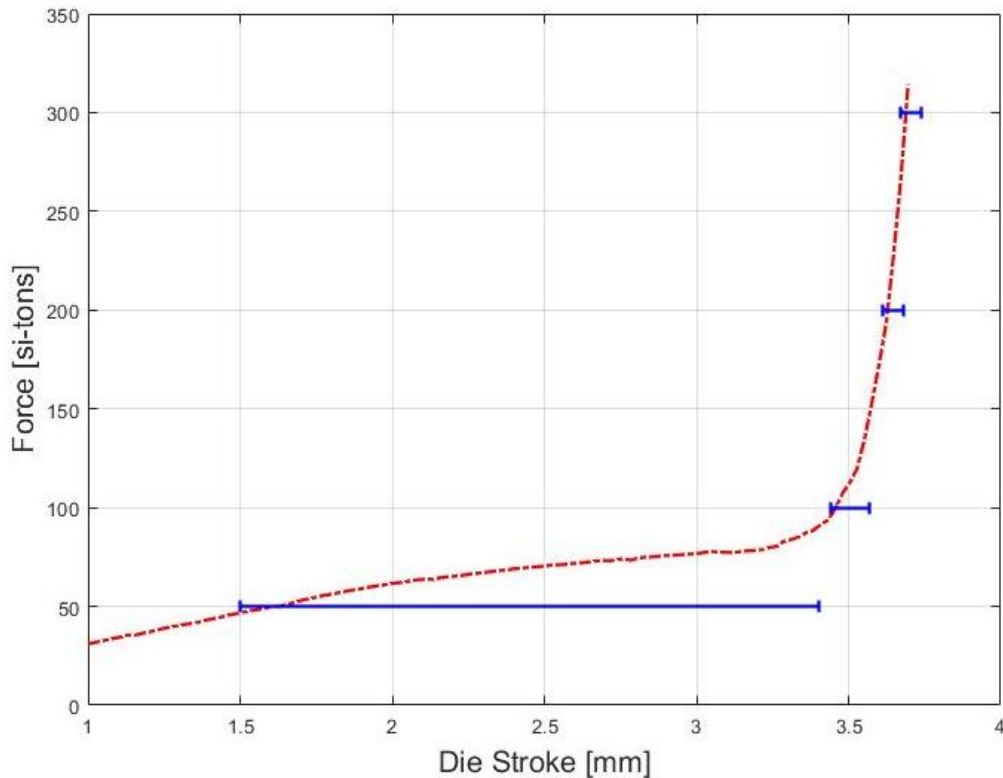
Figure 106: Force versus die stroke with error bars for sensitivity analysis of half-feed large bottom blade forging punch and die set

Table 46 displays the dies stroke of the DEFORM-3D half-feed combine harvester top blade forging simulation at pressing forces of 50, 100, 200, and 300 metric tons for the five stock materials tested. Figure 107 shows the force versus die stroke graph for AISI 1070 in red with the blue horizontal error bars corresponding to the range of die strokes for the five stock materials tested. The largest measured range of the die strokes between the five stock materials is 1.58 mm, which occurs at a press force of 50 metric tons. As the press force increases, the range of the die strokes decreases to 0.35 mm, 0.09 mm, and 0.08 mm for pressing forces of 100, 200, and 300 metric tons. Therefore, at pressing forces above 200 metric tons the half-feed top forging punch and die is not sensitive to varying yield stresses in the range of 500 – 590 MPa. The original half-feed top blade was found to be 3.46 mm; so, a pressing force of 200-300 metric tons is recommended to allow for the grinding of the bottom of the blade.

Table 46: Sensitivity analysis results for half-feed top blade forging punch and die set

| Material	σ_{UTS} (MPa)	Die Stoke (mm)			
		50 metric tons	100 metric tons	200 metric tons	300 metric tons
AISI 1008	370	3.04	3.50	3.65	3.72
AISI 1035	620	1.56	3.31	3.59	3.66
AISI 1043	710	1.46	3.15	3.57	3.65
AISI 1045	660	1.68	3.30	3.56	3.64
AISI 1070	640	1.58	3.27	3.58	3.68
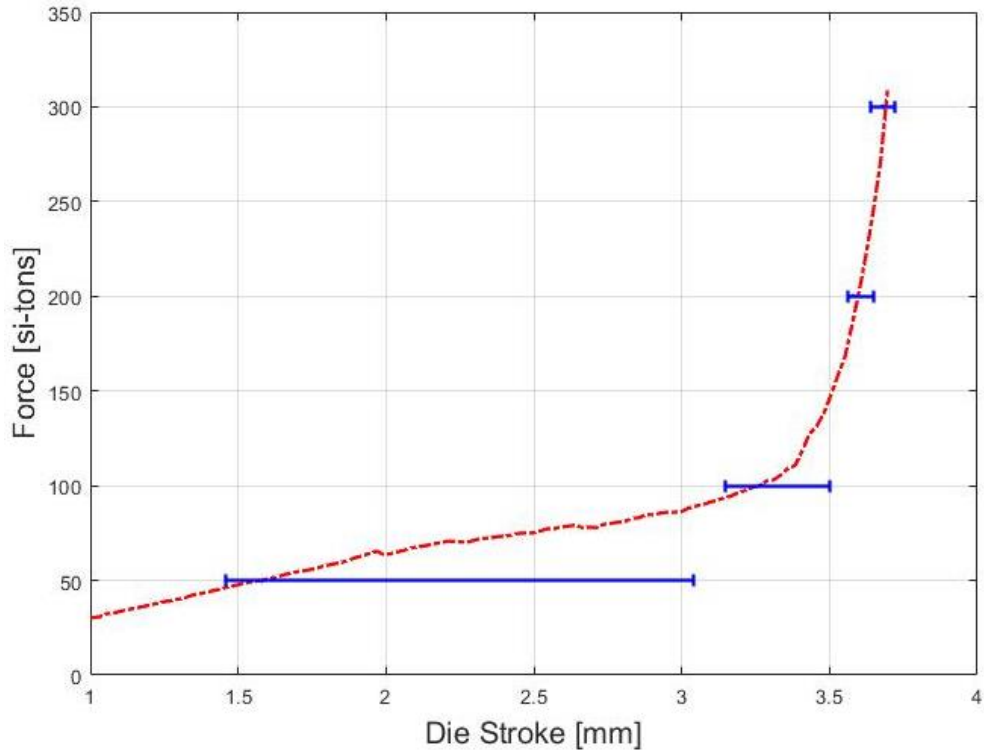
Figure 107: Force versus die stroke with error bars for sensitivity analysis of half-feed top blade forging punch and die set

Table 47 displays the recommended pressing forces for the full feed and half feed combine harvester blades. Hydraulic presses with maximum pressing forces more than 100 metric tons are currently operational in several small machine shops within Bangladesh. However, no press with a maximum capacity of 300 metric tons is documented in the agricultural spare parts market within Bangladesh. Therefore, it is recommended that the initial local manufacturing of combine harvester blades in Bangladesh be full-feed combine harvester blades so that no additional hydraulic presses must be purchased by the local manufacturers.

Table 47: Recommended Pressing Force for Sensitivity Analysis

Blade	Pressing Force (metric tons)
Full-feed	100-300
Half-feed small bottom blade	300
Half-feed large bottom blade	300
Half-feed top blade	200-300

3.7.6 DEFORM Validation

A mesh convergence study was completed on the DEFORM model of the experimental testing to determine the initial of the accuracy of the DEFORM 3D Forming Express preprocessor system defined mesh sizes. Table 48 displays number of mesh elements and nodes and the corresponding die stroke at the maximum press force of 50 metric tons. Figure 108 displays a graph of the die stroke versus the number of mesh elements. The course and normal mesh sizes predict a less accurate die stroke at 50 metric tons, however the fine and very fine meshes predict very similar results. Therefore, the fine and very fine meshes are converged in terms of die stroke (Mesh Convergence, 2017).

Table 48: Results of mesh convergence for DEFORM simulation of experimental testing

Mesh	Elements	Nodes	Die Stroke (50 metric tons) (mm)
Course	11845	2876	3.66
Normal	18947	4526	3.64
Fine	34295	7976	3.48
Very Fine	51703	11970	3.48
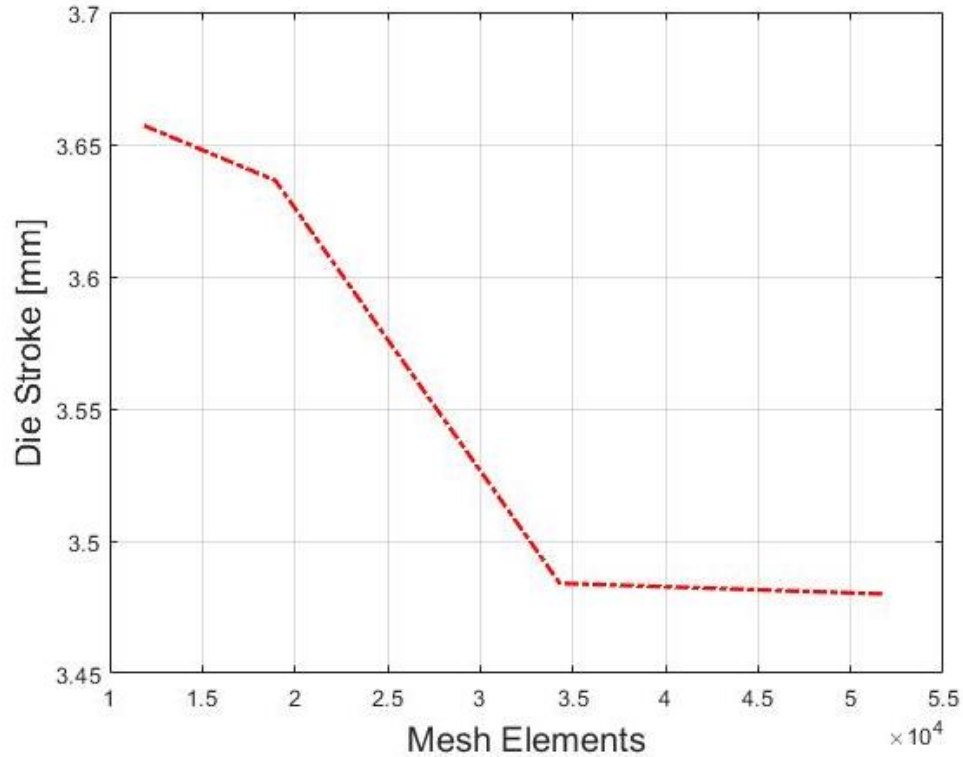
Figure 108: Mesh convergence of DEFORM simulation of experimental test

After the initial mesh convergence of the DEFORM simulation was completed, the

validation of the DEFORM model is performed by comparing the results of the

experimental testing to the results of the DEFORM simulation of the experimental testing

computed in the 3D Forming Express preprocessor. The total die stroke of the DEFORM

model is compared to the results of the experimental testing. The very fine mesh, shown

in Table 48, was used for the validation study.

As mentioned in the previous section the average thickness of the flash around the

edge of the test blanks was found to be 0.54 mm. The thickness of the aluminum 6061-T6

used was 4.10 mm; therefore, the average total die stroke during testing was found to be

3.56 mm. The total die stroke of the DEFORM 3D Forming Express model was found to

be 3.45 mm at a force of 50 ton/45.35 metric ton. Therefore, the difference in die stroke

was found to be 0.11 mm, which corresponds to a percent difference between the

experimental testing and DEFORM simulation of 2.3%. During the machining of the

bending punch and die standard machining tolerances of $\pm 0.005''$ or ± 0.125 mm were

used. As the error between the DEFORM simulations and experimental testing are

smaller the standard machining tolerances, the error is considered acceptable. Therefore,

the DEFORM simulation of the experimental testing in the 3D Forming Express

preprocessor is validated for the very fine mesh size. Figure 109 shows the force versus

die stroke graph for the DEFORM simulation of the experimental testing.
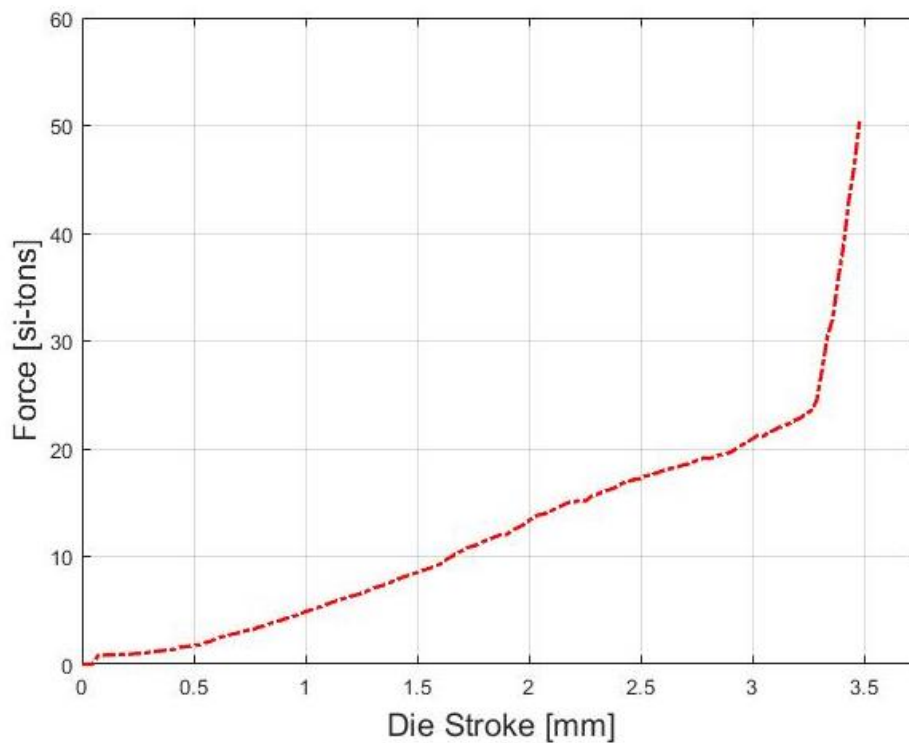
Figure 109: Force versus die stroke for DEFORM forging simulation of experimental test

3.7.7 Discussion and Recommendations

The cost analysis shown in Section 3.3 determined the cost per part of manufacturing the spare combine harvester blades to be $0.27, $0.19, $0.17 for the low-, medium-, and high-volume manufacturing processes. CSISA-MEA partners in Bangladesh determined the dealer's sales price of the full feed and half feed spare combine harvester blades to be between $1.08 and $3.76. Assuming a 200% price markup by the dealers, the production of spare combine harvester blades by spare parts manufacturers Bangladesh was found to be economically viable. Table 29 presents the breakdown of the cost per part of the low-, medium-, and high-volume manufacturing process along with the dealer's sales price for the full-feed and half-feed combine harvester blades.

The market analysis shown in Section 3.3 calculated the estimated market size for spare combine harvester blades in Bangladesh to $135,900 \frac{\text{blades}}{\text{year}}$. Therefore, the low- and medium-volume production processes were determined to be the optimal manufacturing methods in Bangladesh. The yearly production of the low-volume method was determined to $153,300 \frac{\text{blades}}{\text{year}}$; therefore, the low-volume method is optimal for manufacturers who will run production continuously. The yearly production of the medium-volume production process was determined to be $460,800 \frac{blades}{year}$; therefore, the medium-volume method is recommended if the spare parts manufacturer will produce the blades to order for the spare parts dealers.

The DEFORM simulations of the final forging punch/die set with and without a gutter, presented in Subsection 3.7.4, shows the increase in die stroke at varying forming

forces with the addition of a gutter. Therefore, it is recommended that a gutter of equal

dimensions to that of the final half feed small bottom blade punch plate be machined in

the current prototype punch plate so that further testing can be conducted. Table 48

shows the dimensions for the gutters for the full feed and half feed forging punch plates.

The side width refers to the width along the side edges of the cavity and the top width

refers to the width along to the top edge of the cavity. The distance from the blade cavity

to the gutter is 1.5 mm for all punch plates and all edges of the gutter have a 0.5 mm

chamfer applied. Machining of the forging punch base and die are recommended to

replicate the design of the final forging punch base. The machining of the forging die

would consist of removing the edges of the pocket on three sides and machining the

lineup block, or raised portion, into the fourth side. The machining of the forging punch

base would consist of machining the lower left corner so that the forging punch base

engages properly with the forging die. It is recommended that additional punch plates be

machined for testing or production of the three blades not tested during the experimental

testing.

Table 49: Punch plate gutter dimensions

Blade	Width – Side (mm)	Width – Top (mm)	Depth (mm)
Full feed	8.0	6.0	1.0
Half feed small	6.0	6.0	2.0
Half feed large bottom blade	6.0	6.0	2.0
Half feed top blade	6.0	8.0	2.0

The forging sensitivity analysis located in Subsection 3.7.5 determined the

recommended forging pressing forces for the full-feed and half-feed combine harvester

blades as shown in Table 47. A pressing force of 100-300 metric tons is recommended

for the forging of the serrated edge of the full feed combine harvester blade. A pressing force of 200-300 metric tons is recommended for the half feed top blade while a pressing force of 300 metric tons is recommended for both the half feed small bottom and large bottom blade. Hydraulic presses with maximum pressing forces more than 100 metric tons are currently operational in several small machine shops within Bangladesh. However, no press with a maximum capacity of 300 metric tons is documented in the agricultural spare parts market within Bangladesh. Therefore, it is recommended that the initial local manufacturing of combine harvester blades in Bangladesh be full-feed combine harvester blades so that no additional hydraulic presses must be purchased by some local manufacturers. The recommended stock material for the full-feed combine harvester blades is AISI 1070. However, the results of the sensitivity analysis showed that only minor deviations in die stroke are expected as a result of variations in stock material tensile strengths of the range of 620-710 MPa. Stock material hardness can be determined and converted into ultimate tensile strength through the methods shown in Subsection 3.7.2.

For the manufacturing of half-feed combine harvester blades it is recommend that a press with a maximum force of at least 300 metric tons is used so that an adequate die stroke is reached for all the three blades. As there is no documentation of a 300 metric tons press among the Bangladesh spare parts manufactures, it is recommended that the manufacturing of the half-feed combine harvester blades be developed after a successful implementation of the full-feed combine harvester blade manufacturing process. This is due to the increased cost of the 300 metric tons press required to create the serrated edge of the half-feed combine harvester blades.

3.7.8 Section Summary

The Results and Discussion section of Chapter 3 consists of seven main subsections: XRF Results, Hardness Testing Results, Experimental Testing Results, DEFORM simulation results, DEFORM bending sensitivity analysis, DEFORM validation, and Discussion and Recommendations. The XRF Results section presents the material composition results and comments on their application on selecting the appropriate stock materials for combine harvester blade manufacturing in Bangladesh. The Hardness Testing Results section presents the results of the hardness testing conducted on the original and locally produced combine harvester blades. The use of hardness testing in stock material selection and quality control testing is discussed. The Experimental Testing Results section compares the results from the experimental testing of the forging punch and die set to that of the original combine harvester blades. In the DEFORM results section, the DEFORM simulation results of the final design of the forging punch and die set with and without a flash gutter are compared to determine the effects of the flash gutter on the relationship between press force and die stroke. The DEFORM Bending Sensitivity Analysis section presents the results of the sensitivity analysis which determine the effect of stock material tensile stress on the pressing force versus die stroke relationship. The DEFORM Validation section provides verification and validation of the DEFORM forming model through mesh convergence and experimental testing. Finally, the Discussion and Recommendations section discusses the potential for spare parts manufacturers in Bangladesh to produce combine harvester blades accurately

while making a profit. The recommended equipment for manufacturing full feed and half feed combine harvester blades is also discussed.

3.8 Chapter Summary

Chapter 3 is divided into seven main sections. Section 1 introduces the operation of the combine harvester and combine harvester cutter bar as well as the current state of the local rice transplanter claw manufacturing. Section 2 provides a literature review of published literature, video media, and online marketplaces regarding the manufacturing of combine harvester blades. Section 3 describes the characterization of the original and locally produced combine harvester blades and the development of the manufacturing process through a combination of factory layout, cost, and market analysis. Section 4 provides a breakdown of the design of the required tooling for the manufacturing processes determined in Section 3. Section 5 provides a description of the experimental testing and procedures for the forging punch and die set developed for the fabrication of the serrated edge of the combine harvester blades. Section 6 describes the finite element analysis software setup which was used for all FEA simulations. Section 7 provides the results and discussion of the characterization of the original and locally produced combine harvester blades, experimental testing, and finite element simulations. Finally, recommendations of equipment/machinery for the manufacturing of combine harvester blades are made for the small machine shops and CSISA-MEA staff in Bangladesh.

The next chapter looks to provide a conclusion summary of the material presented in this thesis along with any drawbacks of this study and future work.

CHAPTER 4

CONCLUSION AND FUTURE WORK

Mechanization has been listed as a top priority for the agricultural sector of Bangladesh because a decreasing agricultural labor force and rising wages have cut into farmers' low profit margins and left them unable to quickly harvest crops in cases of emergencies such as storms and flooding. The mechanization of operations such as land preparation, pesticide application, irrigation, and threshing have become prevalent since at least 2019. However, mechanization of planting and harvester has yet to be commonplace with less than one percent of rice planting and eight percent of rice harvesting being mechanized as of 2021. Recently implemented government programs have incentivized farmers to purchase more advanced machinery and have resulted in an increase in the combine harvester market from $4.25 million in 2017 to $33.33 million in 2019 (Alam, 2022). The increase in mechanization of transplanting and harvesting has led to the import of rice transplanter and combine harvester spare parts from China. This thesis provides the resources necessary for small machine shops in Bangladesh to advance their manufacturing capabilities by creating additional manufacturing processes for the fabrication of the rice transplanter claws and combine harvester blades.

The initial manufacturing analysis was completed through analysis of the manufacturing markers on the original rice transplanter claws and combine harvester blades. Morphological charts of manufacturing processes were then created based on the previous inspection of the parts. Low-, medium-, and high-volume production manufacturing processes were created through combinations of manufacturing processes

listed in the morphological charts. A cost analysis of the three manufacturing processes was then completed to determine the production cost for a single part. The production cost of the low-, medium-, and high-volume production of the rice transplanter claws and combine harvester blades were then compared to the current prices of the imported spare parts offered. The comparison of the production costs and the dealer's sales prices revealed that all three manufacturing processes are economically viable for producing both rice transplanter claws and combine harvester blades at a profit. A market size analysis was then complete based upon the number of rice transplanters and combine harvesters in use in Bangladesh. The results of the market size analyses were analyzed, and the most suitable manufacturing processes were selected for producing the agricultural spare parts manufactures in Bangladesh.

Next, the design of the required blanking, bending, and forging punch and die sets were completed. The design of the blanking punch and die sets for the rice transplanter claws and combine harvester blades was completed using references such as Suchy's *Handbook of Die Design* and Boljanovic and Paquin's *Die Design Fundamentals*. The rice transplanter bending die design was completed using a combination of sheet metal bending analysis and FEA simulations. The design of the combine harvester forging punch die, base, and punch plates was completed through FEA analysis and collaboration with the Montgomery Machining Mall to verify that the forging punch and die parts can be machined on a 3-axis CNC mill, which is most common in Bangladesh.

The initial prototype bending, and forging punch and die sets were machined from A2 tool steel and tested on a 50-ton hydraulic press at Georgia Tech so that the DEFORM-3D bending and forging models could be validated. The validation of the

DEFORM-3D rice transplanter bending die was completed by comparing width measurement along the rice transplanter claw of the DEFORM-3D simulation and experimental testing. The width differences were found to be 0.05 mm or 0.29%. The validation of the combine harvester forging die testing and corresponding DEFORM-3D model was completed by analyzing the differences in die stroke at a pressing force of 50 tons/45.35 metric tons. The difference between the die stroke of the prototype forging die set and DEFORM-3D simulation was found to be 0.08 mm or 2.3%. The machining tolerances held during the machining of the bending and punch die sets were of $\pm 0.005"$ or ± 0.125 mm, therefore the DEFORM-3D model of the bending and forging operation were considered validated.

Further simulations were conducted to determine the effects of future design changes to the bending and forging punch and die sets. The bending radius of the bending die set was increased from 1.5 mm to 3.0 mm, which resulted in a is 0.05 mm width difference between the DEFORM simulation and original rice transplanter claw. Flash gutters were added to the combine harvester punch plate which resulted in an increase in die stroke at pressing forces of 100, 200, and 300 metric tons. The resulting final design of the four-combine harvester punch and die sets reach adequate die strokes at varying pressing forces of 100-300 metric tons. Therefore, both the design of both the bending and forging punch and die sets have been shown to accurately reproduce the features of the original parts.

Sensitivity analyses were conducted on both the bending and forging punch and die sets to determine the sensitivity of the punch and die sets to stock material yield strength. Results of the rice transplanting bending die sensitivity analysis indicate that a

linear relationship exists between material tensile stress and the required press force needed to reach a die stroke of 9 mm. For stainless steel 304 and 316 the force required to bend the rice transplanter claw was found to be 22.34 -23.24 metric tons. Therefore, a press with a maximum force of at least 50 metric tons is recommended. The press brake rice transplanter bending analysis indicated that a maximum force of 1.05 metric tons was needed to create one bend in the rice transplanter claw. Therefore, a press brake with a maximum force of at least 2 metric tons is recommended to create the bend in the rice transplanter claws. The results of the combine harvester forging die sensitivity analysis results indicate that there is little deviation in the die stroke versus press force relationship for materials with tensile strengths between 620 -710 MPa. The full feed combine harvester forging punch and die set reached adequate die stroke at press forces of 100-300 metric tons. The half-feed combine harvester blades reached adequate die strokes at press forces of 300 metric tons. As 100 metric tons presses are common in machine shops throughout Bangladesh, it is recommended that the full feed combine harvester blades be manufactured before the half-feed combine harvester blade due to the increased cost of the 300 metric tons press. For the manufacturing of the half-feed combine harvester blades it is recommended that a 300 metric tons press be used for the manufacturing of all three blades.

Finally, the shortcomings of this study as well as future work are identified. The cost analyses presented for the low-, medium-, and high-volume manufacturing processes require accurate cost of machinery to be accurate. Due to import duties and taxes imposed in Bangladesh, accurate costs of machinery are hard to obtain and must be estimated based upon machinery prices in India or China. Interest rates are also not

considered in the cost analysis. The estimated market size for the rice transplanter claws and combine harvester blades is based on an estimation of the number of times these parts are replaced per year. More accurate data regarding the replacement of the rice transplanter claws and combine harvester blades is needed to determine a fully accurate market size. Additionally, the sensitivity analysis of the forging punch and die sets consider only five stock materials. Analyzing additional stock material will provide a better understanding of the variation in the force versus die stroke relationship at varying material tensile strengths. This study may be improved by performing additional DEFORM-3D simulations to determine the stresses in the forging punch and die sets so that the appropriate stock material can be selected so that the yield strength is not reached during forging operation with a pressing force of 300 metric tons.

APPENDIX A

Rockwell Hardness Conversion Table

Table A1: Rockwell hardness to tensile conversion chart

Rockwell Hardness		Tensile Strength (psi)
B Scale 100 kg	C Scale 150 kg	
	59	329000
	59	324000
	59	323000
	57	309000
	56	297000
	55	285000
	54	247000
	52	263000
	51	253000
	50	243000
	48	235000
	47	225000
	46	217000
	43	202000
	42	195000
	40	188000
	39	182000
	38	176000
	37	170000
	36	166000
	34	160000
	33	155000
	32	150000
	31	145000
	30	141000
	29	137000
	27	133000
	25	129000
	24	126000
100	23	122000
99	22	118000
98	20	115000
97	18	111000
96	17	105000

96	16	102000
95	15	100000
94		98000
93		95000
92		93000
91		90000
90		89000
89		87000
88		85000
87		83000
86		81000
85		79000
83		76000
81		73000
79		71000
76		67000
74		65000
72		63000
70		60000
68		58000
66		56000

APPENDIX B

Granta EduPack Settings

Table B1: ANSYS Grant EduPack rice transplanter claw part cost estimation settings

ANSYS Granta EduPack Part Cost Estimator Settings	
Material	Stainless Steel 304 Annealed
Value of scrap material	0%
Part mass	0.0777 lb.
Part length	0.377 ft
Primary Process	Cold closed die forging
Availability	Custom form
Part complexity	Simple
Load Factor	50 %
Overhead rate	$4 \frac{USD}{hr}$
Capital write-off time	5 yrs.
Secondary Process	Press forming
Part Complexity	Standard
Amount of scrap	10%
Scrap recycled	Yes

Table B2: ANSYS Grant EduPack combine harvester blade part cost estimation settings

ANSYS Granta EduPack part cost estimator settings for combine harvester blades	
Material	AISI 1070, as rolled
Value of scrap material	0%
Part mass	0.165 lb.
Part length	0.233 ft
Batch Size	100-1e+06
Number of values	15
Primary Process	Cold closed die forging
Availability	Custom form
Part complexity	Simple
Load Factor	50 %
Overhead rate	$3.36 \frac{USD}{hr}$
Capital write-off time	5 yrs.
Secondary Process	Cold closed die forging
Part Complexity	Complex
Amount of scrap	10%
Scrap recycled	Yes

APPENDIX C

Machinery Cost

Table C1: Rice transplanter claw and combine harvester claw machinery costs

Cost List		
Equipment	Price [USD]	Links
300-ton Hydraulic press	6827	https://www.indiamart.com/proddetail/hydraulic-power-press-4161786973.html?pos=1&pla=n
40-ton press brake	9,178	https://www.indiamart.com/proddetail/hydraulic-press-brake-12394779130.html?pos=7&kwd=press%20brake&tags=A||||7613.566 |Price|product|
50-ton mechanical press	1300	https://www.indiamart.com/proddetail/h-frame-power-press-machine-10100211697.html?pos=6&kwd=press&tags=A|||8258.9375|Price|proxy|
Drill Press	140	https://www.indiamart.com/proddetail/h-frame-power-press-machine-10100211697.html?pos=6&kwd=press&tags=A||||8258.9375|Price|proxy|
Grinder	43	https://fixit.com.bd/product/1010w-12000rpm-100mm-angle-grinder-ingco-brand-ag10108-2/
Bench Grinder	72	https://dir.indiamart.com/search.mp?ss=bench+grinder&cityid=70772&cq=Kolkata&mcatid=14562&catid=785&prdsrc=1
Band saw	523	https://www.indiamart.com/proddetail/vertical-band-saw-machine-15823339497.html?pos=15&kwd=metal%20band%20saw&tags=A||||8132.985|Price|product|
Piercing punch	1.95	https://www.indiamart.com/proddetail/piercing-punches-23604633155.html?pos=6&kwd=piercing%20punch&tags=A||Pref||1427.5057|Price|product|

REFERENCES

Acuren. (2019, June 12). *Optical emission spectroscopy (OES)*. Retrieved May 6, 2022, from https://www.acuren.com/engineering/field-engineering/optical-emission-spectroscopy/

Aerospace Alloy. (2019). *Spring Steel EN42J / C80 sheet plate*. Retrieved from https://www.aerospacealloy.com/spring-steel-en42j-c80-sheet-plate-manufacturer-supplier.html

AISI 1008 Carbon Steel. AZO Materials. (2012, September 11). Retrieved June 9, 2022, from https://www.azom.com/article.aspx?ArticleID=6538

Alam, M. M., Khan, M. I. N., Saha, C. K., Rahman, A., & Bhuyian, M. G. K. (2017). *Manufacturing of agricultural machinery in Bangladesh: opportunities and constraints*. CIGR, 19(1), 122–135.

Alam, M. M. (2022, March). *Trend of Agricultural Machinery and Spare Parts Manufacturing and Sales in Bangladesh*. Agricultural Mechanization in Bangladesh - The Future. Dhaka; Bangladesh.

Annealed 304 Stainless Steel. MakeItFrom.com. (2020, May 30). Retrieved June 10, 2022, from https://www.makeitfrom.com/material-properties/Annealed-304-Stainless-Steel

Annealed 316 Stainless Steel. MakeItFrom.com. (2020, May 30). Retrieved June 10, 2022, from https://www.makeitfrom.com/material-properties/Annealed-316-Stainless-Steel

Annealed 410 Stainless Steel. MakeItFrom.com. (2020, May 30). Retrieved June 10, 2022, from https://www.makeitfrom.com/material-properties/AISI-410-S41000-Stainless-Steel

Annealed and Cold Drawn 1045 Carbon Steel. MakeItFrom.com. (2020, May 30). Retrieved June 10, 2022, from https://www.makeitfrom.com/material-properties/Annealed-and-Cold-Drawn-1045-Carbon-Steel

Annealed and Cold Drawn 1070 Carbon Steel. MakeItFrom.com. (2020, May 30). Retrieved June 9, 2022, from https://www.makeitfrom.com/material-properties/Annealed-and-Cold-Drawn-1070-Carbon-Steel/

Ashby, M. (2009). Granta Ces 2009 EduPack Material and Process Selection Charts. Granta Design Limited.

ASTM Standard A370 – 21, 2021, "*Standard Test Methods and Definitions for Mechanical Testing of Steel Products,*" ASTM International, West Conshohocken, PA, 2021, www.astm.org

ASTM Standard E140 – 12b, 2019, "*Standard Hardness Conversion Tables for metals Relationship Among Brinell Hardness, Vickers Hardness, Rockwell Hardness, Superficial Hardness, Knoop Hardness, Scleroscope Hardness, and Leeb Hardness,*" ASTM International, West Conshohocken, PA, 2019, www.astm.org

Bangladesh Rice Research Institute. (2011). *Rice in Bangladesh*. Bangladesh Rice Knowledge Bank. Retrieved June 13, 2022, from http://www.knowledgebank-brri.org/riceinban.php

BESCO Harvester blade mould and punch press [Video]. (2020, November 19). YouTube. https://www.youtube.com/watch?v=Ok3Fag1fPs0&ab_channel=%E8%96%9B%E4%BA%AD

BITAC. (n.d.). *Material Price List*. Dhaka, Bangladesh; Tool and Technology Institute.

Boeijen, A. van, Daalhuizen, J., & Zijlstra, J. (2020). *Delft Design Guide: Perspectives, models, approaches, methods*. BIS Publishers.

Boljanovic, V., & Paquin, J. R. (2006). *Die Design Fundamentals* (Third). Industrial Press.

Callister, W. D. (2003). *In Materials Science and Engineering - An Introduction* (Sixth, p. 139). Wiley.

China 45 Steel. The World Material. (2022). Retrieved June 13, 2022, from
https://www.theworldmaterial.com/china-45-steel/

Clearence Calculation. Matrix Tools. (2019, September 11). Retrieved March 20, 2022,
from https://www.matrixtools.eu/en/clearence-calculation/

Cold Drawn 1008 Carbon Steel. MakeItFrom.com. (2020, May 30). Retrieved June 9,
2022, from https://www.makeitfrom.com/material-properties/Cold-Drawn-1008-
Carbon-Steel

Cold Drawn 1035 Carbon Steel. MakeItFrom.com. (2020, May 30). Retrieved June 9,
2022, from https://www.makeitfrom.com/material-properties/Cold-Drawn-1035-
Carbon-Steel

Daily sun. (2022, June 12). *Bangladesh ranks third in rice production for four
consecutive years*. Retrieved June 13, 2022, from https://www.daily-
sun.com/post/625938/Bangladesh-ranks-third-in-rice-production-for-four-
consecutive-years

Discover Agriculture. (2020, October 17). *How to prepare RICE SEEDLINGS for
Transplantation | Paddy / Rice Nursery Bed Preparation* [Video]. YouTube.
https://www.youtube.com/watch?v=R2rqGqLCDNg&ab_channel=DiscoverAgricul
ture

Fuad, M. A. F., & Flora, U. M. A. (2019). *Farm mechanization in Bangladesh: a Review*.
International Journal of Research in Business Studies and Management, 6(9), 15–
29.

Grade 65Mn Steel. The World Material. (2022). Retrieved June 8, 2022, from
https://www.theworldmaterial.com/65mn-high-carbon-spring-steel/

Greenly Machinery. (2012). Retrieved June 7, 2022, from http://www.greenly-
agparts.com/

Grigor'ev Igor' Sergeevič, Mejlihov Evgenij Zalmanovič, & Radcig Aleksandr
Aleksandrovič. (1997). *Handbook of physical quantities*. CRC Press.

High Strength Steel Design/Formability Task Force of the Auto Steel Partnership. (2001). Die Design and Construction Guidelines for HSS Dies. In *High Strength Steel (HSS) stamping design manual*. essay.

Hoshino, S. (1974). *Recent Advances on Rice Transplanter*. Japan Agricultural Research Quarterly, 8(4), 209–213.

Inspira. (2022). (rep.). *Raw Materials Market Assessment for Agro-Machines and Spare Parts* (pp. 27–30). Dhaka.

IRRI Rice Knowledge Bank. (2014). *How to prepare the seedlings for transplanting*. Retrieved from http://www.knowledgebank.irri.org/step-by-step-production/growth/planting/how-to-prepare-the-seedlings-for-transplanting#modified-mat-nursery

Jatinder Singh Kundi. (2013, July 17). *Induction Heater Combine blade 20Kw 50Khz* [Video]. YouTube. https://www.youtube.com/watch?v=q4_Pn3qnFCw&ab_channel=JatinderSinghKundi

Jhone Deer Harvester Repair. (2020, June 15). *Harvest cutter bar repair* [Video]. YouTube. https://www.youtube.com/watch?v=1jBAeAnosW0&ab_channel=Jhonedeerharvesterrepair

JRS Farmparts. (n.d.). *Harvesting Blade*. indiamart.com. Retrieved June 8, 2022, from https://www.indiamart.com/proddetail/harvesting-blade-17016885130.html?pos=1&kwd=harvester+blade&tags=A%7C%7C%7C%7C8190.9683%7CPrice%7Cproduct%7C

Kalpakjian, S., & Schmid, S. R. (2008). *Bending of Sheet and Plate. In Manufacturing Processes for Engineering Materials* (Fifth, pp. 360–371). essay, Pearson Education Inc.

Kubota SPV6C Rice Transplanter Planting Assembly. Alibaba. (n.d.). Retrieved June 13, 2022, from https://www.alibaba.com/product-detail/KUBOTA-SPV6C-RICE-TRANSPLANTER-FINGER-PLANTING_62441025764.html

Massachusetts Institute of Technology. (2017). *Mesh Convergence*. Retrieved June 5, 2022, from https://abaqus-docs.mit.edu/2017/English/SIMACAEGSARefMap/simagsa-c-ctmmeshconverg.htm

Ministry of Agriculture, *National Agricultural Mechanization Policy 2020* (2020). Dhaka; Ministry of Agriculture. Retrieved March 1, 2022, from https://moa.gov.bd/sites/default/files/files/moa.portal.gov.bd/policies/db06a170_6d 62_4f59_b7fd_d9477ed941c3/09.%20National%20Agriculture%20Macanisum%20 Policy2020.pdf

Nath, B. , Paul, S. , Huda, M. , Hossen, M. , Bhuiyan, M. and Islam, A. (2022) *Combine Harvester: Small Machine Solves Big Rice Harvesting Problem of Bangladesh*. Agricultural Sciences, **13**, 201-220. doi: 10.4236/as.2022.132015.

OnlineMetals, (2019). *Hardness conversion table: Brinnel/Rockwell tensile strength*. Retrieved from https://www.onlinemetals.com/en/hardness-conversion-table

Qingdao Ablson Machinery Co. Ltd. . (n.d.). *Planting claw for SPV6CMD/SPW48C/68C riding rice transplanter*. Retrieved from https://www.alibaba.com/product-detail/Planting-claw-for-SPV6CMD-SPW48C-68C_1600499424126.html?spm=a2700.galleryofferlist.normal_offer.d_title.db8d49 44tR0MJ1

SAE AISI 1080 Steel Properties. The World Material. (2019). Retrieved June 8, 2022, from https://www.theworldmaterial.com/astm-sae-aisi-1080-steel-properties-heat-treatment-composition/

Sawblade.com. (2015). *Band Saw Blade Speed and Feed Chart*. Retrieved May 23, 2022, from https://www.sawblade.com/band-saw-blade-speed-and-feed-chart.cfm

Scientific Forming Technologies Corporation. (2012). DEFORM 3D. *Products*. Retrieved March 20, 2022, from https://www.deform.com/products/deform-3d/

Statology. (2020, November 18). *How to Perform Polynomial Regression in Excel*. Retrieved March 1, 2022, from https://www.statology.org/polynomial-regression-excel/

Steel Grades. (2018). *AISI 1566*. Retrieved June 8, 2022, from https://www.steel-grades.com/Steel-Grades/Carbon-Steel/AISI-1566.html

K, Ivana. *Handbook of Die Design*. Second ed., McGraw-Hill, 2006.

Tempered 431 Stainless Steel. MakeItFrom.com. (2020, May 30). Retrieved June 10, 2022, from https://www.makeitfrom.com/material-properties/Tempered-T-431-Stainless-Steel

Thermo Fisher Scientific - US. (n.d.). *Niton™ FXL field X-ray lab*. Retrieved March 1, 2022, from https://www.thermofisher.com/order/catalog/product/NITONFXLXRF

Thermo Fisher Scientific. (n.d.). *ARL™ OPTIM'X WDXRF Spectrometer*. Retrieved May 6, 2022, from https://www.thermofisher.com/order/catalog/product/IQLAAHGABMFAASMACH?SID=srch-srp-IQLAAHGABMFAASMACH

The World Bank. (2020). *Population Density (people per sq. km of land area) - Bangladesh*. Retrieved from https://data.worldbank.org/indicator/EN.POP.DNST?locations=BD

United Nations Population Fund. (2022). *World Population Dashboard -Bangladesh* Retrieved from https://www.unfpa.org/data/world-population/BD

Viking Drill and Tool. (2015). *Drill Feeds and Speeds*. Retrieved May 23, 2022, from http://www.vikingdrill.com/viking-Drill-FeedandSpeed.php

Weifang Jintan Harvester Blade Factory. (n.d.). *Blade Factory for Combine Harvester Combine*. Made-in-China. Retrieved June 8, 2022, from https://harvesterblade.en.made-in-china.com/product/CSjmzAMUHPYi/China-Blade-Factory-for-Combine-Harvester-Combine.html

Wirth, K., & Barth, A. (2020, January 21). *X-ray fluorescence (XRF). Geochemical Instrumentation and Analysis*. Retrieved May 1, 2022, from https://serc.carleton.edu/research_education/geochemsheets/techniques/XRF.html